AD-A081 998 EIC CORP NEWTON MASS F/G 10/3
INVESTIGATIONS OF THE SAFETY OF LI/SOCL2 BATTERIES.(U)
FEB 80 K M ABRAHAM, R M MANK, G L HOLLECK DAAB07-78-C-0564
UNCLASSIFIED C-536 DELET-TR-78-0564-F NL

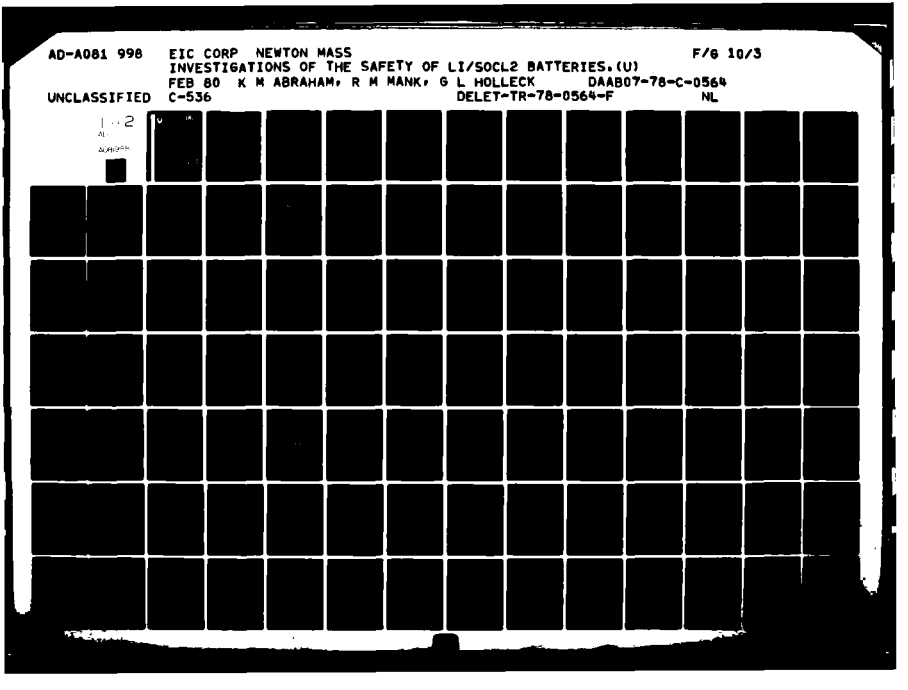

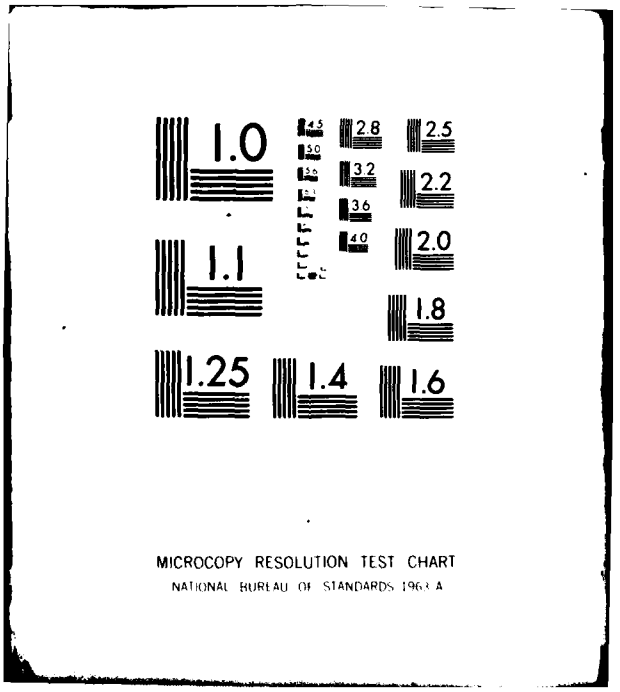
1.0
1.1
1.25
1.4
1.6
1.8
2.0
2.2
2.5
2.8
3.2
3.6
4.0
4.5
5.0
5.6
MICROCOPY RESOLUTION TEST CHART
NATIONAL BUREAU OF STANDARDS 1963 A

Research and Development Technical Report
DELET-TR-78-0564-F

INVESTIGATIONS OF THE SAFETY OF Li/$SOC1_2$ BATTERIES

Kuzhikalail M. Abraham
Richard M. Mank
Gerhard L. Holleck

EIC CORPORATION
55 Chapel Street
Newton, MA 02158

February 1980

Final Report for Period 30 Sept. 1978 - 29 Sept. 1979

Prepared for:
ELECTRONICS TECHNOLOGY & DEVICES LABORATORY

ERADCOM

US ARMY ELECTRONICS RESEARCH AND DEVELOPMENT COMMAND
FORT MONMOUTH, NEW JERSEY 07703

NOTICES

Disclaimers

The citation of trade names and names of manufacturers in this report is not to be construed as official Government indorsement or approval of commercial products or services referenced herein.

Disposition

Destroy this report when it is no longer needed. Do not return it to the originator.

UNCLASSIFIED

SECURITY CLASSIFICATION OF THIS PAGE (When Data Entered)

(19) REPORT DOCUMENTATION PAGE	READ INSTRUCTIONS BEFORE COMPLETING FORM
1. REPORT NUMBER (18) DELET-TR-78-0564-F	2. GOVT ACCESSION NO. / 3. RECIPIENT'S CATALOG NUMBER (9)
4. TITLE (and Subtitle) (6) INVESTIGATIONS OF THE SAFETY OF Li/$SOCl_2$ BATTERIES.	5. TYPE OF REPORT & PERIOD COVERED Final Report. 30 Sept 1978-29 Sept 1979
	6. PERFORMING ORG. REPORT NUMBER (14) C-536
7. AUTHOR(s) (10) Kuzhikalail M. Abraham, Richard M. Mank and Gerhard L. Holleck	8. CONTRACT OR GRANT NUMBER(s) (15) DAAB07-78-C-0564
9. PERFORMING ORGANIZATION NAME AND ADDRESS EIC CORPORATION 55 Chapel Sreet Newton, MA 02158	10. PROGRAM ELEMENT, PROJECT, TASK AREA & WORK UNIT NUMBERS (16) 1L162705AH94-11-218
11. CONTROLLING OFFICE NAME AND ADDRESS U.S. Army Electronics Research & Development Command, Attn: DELET-PR Fort Monmouth, New Jersey 07703	12. REPORT DATE (11) February 1980 (17) 11
	13. NUMBER OF PAGES 91
14. MONITORING AGENCY NAME & ADDRESS(if different from Controlling Office) (12) 105	15. SECURITY CLASS. (of this report) UNCLASSIFIED
	15a. DECLASSIFICATION/DOWNGRADING SCHEDULE

16. DISTRIBUTION STATEMENT (of this Report)

Approved for Public Release; Distribution Unlimited.

17. DISTRIBUTION STATEMENT (of the abstract entered in Block 20, if different from Report)

18. SUPPLEMENTARY NOTES

19. KEY WORDS (Continue on reverse side if necessary and identify by block number)

Lithium thionyl chloride battery, forced overdischarge, explosion hazards, charging behavior, IR spectra, cyclic voltammetry, SO_2Cl_2, $SOCl^+AlCl_4^-$ Cl_2, Li_2S, SCl_2, $LiAlSCl_2$.

20. ABSTRACT (Continue on reverse side if necessary and identify by block number)

Forced overdischarge behavior of Li/$SOCl_2$ cells was studied using spirally wound C-size and small prismatic cells. Cathode and anode limited cells were tested. Cathode limited cells could be forced overdischarged for long periods of time without explosions. Anode limited cells, on the other hand, were found to be potentially hazardous. Our data suggest that anode limited cells are likely to explode during forced overdischarge.

DD FORM 1 JAN 73 1473 EDITION OF 1 NOV 65 IS OBSOLETE

UNCLASSIFIED

SECURITY CLASSIFICATION OF THIS PAGE (When Data Entered)

408525

The behavior of $Li/SOCl_2$ cells during application of a "charge" current was investigated using C-size cells. It was possible to subject either new or partially discharged cells to a "charging" current without apparent hazard. The charging reactions involve a sequence of regenerative processes so that only small amounts of chemicals accumulate in the cells.

Cyclic voltammetry and infrared spectrometry were employed as analytical tools to characterize the reaction products in $Li/SOCl_2$ cells during various modes of operation. Sulfur dioxide is produced during early stages of discharge. The nature of products formed during forced overdischarge depends on whether the cells are cathode or anode limited.

Infrared spectral data indicated that $LiAlSCl_2$ is formed in cathode limited $Li/SOCl_2$ cells during forced overdischarge and resistive load overdischarge. These compounds are formed from the reaction of Li_2S, produced in the cell under these operational modes, with $LiAlCl_4$. It has been found that the lithium thioaluminum compounds can also be prepared from the reaction between Li_2S and $AlCl_3$.

From anode limited cells, Cl_2 and a compound exhibiting IR absorption at 1070 cm^{-1} were detected after forced overdischarge. These materials are formed by oxidation reactions at the anode.

Analysis of solutions from cells discharged without Li on the anode showed SO_2Cl_2, $SOCl^+AlCl_4^-$ SCl_2, Cl_2 and a material absorbing at 1070 cm^{-1} in the IR spectrum as products. Some SO_2 was also found in these solutions.

The products detectable after "charging" a $Li/SOCl_2$ cell were SO_2Cl_2, SCl_2, SO_2, Cl_2 and the material exhibiting absorption in the infrared spectrum at 1070 cm^{-1}.

On the basis of materials characterized from IR spectral and cyclic voltammetry data, a mechanism is proposed for the oxidation reactions in $SOCl_2/LiAlCl_4$ solutions.

Preliminary studies indicated that $Li_2S/AlCl_3$ based electrolytes may be useful as alternatives to $LiAlCl_4$ in $Li/SOCl_2$ batteries.

TABLE OF CONTENTS

TABLE OF CONTENTS
(continued)

LIST OF ILLUSTRATIONS

LIST OF ILLUSTRATIONS
(continued)

LIST OF ILLUSTRATIONS
(continued)

LIST OF TABLES

I. INTRODUCTION

In recent years there has been considerable research and development on ambient temperature, high energy density Li cells. A particularly promising system is based on $SOCl_2$ (1,2). Here, $SOCl_2$ serves as both a solvent and depolarizer for the cell. These cells have delivered 100 Whr/lb and 40 W/lb at the 2.5-hour rate and, as usual, higher energy densities at lower discharge rates (3). They can deliver as much as 300 Whr/lb at low rates (4). Clearly this is a very promising system with many applications where high energy density and high rate are required.

The cell has two problems: (1) under a variety of circumstances, the cell has shown a tendency to explode, (2) after high temperature storage, it shows voltage delay.

The objective of this program is to explore the causes and find solutions to the explosion hazards in the Li/$SOCl_2$ cells. Three types of explosion have been reported: (1) cells explode on short circuit; (2) cells explode on forced overdischarge; (3) cells explode on resistive load overdischarge. Clearly, any high rate, high energy density system such as Li/$SOCl_2$ has the possibility of a thermal runaway type of explosion. It is not surprising that a hermetically sealed D-cell, which can deliver in excess of 20 amps, might explode when short circuited -- it just is not possible to remove the waste heat. However, this problem appears to have been solved with low pressure vents (100-300 psi) and with appropriate fuses incorporated into the cell (5,6).

The other two types of explosion are of greater concern. The forced overdischarge situation may be experienced by a cell in a battery package. Explosion on resistive load overdischarge implies that any completely discharged cell still connected to a piece of equipment is a hazard. No clear documentation of the explosion hazard on resistive load overdischarge is found in the literature. Forced overdischarge explosions have been documented for D-size (5) and C-size (7,8) Li/$SOCl_2$ cells. This type of explosion, occurring after cell-voltage reversal, takes place without prior temperature or pressure rise and appears to be chemical in its origin. Our results seem to show that forced overdischarge explosions would occur only in anode limited cells (7,8). Individual electrode potential measurements during discharge and overdischarge showed that the anode was at $\geq$4.0V for a considerable length of time prior to an explosion. The nature of the explosion suggests that they are caused by sensitive chemicals generated in oxidation reactions of $SOCl_2$ or other materials present in the cell.

In the present program we have further studied the behavior of Li/$SOCl_2$ cells during forced overdischarge. These studies were directed towards answering the following questions: (1) What is the effect of current density? (2) What

roles do cell geometry and cell size play? (3) What is the role of the supporting electrolyte? (4) What is the explosive material? (5) What initiates the explosion and what is the mechanism of propagation?

We have also examined the behavior of $Li/SOCl_2$ cells during resistive-load overdischarge and during the application of a positive current to the cathode (charging).

Since the ultimate solution to the explosion hazards requires a detailed understanding of the chemical and electrochemical reactions which occur under use and abuse conditions, a considerable amount of analytical work was carried out to clearly understand safety related chemistry. The principal analytical techniques have been cyclic voltammetry and IR spectrometry.

II. PHENOMENOLOGICAL STUDIES

1. Experimental Procedures

Two types of test vehicles were employed for these studies. They were C-size and small prismatic laboratory cells.

1.1 C-Size Cells

C-size $Li/SOCl_2$ cells with spirally wound electrodes were constructed and specially instrumented for measuring individual electrode potentials and temperature. Special emphasis was placed on the configuration of these cells, i.e., whether they were cathode or anode limited.

- Cell Construction

C-cells were constructed using the typical parameters given below:

C Cathode: 10" × 1.5"; 0.024" thick. The cathode contained 1.70 ± 0.2g of the cathode mix, comprising 85% Shawinigan carbon and 15% Teflon, bonded on expanded Ni, 5Ni5-5/0.

Li Anode: 10" × 1.5"; 0.017" thick Li foil pressed on expanded Ni, 5Ni7-4/0.

In some cells, electrode parameters varied slightly from those given above. These are appropriately indicated in the text.

Separator: 2" × 11.5"; 0.005" thick, all-glass filter paper containing 4% PVA binder (Mead Paper Specialty, Catalog No. 934-S).

Electrolyte: 12 ml 1.8M $LiAlCl_4/SOCl_2$. The electrolyte was prepared as described below.

Cell Containers: Stainless steel (No. 316) can; height = 2.1", OD = 1.00").

The Li anode, the carbon cathode and the glass filter paper separator were wound into a tight roll such that the Li formed the outer layer of the roll. The roll was then introduced into the can which contained two layers of the 5 mil thick separator at the bottom as an insulator. The can served as the negative terminal. The cell top consisted of a stainless steel plate with a Viton rubber gasket. The cell top was held tightly in place by threaded steel bolts leading to a bottom plate. Compression springs were used and adjusted such as to allow cell venting above a pressure of 120 psi. The positive lead connection was made through a Conax feedthrough attached to

the top of the steel plate. A reference electrode, consisting of a piece of Li foil attached to a nickel wire, was positioned on top of the cell package before sealing the cell. The reference electrode lead was also taken through the Conax fitting. Temperature measurements were made with a copper-constantan thermocouple junction placed either on the cell wall or at the center of the electrode package. In the latter case it was introduced into the cell package through the Conax fitting. It was electrically insulated by Teflon tape or Teflon shrink tube. A schematic of a fully sealed cell is shown in Figure 1.

1.2 Small Prismatic $Li/SOCl_2$ Cells

The prismatic $Li/SOCl_2$ cell comprised an electrode package assembled with alternating carbon and Li electrodes, each separated by a 5 mil fiber glass separator. A schematic of the electrode arrangement is shown in Figure 2. The package was introduced into a rectangular glass vial, 0.8 × 2.4 × 4.0 cm and the glass vial was tightly closed with rectangular coverplates in a manner similar to that in the C-cells. Except for the rectangular shape, the cell assembly resembles that of the C-cell shown in Figure 1. The electrode connections were made through the Conax fitting on the coverplate. A Li reference electrode was also placed in each cell.

1.3 Electrolyte Preparation

Experiments were carried out using $LiAlCl_4$ and $Li_2O/AlCl_3$ based electrolytes. Lithium tetrachloroaluminate, $LiAlCl_4$, was initially synthesized as the melt and purified by electrolysis. In this preparation, 1 mol of LiCl (Fisher L-121), which was predried in vacuum (10^{-3} torr) at 400°C for ∿4 hr, and 1 mol of $AlCl_3$ (Fluka, puriss) were melted together in a Pyrex container. The temperature was maintained at ∿190°C. The product was light yellow. The melt was purified by anodizing a piece of Pure Al (Ventron m5N ingot) against an Al wire cathode. The anodization was continued for ∿24 hr at 4 mA/cm^2 (40 mA). At the end of electrolysis, the melt was water white. The cooled melt was powdered with a mortar and pestle. The $LiAlCl_4/SOCl_2$ electrolyte of appropriate concentration was prepared by dissolving the salt in $SOCl_2$ (Eastman Kodak, Catalog No. 246) at room temperature.

The electrolyte based on $Li_2O/AlCl_3$ (9) was prepared by stirring Li_2O (ROC/RIC) with a solution of $AlCl_3$ in $SOCl_2$ at room temperature for more than 48 hr. To ensure complete conversion of $AlCl_3$ into ionic species, the Li_2O and $AlCl_3$ were originally mixed in the ratio 1.25:2. The reaction was followed by IR spectrometry (Fig. 3). At the end, the unreacted Li_2O was filtered off.

2. Forced Overdischarge Behavior of $Li/SOCl_2$ Cells

Forced overdischarge behavior of Li/SOCl2 cells was examined using C-size and small prismatic laboratory size cells. Individual electrode potential measurements were made to determine whether the cells were anode or cathode limited.

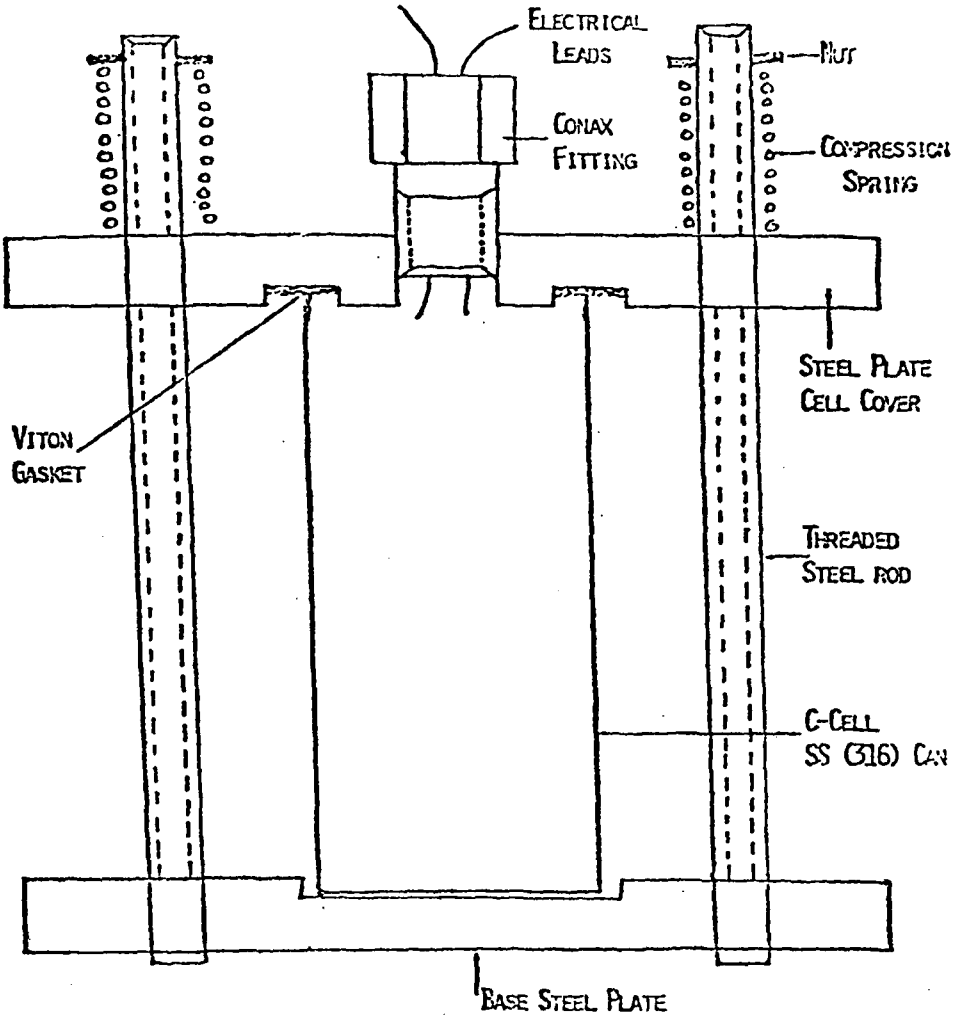

Fig. 1. A schematic view of an assembled $Li/SOCl_2$ C-cell.

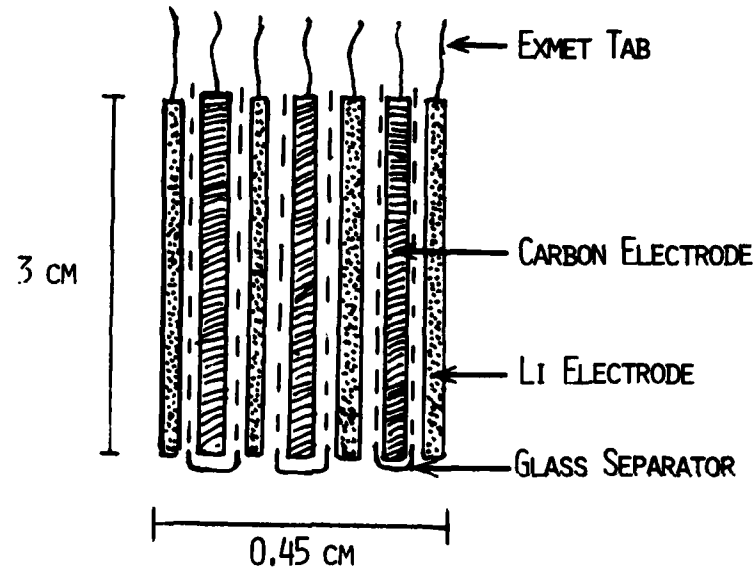

Fig. 2. A typical arrangement of electrodes in a prismatic cell.

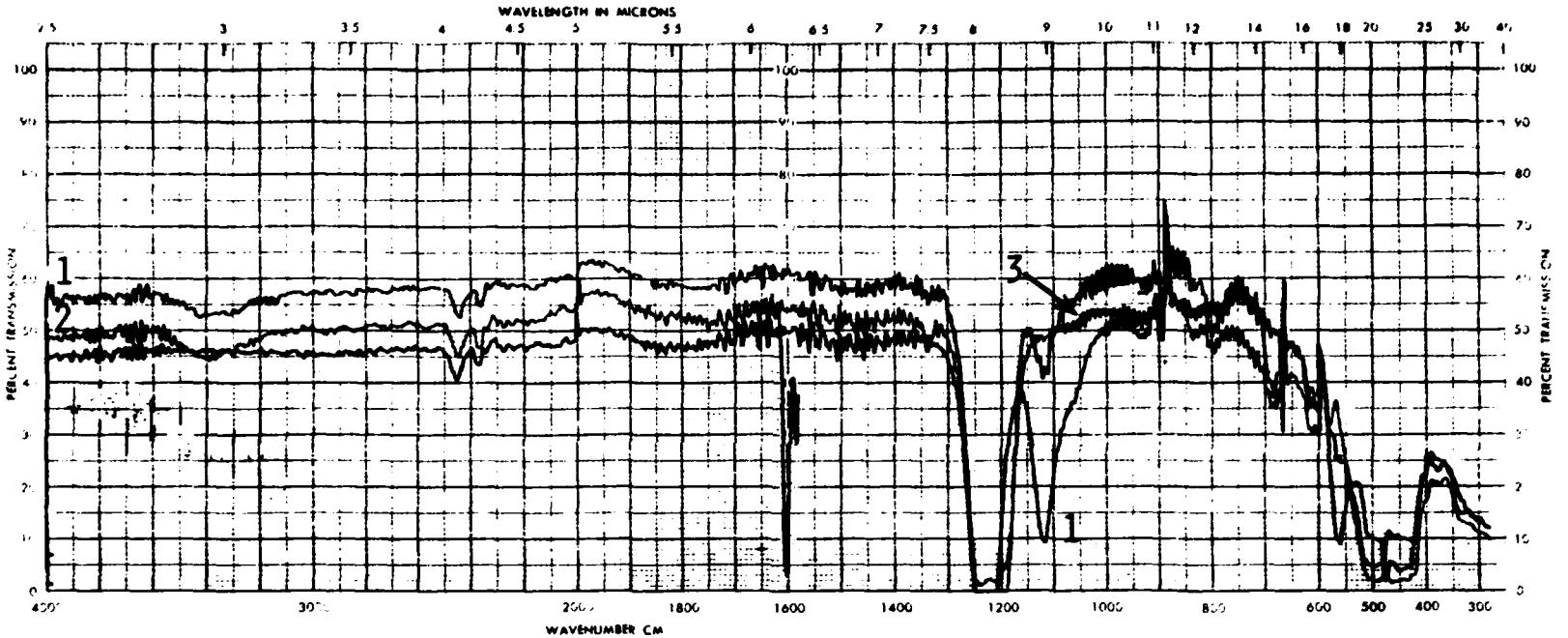

Fig. 3. Infrared spectrum of $SOCl_2$/1M $AlCl_3$ solution as a function of added Li_2O. (1) $SOCl_2$/1M $AlCl_3$ solution; (2) $SOCl_2$/1M $AlCl_3$ solution with 0.5M Li_2O stirred for >48 hr; (3) $SOCl_2$/1M $AlCl_3$ with 0.7M Li_2O stirred for >48 hr.

2.1 Results and Discussion

2.1.1 Cathode Limited Cells

In a cathode limited cell, the end of cell life is caused either by blockage of the carbon current collector by discharge products or by depletion of the $SOCl_2$ depolarizer. In either event, at the end of discharge the cathode potential changes towards and on overdischarge beyond the Li electrode potential. During forced overdischarge, Li is plated onto and into the carbon resulting in very small cell voltages, ~100 mV. Detailed parameters of the C-size cells tested, C-7 and C-2, are shown in Table 1.

Cell C-7 was built with the thermocouple junction placed inside the cell at the center of the electrode package. The junction was situated at about the half-way mark of the full length of the electrode package. The cell was discharged and overdischarged at 100 mA (0.66 mA/cm^2 of Li electrode area). Voltage/time plots of the cell potential and the potential of the Li-anode vs. a Li reference electrode and a plot of temperature vs. time are shown in Figure 4. The discharge capacity of 4.2 Ah to zero volt corresponds to a cathode utilization of 2.74 Ah/g carbon and suggests that the end of cell life occurred due to cathode blockage. The anode potential remained close to zero volt during most of the discharge. However, towards the end of discharge, as the cell voltage approached zero, there was a temporary polarization of the anode to more positive potentials. This temporary anode polarization probably reflects the inhomogeneous current distribution at the end of the useful carbon electrode life resulting in high local current densities at the Li electrode. The average current density corresponding to the 100 mA discharge was 0.66 mA/cm^2. The high overvoltages at both electrodes in this transition region also result in increased heat generation leading to a temperature peak. The cell was overdischarged also at 100 mA. They did not explode even after 10.5 Ah of overdischarge. The total charge passed through the cell now was 15 Ah. The amount of Li and $SOCl_2$ originally present was 8.18 Ah and 7.4 Ah respectively.

Cell C-2 was tested at 200 mA (1.32 mA/cm^2 of Li electrode area). Its behavior during discharge and overdischarge (Fig. 5) is similar to that of Cell C-7. The cell yielded 3.5 Ah capacity, equivalent to a cathode utilization of 2.23 Ah/g carbon. The cell did not explode even after 25 Ah of overdischarge. The results agree with our previous observation (7,8) that cathode limited cells can be forced overdischarge for long periods of time without apparent problems. Furthermore, the data shows that the internal cell temperature remains close to ambient both during discharge and overdischarge. It appears that during forced overdischarge of cathode limited cells, Li dendrites form on the carbon electrode and lead to internal short circuits which readily accommodate the major part of the current. This situation does not appear to constitute a specific hazard.

The small prismatic laboratory cells exhibited behavior similar to C-size cells. The discharge and overdischarge behavior of Cell P-4, shown

TABLE 1

CELL PARAMETERS FOR CATHODE-LIMITED $Li/SOCl_2$ C-CELLS

	Carbon Electrode			Lithium Electrode		Electrolyte $SOCl_2$/1.8M $LiAlCl_4$		
Cell No.	Average Thickness (mm)	Total Area (cm^2)	Amount of Carbon (g)	Total Area* (cm^2)	Amount of Li (Ah)	Vol. (ml)	Capacity (Ah)	Discharge Current (mA)
C-7	0.66	184	1.53	152	8.18	12	7.4	100
C-2	0.66	184	1.57	160	6.3	12	7.4	200

*Area corrected for Li not facing carbon cathode.

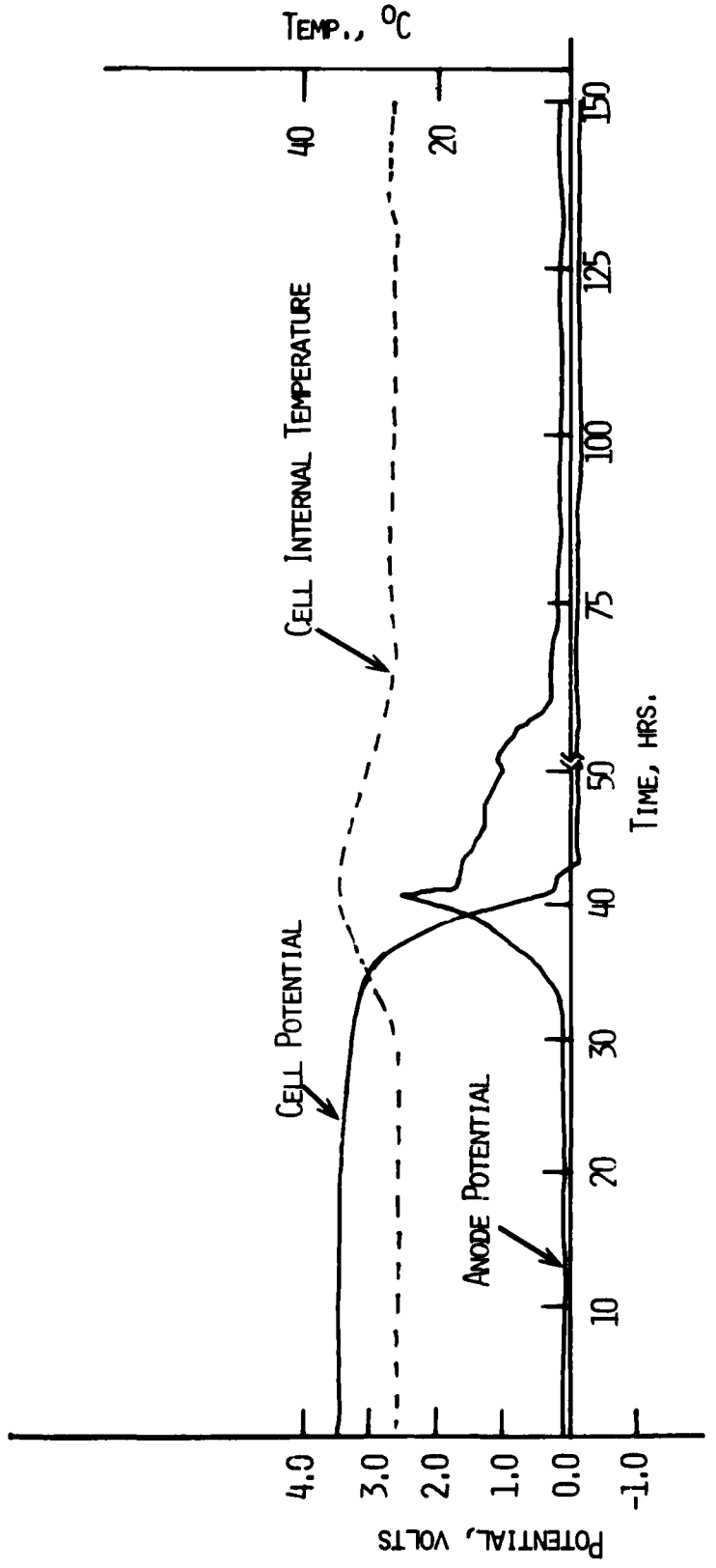

Fig. 4. Galvanostatic discharge and overdischarge curves for Li/$SOCl_2$ cell C-7. Current = 100 mA.

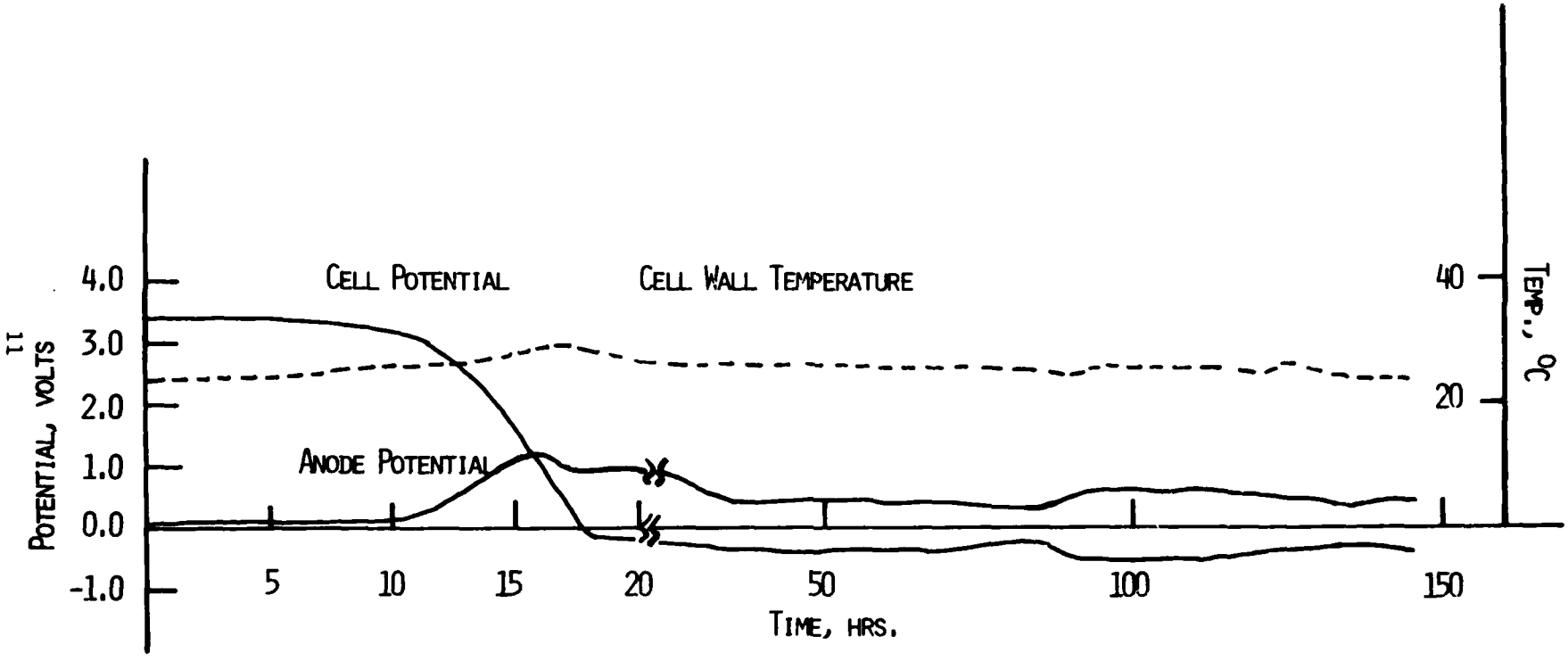

Fig. 5. Galvanostatic discharge and overdischarge curves for Li/$SOCl_2$ cell C-2. Current = 200 mA.

in Figure 6 is typical. The cell construction parameters are shown in Table 3. Cathode limitation of the cell is evidenced by the Li electrode potentials which remained close to zero during discharge and overdischarge. A temporary anode polarization at the end of discharge was observed as in the case of the C-cells. The discharge current of 36 mA corresponded to a current density of 1 mA/cm2 of the Li electrode area. The discharge capacity of 880 mAh was equivalent to a cathode utilization of 2.82 Ah/g carbon which is similar to that found in the C-cells. The cell was overdischarged for 120 hr (4.32 Ah) without explosion. The total charge passed would be equivalent to $>5e^-/SOCl_2$. The result indicates that short circuit occurs in forced overdischarge of prismatic $Li/SOCl_2$ cells as observed in spirally wound cells.

- Post-Test Examination of Cathode Limited Cells

Post-test examination revealed that in all cathode limited cells, inspite of the long periods of overdischarge, some Li remained on the anode. This and the low Li electrode polarization strongly support short circuiting due to Li dendrites. Thus, during overdischarge the majority of the current does not result in plating of Li onto the cathode.

The carbon cathodes in these cells have become very brittle and easily breakable. The electrode surface is covered, often non-uniformly, with discharge products, predominantly LiCl. Cathodes from cells which have been overdischarged for long periods of time have consistently shown extreme moisture sensitivity, often catching fire in contact with water. The handling and disposal of cathodes from overdischarged cathode limited cells requires special care. The fire hazard of the cathode may be due to the high surface area of Li plated onto it during overdischarge. It is also possible that the majority of the plated Li is present as an intercalate of carbon (10) and this form may be more sensitive (less easily passivated) than Li foil itself.

2.1.2 Anode Limited Cells

In anode limited cells, the end of cell life is determined by Li electrode polarization. This can be either due to Li depletion or due to loss of contact between Li and the Exmet grid. The parameters for various cells tested are given in Table 2.

Cell C-1 was discharged and overdischarged at 100 mA (0.64 mA/cm^2 of Li electrode area), Figure 7. The cell yielded a capacity of only 2.5 Ah, although the amount of Li originally present was 6.1 Ah. It appears that the Li electrode prematurely polarized due to loss of contact of Li with Exmet grid. The Li had been pressed onto the grid at a pressure less than 50 psi. It may be noted that towards the end of discharge the cell voltage showed fluctuations which were also reflected in the anode potentials. It appears that the voltage fluctuations are related to the breaking and making of contact of the Li foil with the anode Exmet grid. The cell was overdischarged also at 100 mA. The fluctuations of the anode potential continued during overdischarge reaching occasionally $\sim$8V vs. Li^+/Li. The cell exploded

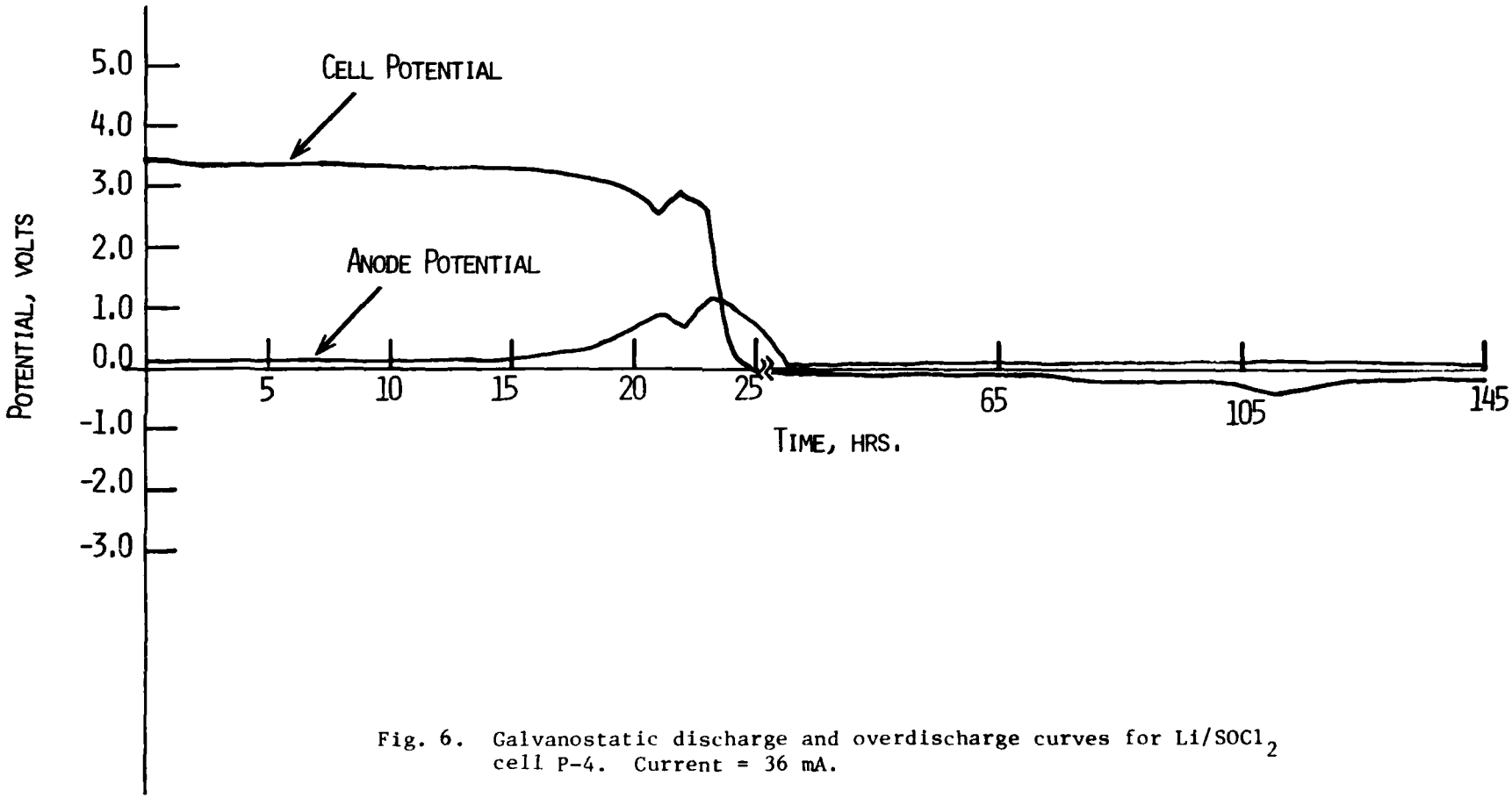

Fig. 6. Galvanostatic discharge and overdischarge curves for $Li/SOCl_2$ cell P-4. Current = 36 mA.

TABLE 2

CELL PARAMETERS FOR ANODE-LIMITED $Li/SOCl_2$ C-CELLS

	Carbon Electrode			Lithium Electrode		Electrolyte $SOCl_2$/1.8M $LiAlCl_4$		
Cell No.	Average Thickness (mm)	Total Area (cm^2)	Amount of Carbon (g)	Total Area* (cm^2)	Amount of Li (Ah)	Vol. (ml)	Capacity (Ah)	Discharge Current (mA)
C-1	0.72	184	1.60	156	6.1	12	7.4	100
C-3	0.66	189	1.60	156	6.1	12	7.4	200
C-6	0.67	179	1.58	161	6.3	12	7.4	100

*Area corrected for Li not facing carbon cathode.

TABLE 3

CELL PARAMETERS FOR SMALL PRISMATIC CELLS

Cell No.	Cell Configuration	Carbon Electrode: Average Thickness (mm)	Carbon Electrode: Total Area Facing Li (cm^2)	Carbon Electrode: Approximate Amount of Carbon (mg)	Lithium Electrode: Area (cm^2)	Lithium Electrode: Amount (Ah)	Electrolyte $LiAlCl_4/SOCl_2$: Con. $LiAlCl_4$ (M)	Electrolyte $LiAlCl_4/SOCl_2$: Vol. (ml)	Capacity (Ah)	Discharge Current (mA)
P-4	Li/C/Li/C/Li/C/Li (cathode limited)	0.61	36	320	36	2.01	1.8	3	1.84	36
P-5	C/Li/C/Li/C (anode limited)	0.61	24	320	24	0.70	1.8	3	1.84	24
P-8	C/Li/C/Li/C (anode limited)	0.68	24	420	24	0.70	1.8	2	1.23	24
P-15	Cathode limited	0.70	36	450	36	2.01	1.00*	3	1.84	36

*$Li_2O/AlCl_3$ based electrolyte.

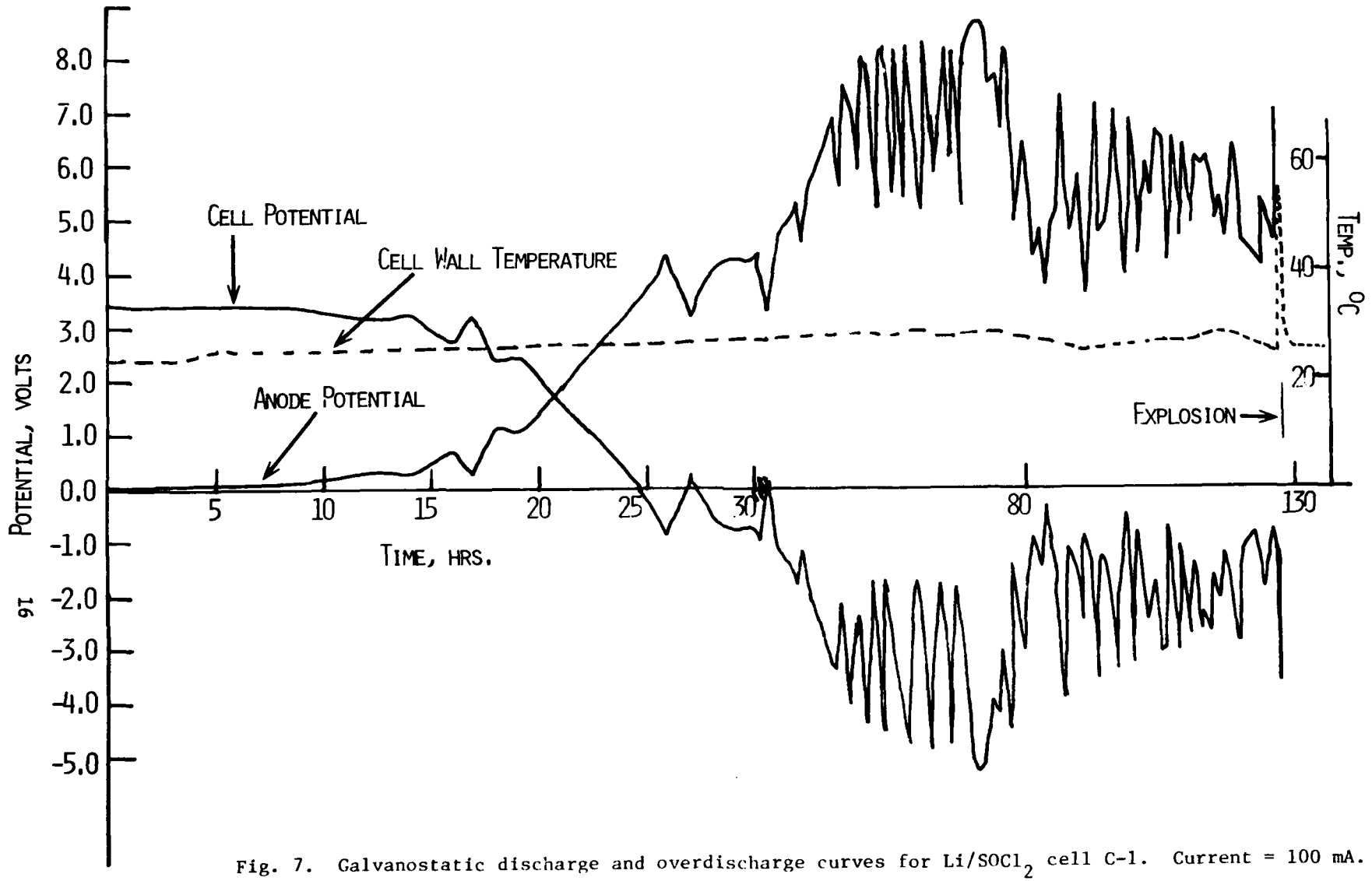

Fig. 7. Galvanostatic discharge and overdischarge curves for $Li/SOCl_2$ cell C-1. Current = 100 mA.

at the 126th hr of test. The temperature, measured here at the external cell wall, increased sharply. There was no gradual increase in temperature prior to the explosion. In fact the temperature decreased for several hours prior to the explosion as a result of reduced cell polarization. The cell vent opened as a result of the explosion. We found fused metal at the mouth of the nickel can where this venting occurred indicating that the materials which escaped during the venting were extremely hot. Post-test examination revealed that the explosion damage was almost exclusively confined to the anode. Large areas of the anode grid were missing whereas the cathode remained intact. The explosion occurred at the part of the cell opposite to the location of the thermocouple. This accounts probably for the relatively low peak temperature measured. The local temperatures in the cell must have been much higher than this. The general character of this explosion closely resembled our earlier observations (7,8). However, this was the first time we encountered an explosion upon overdischarge of a C-cell at 100 mA. All previous explosions occurred at 50 mA.

In general, forced overdischarge explosions of anode limited cells appeared to occur at random. The test results of Cells C-3 and C-4 are indicative of this. The construction parameters for these cells are also given in Table 2.

Cell C-3 was discharged at 200 mA (1.26 mA/cm^2 of Li electrode area). The cell capacity to zero volt was 3.5 Ah which was equivalent to a cathode capacity of 2.18 Ah/g carbon. As in Cell C-1, the anode potential showed fluctuations during the end of discharge and during overdischarge. Although the cell was overdischarged for 122.5 hr (24.5 Ah) it did not explode.

Cell C-6 was discharged and overdischarged at 100 mA (0.62 mA/cm^2 of Li electrode area). In this cell temperature was monitored with an internal thermocouple as in the cathode limited cell discussed earlier. During the discharge the temperature remained close to that of the ambient. As the cell potential approached zero volt at the end of discharge the temperature gradually increased to $\sim$36°C and during overdischarge it stabilized at 30°C. The average internal temperature during overdischarge is slightly higher than what was observed in the cathode limited cell tested earlier. The higher temperature may reflect the different types of reaction which occur in anode limited cells when the anode potentials are at values greater than 4V.

Forced overdischarge behavior of anode limited prismatic cells, P-5 and P-8, were also tested. The parameters for these cells are shown in Table 3. Cell P-5, depicted in Figure 8, gave a capacity of 470 mAh. The discharge was limited by Li depletion. The cathode utilization was equivalent to 2.2 Ah/g carbon. The overdischarge proceeded with considerable fluctuations in anode potentials, reaching values as high as 9.0V. The behavior is similar to that found in C-cells. The cell did not explode although it was overdischarged for 70 hr (1.68 Ah).

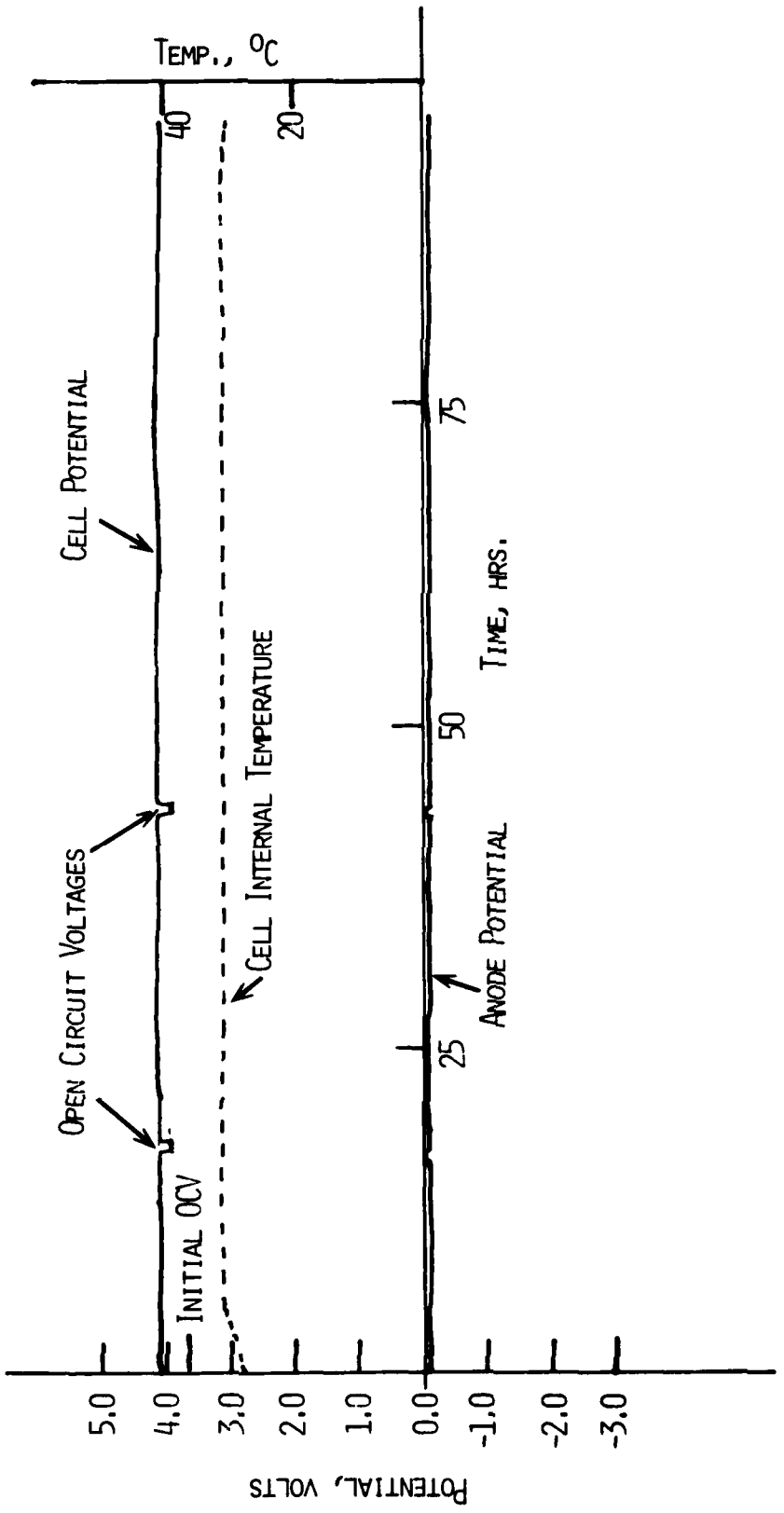

Fig. 8. Galvanostatic "charging" curve for Li/$SOCl_2$ cell C-10. Current = 100 mA.

In Cell P-8, an amount of electrolyte lower than present in Cell P-5 was used. The forced overdischarge behavior was similar to that of Cell P-5. The cell did not explode even after overdischarge for 65 hr (1.6 Ah).

Although none of the anode limited prismatic cells tested exploded, it cannot be unequivocally concluded that these cells are safe. It is possible that the special conditions required to bring about an explosion may not have been present in our cells.

2.2 Conclusions

On the basis of the present results and that of our previous studies (7,8) it may be concluded that the anode limited condition of $Li/SOCl_2$ cells is potentially hazardous. These cells may explode during forced overdischarge.

Cathode limited cells, on the other hand, appear to be safe during forced overdischarge. These cells could be overdischarged for long periods of time without apparent hazard.

3. Behavior of $Li/SOCl_2$ Cells on "Charging"*

It has been alleged that $Li/SOCl_2$ cells explode on charging, although no clear documentation is found in the literature. We have studied the charging behavior of five $Li/SOCl_2$ cells. Four of these were C-size cells, C-10, C-12, C-13 and C-14, and their charging behavior was examined as a function of the state of discharge of the cell as well as the concentration of $LiAlCl_4$. The fifth one was a small prismatic cell, P-15 and the electrolyte in this cell was that based on $Li_2O/AlCl_3$.

3.1 Results

The parameters of the C-cells are shown in Table 4 and those of the prismatic cell are given in Table 3.

Cell C-10 was charged at 100 mA (0.60 mA/cm^2 of Li electrode area). The results are shown in Figure 8. The internal temperature, the cell potential and the potential of the anode vs. a Li reference electrode were measured. The charge proceeded with the cell potential at 4.1V and the anode potential at -0.1V. The cell was charged for 97 hr (9.7 Ah) without change in cell polarization. The total charge passed exceeded both the Li and the $SOCl_2$ which were originally present in the cell in amounts of 7.4 and 7.37 Ah respectively. Open-circuit-voltage measurements after passing charges of 1.8 Ah and 4.4 Ah gave a value of 3.95V as opposed to the initial value of 3.65V. The cell internal temperature gradually increased to 31°C in a period of 4 hr and remained at this value during the entire test.

*The term charging implies that a positive current is applied to the carbon electrode.

TABLE 4

CELL PARAMETERS FOR Li/$SOCl_2$ CELLS TESTED FOR CHARGING BEHAVIOR

Cell No.	Carbon Electrode			Lithium Electrode		Electrolyte $SOCl_2$/1.8M $LiAlCl_4$		
	Average Thickness (mm)	Total Area (cm^2)	Amount of Carbon (g)	Total Area (cm^2)	Amount of Li (Ah)	Vol. (ml)	Capacity (Ah)	Discharge Current (mA)
C-10	0.68	194	1.65	166	7.4	12	7.4	100
C-12	0.64	184	1.74	166	7.4	12	7.4	100
C-13	0.71	184	1.78	151	6.72	12	7.5*	100
C-14	0.69	184	1.86	166	7.4	12	7.5	100

*0.5M $SOCl_2$/$LiAlCl_4$ electrolyte.

After charging, the cell was discharged again at 100 mA. The discharge is shown in Figure 9. The cell yielded a capacity of 3.95 Ah. Note that the initial 0.15 Ah of discharge occurred between 3.8 and 3.6V. This might correspond to the discharge of an accumulated product of charge. The cell was overdischarged also at 100 mA for 3 Ah and showed cathode limitation.

The important point to note is that the cell exhibited safe behavior during charge and the subsequent discharge and overdischarge.

Cell C-12 was initially discharged at 100 mA (Fig. 10) for 2 Ah. The OCV at this stage was measured to be 365V. The cell was then charged for 5.3 Ah also at 100 mA. The charging cell voltage remained at 3.7V for 35 hr (3.5 A) and then at 3.8V for the rest of the charging. The discharge of C-12 after the charge gave an additional capacity of 2.5 Ah, making the total discharge capacity of the cell to be 4.5 Ah, identical to that from a fresh cell. C-12 was overdischarged for 2 Ah, then charged for 2 Ah. Discharging the cell after this last charge did not result in any capacity.

The effect of concentration of $LiAlCl_4$ on charging was investigated in Cell C-13 and C-14 utilizing 0.5M $LiAlCl_4/SOCl_2$ solutions. Cell C-13 was charged at 100 mA for 92 hr (9.2 Ah), Figure 11. It was then discharged, again at 100 mA. The cell capacity to zero volt was 2.3 Ah. The discharge capacity was lower than what was obtained in C-10, tested similarly.

Cell C-14 also utilized 0.5M $LiAlCl_4/SOCl_2$ electrolyte. The cell was tested at 100 mA and the results are shown in Figure 12. After 70 hr of charging, the cell was discharged yielding a capacity of 2.85 Ah. The voltage profiles of C-13 and C-14 are similar to that found in Cell C-10.

The charging behavior of $Li/SOCl_2$ cells utilizing $Li_2O/AlCl_3$ based electrolyte was briefly investigated in Cell P-15. This was a small prismatic cell and its parameters are given in Table 3. The behavior during charging and subsequent discharging, shown in Figure 13 are similar to that of cells utilizing $LiAlCl_4/SOCl_2$ electrolyte.

3.2 Summary and Discussion

The charging behavior of $Li/SOCl_2$ cells was studied using C-size cells. These cells could be "charged" for long periods of time without explosions. In fresh C-cells at 100 mA current, the "charging" proceeded at 4.1V. The cell voltage remained steady at this value even after passing an amount of charge exceeding $2e^-/SOCl_2$. When the cells were discharged after "charging" they yielded capacities comparable to that from fresh cells. These observations suggest that "charging" of $Li/SOCl_2$ cells involve regenerative cell process, probably comprising both redox and chemical reactions.

The charging behavior resembled the discharge characteristics of $Li/SOCl_2$ cells without Li on the anode Exmet (8).

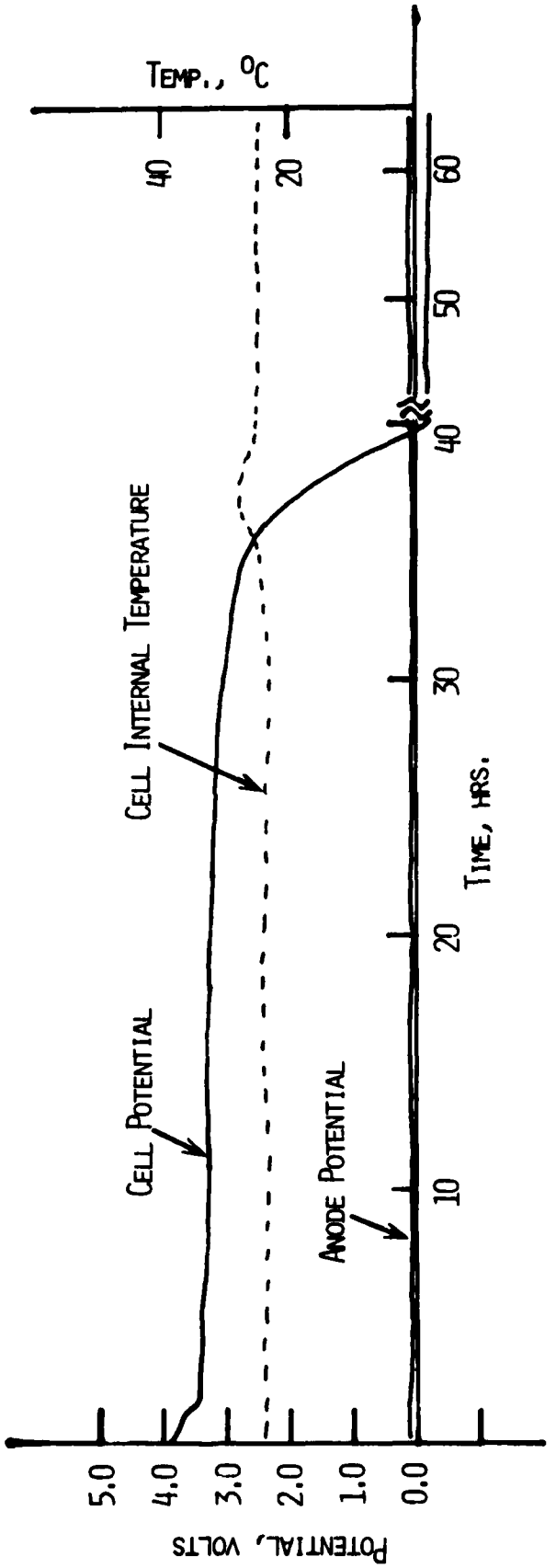

Fig. 9. Galvanostatic discharge and overdischarge curves for Li/$SOCl_2$ cell C-10 after the "charging" shown in Fig. 7. Current = 100 mA.

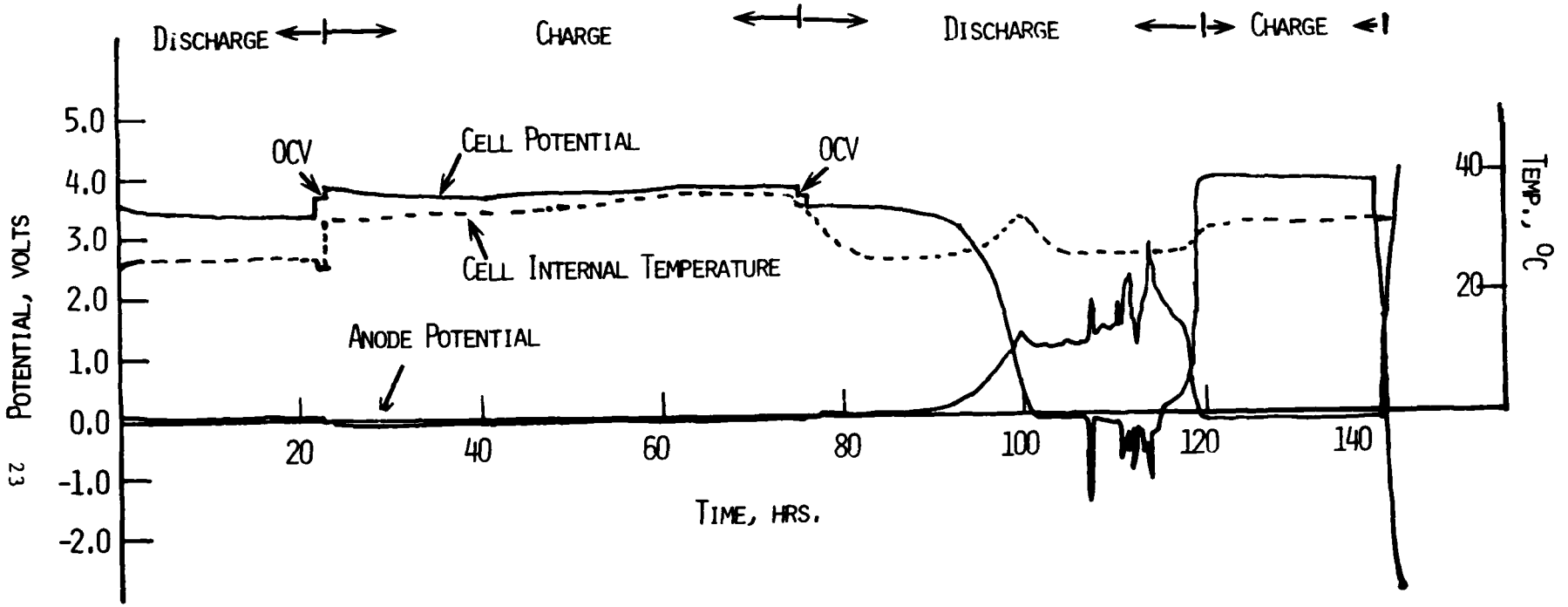

Fig. 10. Galvanostatic discharge and "charge" curves for $Li/SOCl_2$ cell C-12. Current - 100 mA.

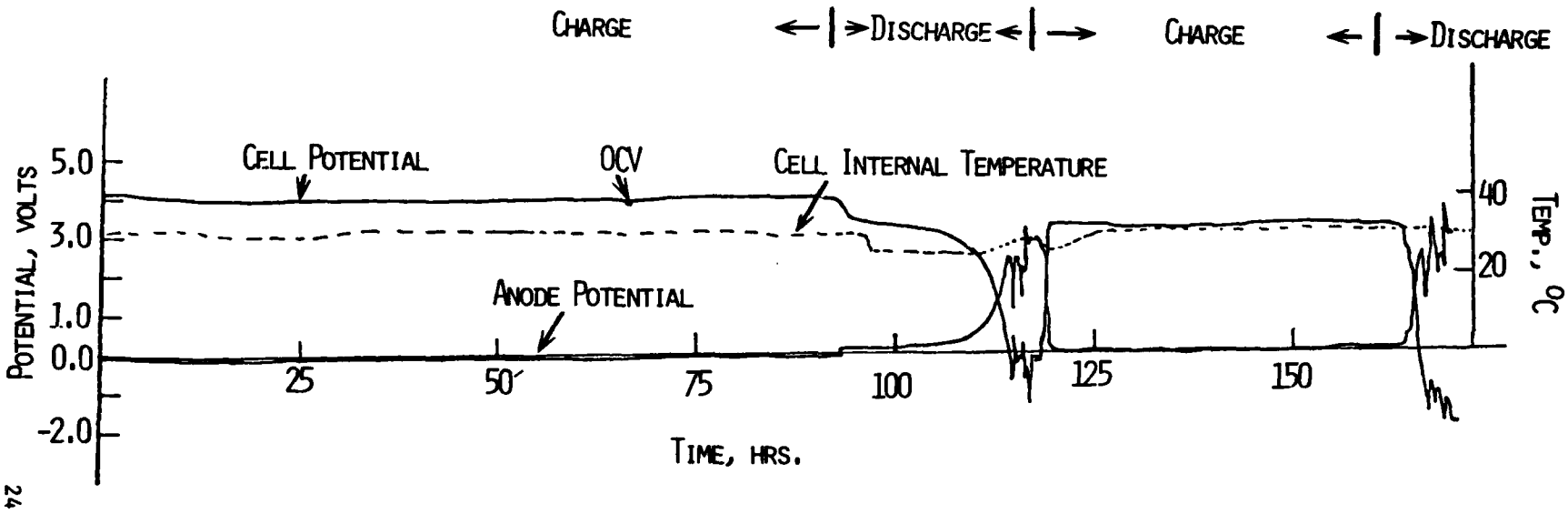

Fig. 11. Galvanostatic "charge" and discharge curves for cell C-13. Current = 100 mA.

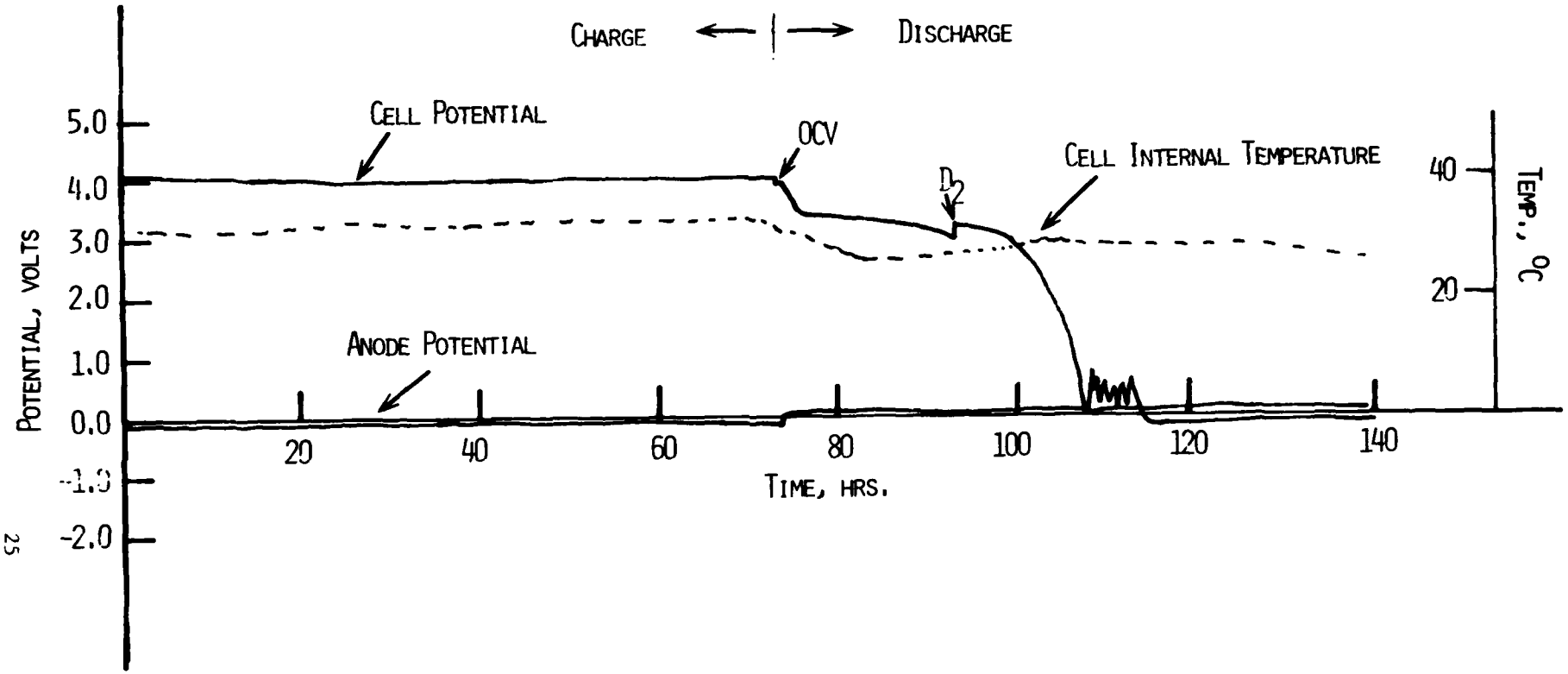

Fig. 12. Galvanostatic "charge" and discharge curves for $Li/SOCl_2$ cell C-14. Current = 100 mA. At D_2 current reduced to 50 mA.

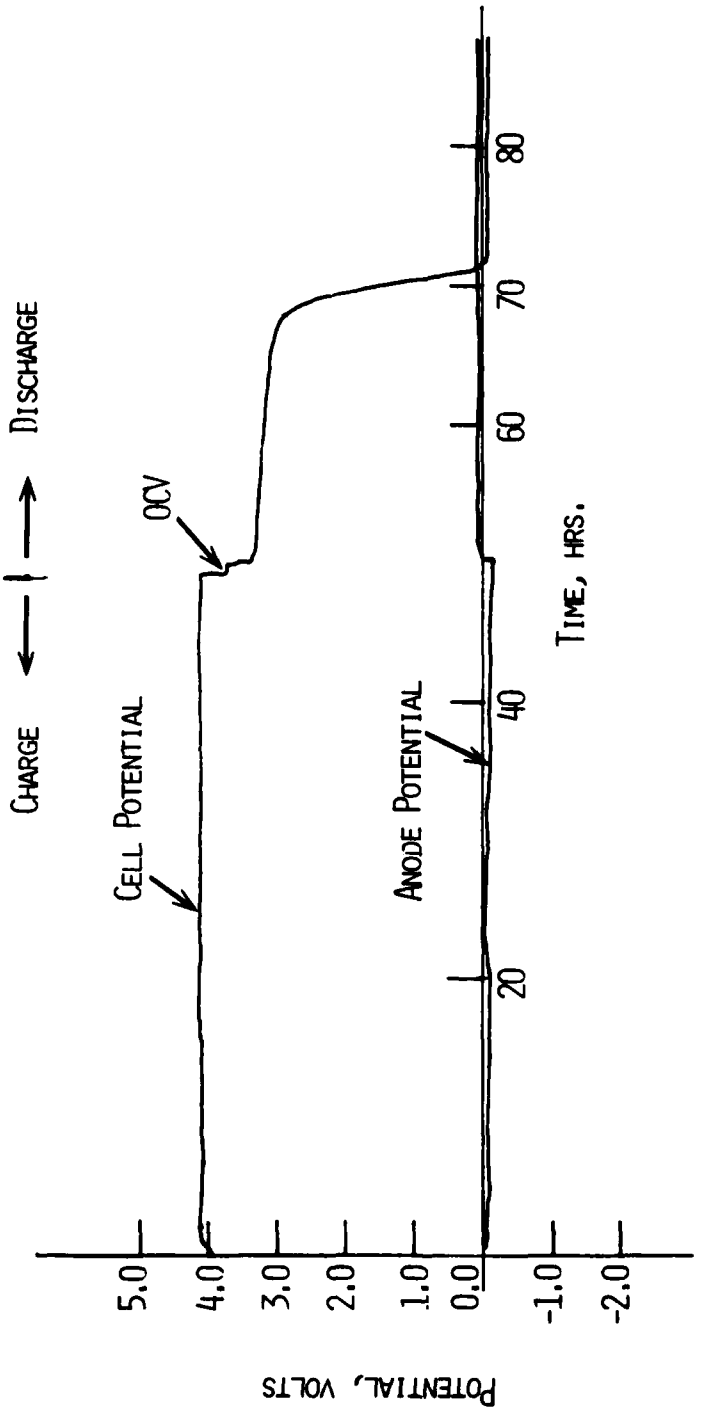

Fig. 13. Galvanostatic "charge" and discharge curves for Li/$SOCl_2$ cell P-15. Current = 36 mA.

The "charging" of a partially discharged cell proceeded at lower potentials, i.e., ~3.8V when the test current was 100 mA. This cell also did not exhibit a change in cell polarization even after long periods of "charging". Moreover, it was possible to discharge the cell after the "charging" and the total discharge capacity was identical to that from fresh cells. A possible reason for lower "charging" potentials in partially discharged cells is the "activation" of the carbon cathode so that the same regenerative reactions occurring in fresh cells occur at lower voltages. However, a different set of reactions cannot be ruled out (see later for analytical data).

The charging behavior of cells utilizing 0.5M $LiAlCl_4/SOCl_2$ solutions was identical to those utilizing 1.8M $LiAlCl_4/SOCl_2$ solutions. However, the discharge capacities after the "charging" was lower in cells with the lower salt concentration. It is interesting to note that both types of cells were built for cathode limitation. But one of these cells utilizing lower salt concentration showed anode limitation. The latter behavior might be related to the "charging" prior to the discharge. The "charging" probably affects the Li anode more when the salt concentration is lower.

The behavior of a cell utilizing $Li_2O/AlCl_3$ based electrolyte was similar to those utilizing $LiAlCl_4$, both during charging and subsequent discharging.

All the cells tested exhibited safe behavior during the charge and the subsequent discharge and overdischarge.

III. ANALYTICAL STUDIES

Ultimate solutions to the explosion hazards in $Li/SOCl_2$ cells require a detailed understanding of the chemical and electrochemical reactions which occur under conditions of operation where explosions are encountered. Electrochemical oxidation reactions involving $SOCl_2$ or other materials present in the cells become of considerable importance during forced overdischarge of anode limited cells and during application of a positive current to the carbon electrode (charging).

1. Electrolysis of $SOCl_2/LiAlCl_4$ Solutions

1.1 Experimental Procedures

Constant current electrolysis of $SOCl_2/LiAlCl_4$ was accomplished in a two compartment pyrex glass cell with a fine porosity (15 μ pore) glass frit separator having ∿2 cm^2 area. The cell was also provided with ports for gas and liquid sampling.

Typically, the cathode consisted of a stack of 3 Teflon bonded carbon electrodes, each having ∿3 cm^2 and 0.7 mm thickness. The anode was fabricated from a thrice-folded piece of expanded nickel metal (5Ni5-5/0, Exmet Corp.) with about 10 cm^2 useful area. Electrical leads were made by means of Ni wire. The anode compartment contained about 6.5 ml of $SOCl_2$/1.8M $LiAlCl_4$ electrolyte and the cathode compartment 1.5 ml of the same solution. The cell exhibited high impedances (∿500 Ω) and the electrolysis was accomplished at small currents between 2 and 5 mA. After various times of electrolysis, samples were withdrawn from the anode and cathode compartments for infrared spectral analyses.* The gases from anode compartment were also analyzed by IR spectrometry using a gas cell fitted KBr or NaCl windows.

1.2 Results and Discussion

Figure 14 shows plots of cell voltage and of anode potential vs. a Li reference electrode (placed in the cathode compartment) for one of the experiments. The anode potential was ∿4.5V vs. Li. The actually measured voltage was about 0.90V larger due to IR drop as evidenced by potential measurements

*All spectra were recorded on a Beckman Acculab 5 dual beam Spectrometer. The instrument covers the range from 4000 cm^{-1} to 375 cm^{-1}. All the liquid spectra were obtained with Beckman TAC cells. These have AgCl windows and can be sealed permanently. The cells were of 0.025 or 0.1 mm path lengths. Spectra of gases were obtained with a Beckman Universal Gas cell (10 cm path length) fitted with NaCl or KBr windows.

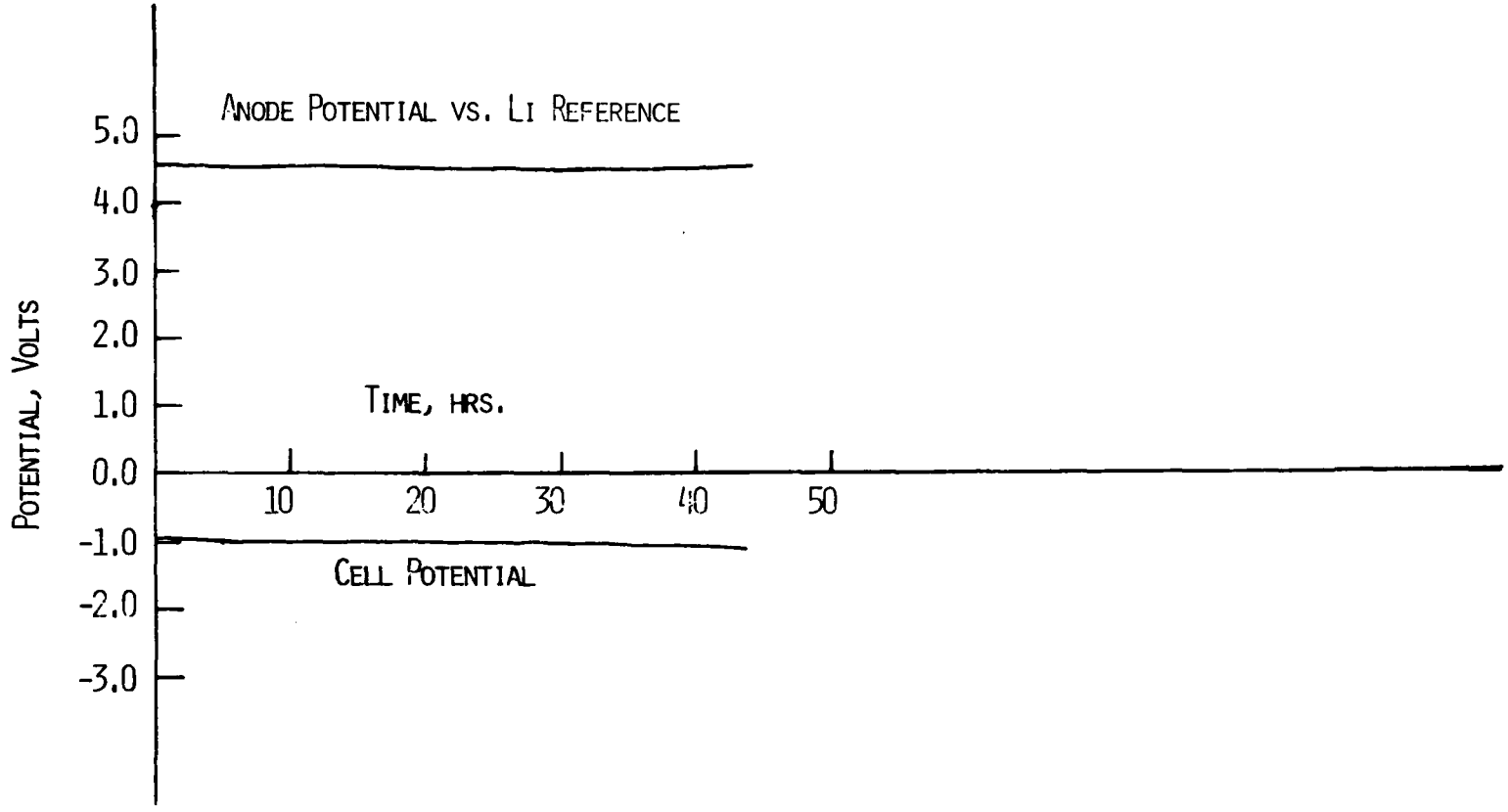

Fig. 14. Voltage/time plots for the electrolysis of $SOCl_2/LiAlCl_4$ (1.8M) solution in a two compartment cell with a 15 μ porosity glass-frit separator. Current, 2 mA. The Li reference electrode is in the cathode compartment. The curves are corrected for iR (~0.9V).

vs. a Li reference electrode placed directly in the anode compartment.* After a passage of 70 mAh, the anolyte and the catholyte were analyzed separately.

- Analysis of Oxidation Products

The IR spectrum of the anolyte is shown in Figure 15. Comparison of this spectrum with the spectrum of $SOCl_2/LiAlCl_4$ solutions shows the presence of two additional peaks at 1415 cm^{-1} and at 1110 cm^{-1}. The peak 1415 cm^{-1} was identified as due to SO_2Cl_2. Neat SO_2Cl_2 exhibits two strong peaks at 1205 cm^{-1} ($\nu 1$, S-O symmetric stretch) and 1415 cm^{-1} ($\nu 6$, S-O asymmetric stretch). In the spectrum of the anolyte, the SO_2Cl_2 peak at 1205 cm^{-1} is hidden inside the absorption peak of $SOCl_2$ at 1230 cm^{-1} ($\nu 1$, S-O symmetric stretch). Thus one of the oxidation products of $SOCl_2/LiAlCl_4$ solution is SO_2Cl_2.

The peak at 1110 cm^{-1} in the anolyte is most probably due tc the S-O symmetric stretching absorption of the complex, $SOCl^+AlCl_4^-$, since a similar absorption peak was found in $AlCl_3$ solutions of $SOCl_2$ or $SOCl_2/LiAlCl_4$ electrolyte (Fig. 16). Aluminum chloride itself does not have any absorption peaks above 800 cm-1. The existence of the complex in an $AlCl_3$ solution of $SOCl_2$ has been established previously (10) from conductivity studies. The present data confirms its existence. The occurrence of S-O symmetric stretching absorption in $SOCl^+AlCl_4^-$ at a lower frequency than that in $SOCl_2$ is consistent with the ionic structure.

Analysis of the gaseous products from the anode compartment was also carried out by IR spectrommetry using a gas cell fitted with KBr windows. Only SO_2Cl_2 was found as the IR-identifiable product in the gas phase.

- Analysis of Reduction Products

The infrared spectrum of the catholyte is shown in Figure 17. The only peak identifiable as due to a product was found at 1335 cm^{-1}. This peak was identified as due to SO_2. Sulfur dioxide exhibits two strong absorptions at 1150 cm^{-1} ($\nu 1$, S-O symmetric stretch) and at 1335 cm^{-1} ($\nu 3$, S-O asymmetric strech). The peak at 1150 cm^{-1} in the spectrum of SO_2 solutions in $SOCl_2$ appears as a shoulder to the $SOCl_2$ peak. It may be noted that LiCl, SO_2 and S were identified previously as reduction products of $SOCl_2/LiAlCl_4$ solutions (11).

*A Li reference electrode could not be placed in contact with the anolyte for long periods of time for reasons of corrosion and loss due to reaction with the solution.

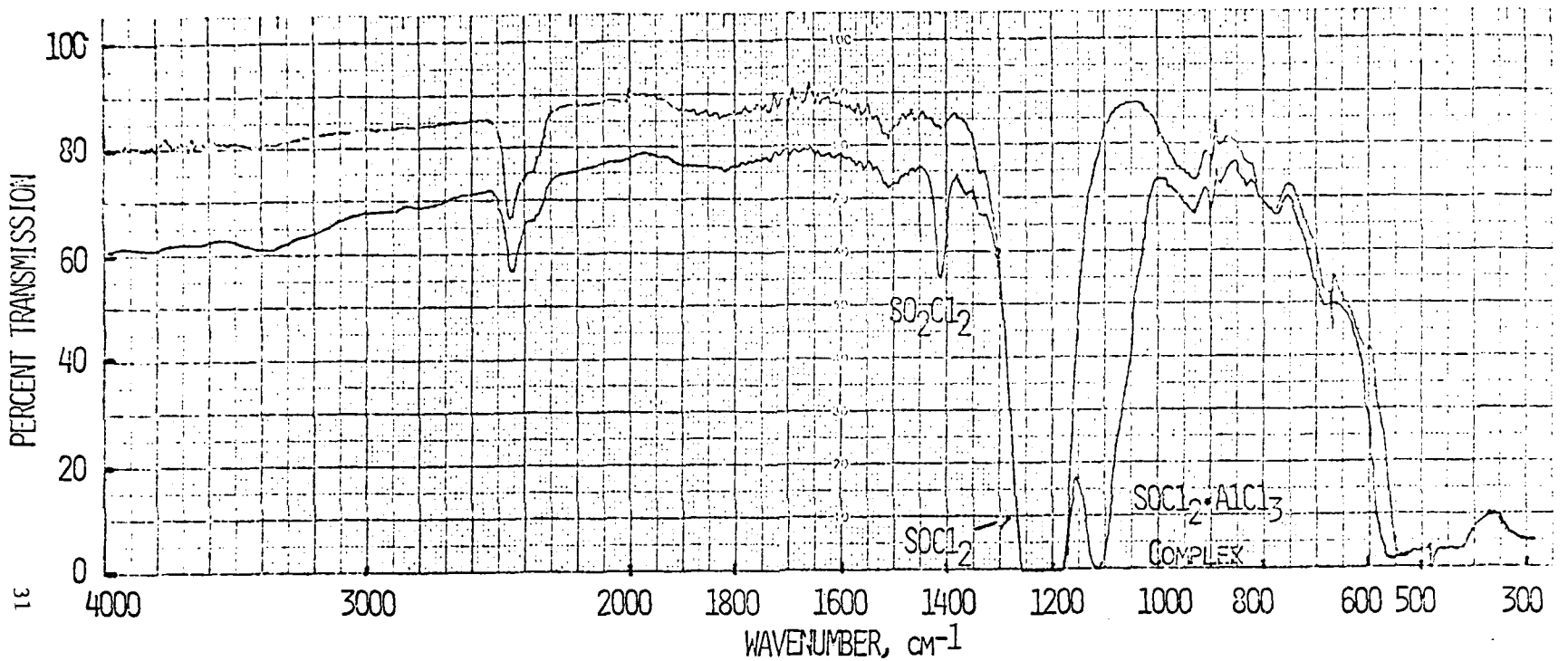

Fig. 15. Infrared spectrum of the anolyte (lower trace) after electrolysis of $SOCl_2$/$LiAlCl_4$ (1.8M) solution. The upper trace is the spectrum of the solution prior to electrolysis.

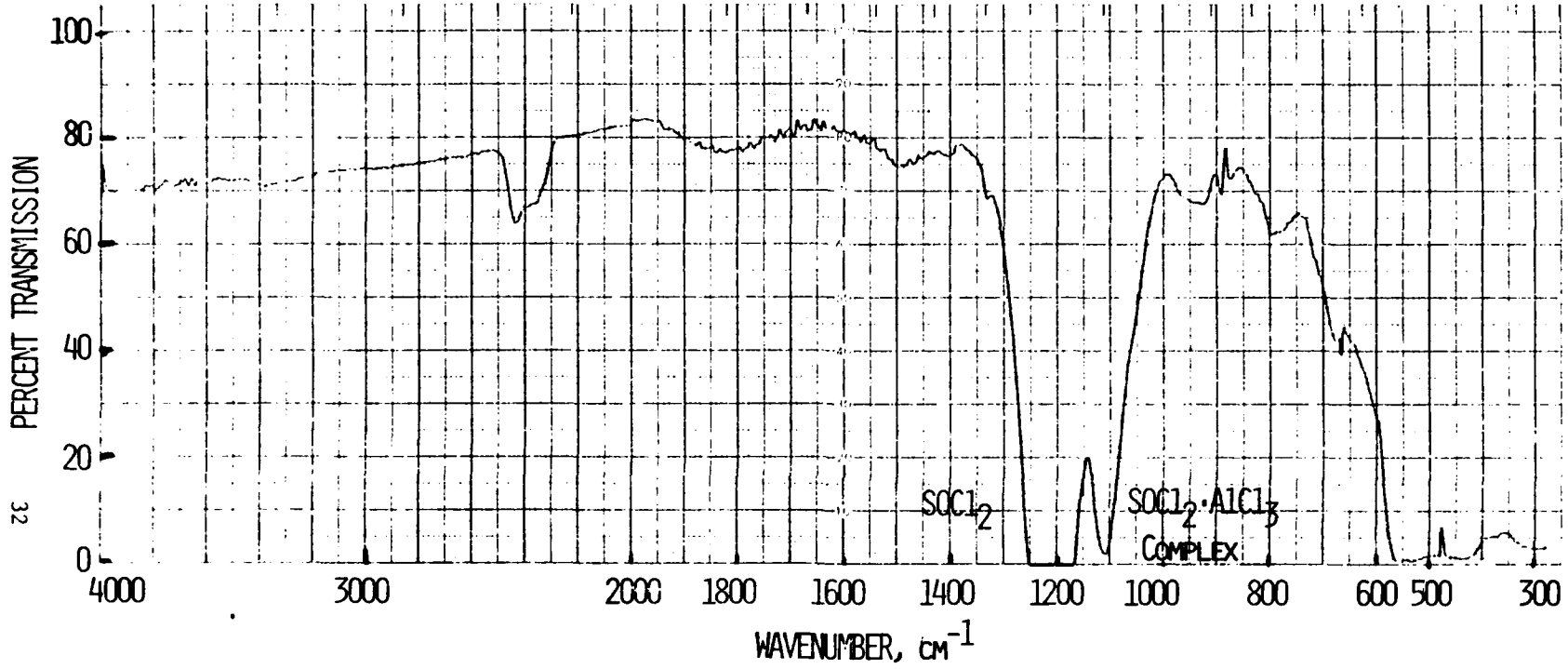

Fig. 16. Infrared spectrum of $SOCl_2/LiAlCl_4$ (1.8M) solution containing 1.8M $AlCl_3$.

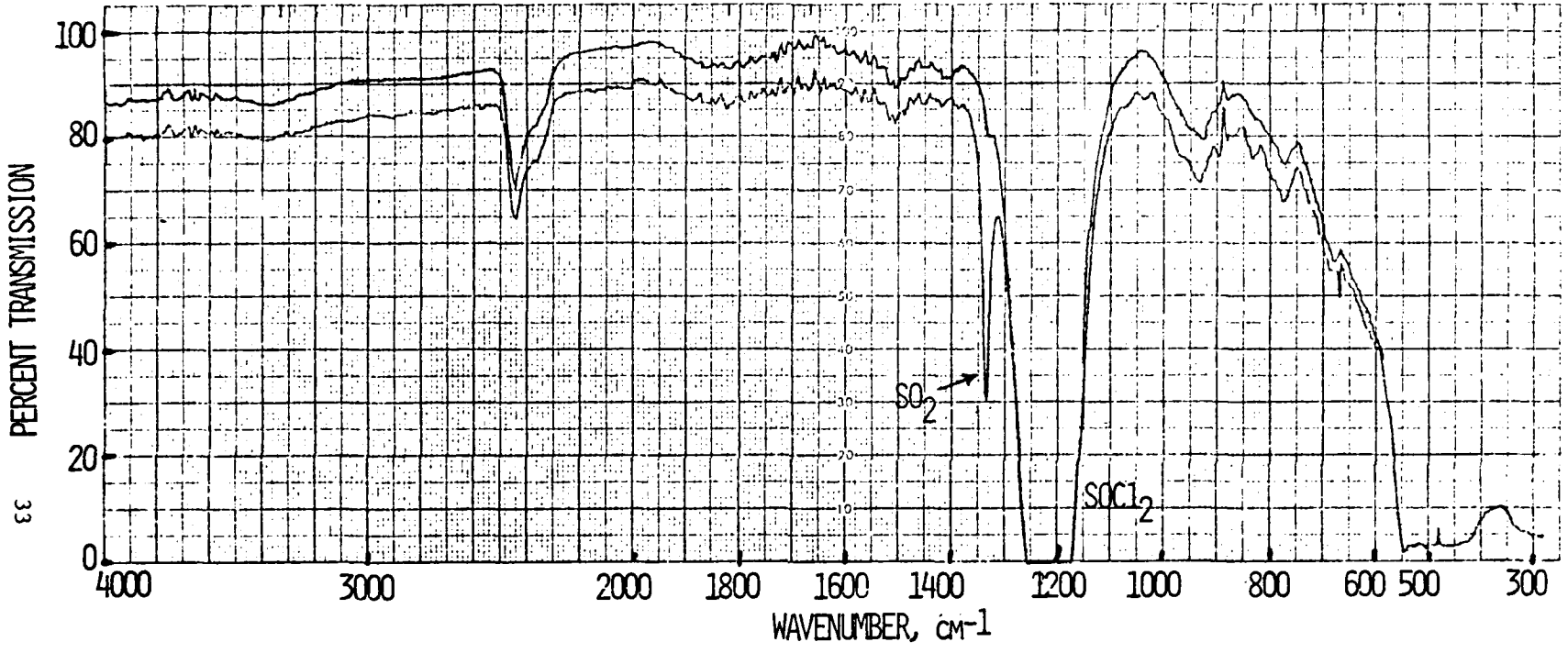

Fig. 17. Infrared spectrum of the catholyte (lower trace) after electrolytes of $SOCl_2$/ $LiAlCl_4$ (1.8M) solution. The upper trace is the spectrum of the solution prior to electrolysis.

2. Cyclic Voltammetry Studies of $SOCl_2/LiAlCl_4$ Solutions

2.1 Experimental Procedures

Cyclic voltammetric studies of $SOCl_2/LiAlCl_4$ (1.8M) solutions were carried out on nickel and carbon electrodes using a three electrode system. A 15 mil lithium ribbon pressed onto a nickel screen served as the reference electrode. The reference electrode was contained in a Luggin capillary and was placed close to the working electrode. The counter electrode consisted of a piece of Li ($\sim$1 cm^2) pressed onto a nickel screen. The Ni working electrode consisted of a 0.5 cm^2 nickel disc (10 mil thick), fitted in a Teflon holder. The carbon working electrode was a 0.10 cm^2 glassy carbon surface. The electrodes were arranged in a 25 ml capacity, three-necked flask. A volume measuring 7 ml of $SOCl_2$/1.8M $LiAlCl_4$ solution was used. The voltammetric scans were performed with an Amel Model 551 potentiostat in conjunction with their Model 566 function generator. The i-E curves were recorded on a Houston Omnigraphic Model 2000 X-Y Recorder or on a Bascom-Turner Series 8000 Recorder provided with microprocessor capabilities.

2.2 Results and Discussion

A typical cyclic voltammogram between 1V and 5V vs. Li^+/Li in $SOCl_2$/1.8M $LiAlCl_4$ on a glassy carbon electrode is shown in Figure 18. A similar voltammogram was obtained also on a Ni electrode and is shown in Figure 19. Although the overall features of the voltammogram are identical on both of the electrodes, the peaks appeared more sharp on the carbon electrode. Also the peaks on Ni are shifted to slightly lower potentials. Therefore most of the studies were performed using the glassy carbon electrode.

- Electrochemical Reduction of $SOCl_2/LiAlCl_4$ Solutions

A cyclic voltammogram in $SOCl_2$/1.8M $LiAlCl_4$ solution, obtained by scanning the carbon electrode cathodically from open circuit voltage (3.6V vs. Li^+/Li) is shown in Figure 20. The scan rate is 0.1V/sec. The onset of a reduction peak occurs at $\sim$3.0V with a peak at 2.6V. This reduction peak may be regarded as due to the reduction of $SOCl_2$ and is in good agreement with previous observations (7,8) on similar electrodes. Following the peak at 2.6V a very weak current peak appears at $\sim$1.8V. No other reduction peaks are observed up to 1.0V. Scanning the electrode below 1.0V showed only the current peak corresponding to the plating of Li on the carbon. The onset of current corresponding to this process occurs at $\sim$0.5V with a peak near 0.0V, Figure 21. This process, however, led to the damage of the carbon electrode surface and therefore in all studies the electrode was scanned only to 1.0V. The anodic scan from 1.0V showed a very weak current peak at 2.55V, and as shown previously (7), this peak may correspond to the oxidation of the material exhibiting the reduction peak at 1.80V. The reduction peak at 1.8V and oxidation peak at 2.55V may correspond to the reduction and oxidation of SO_2. Addition of SO_2 to the solution slightly enhanced the height of the

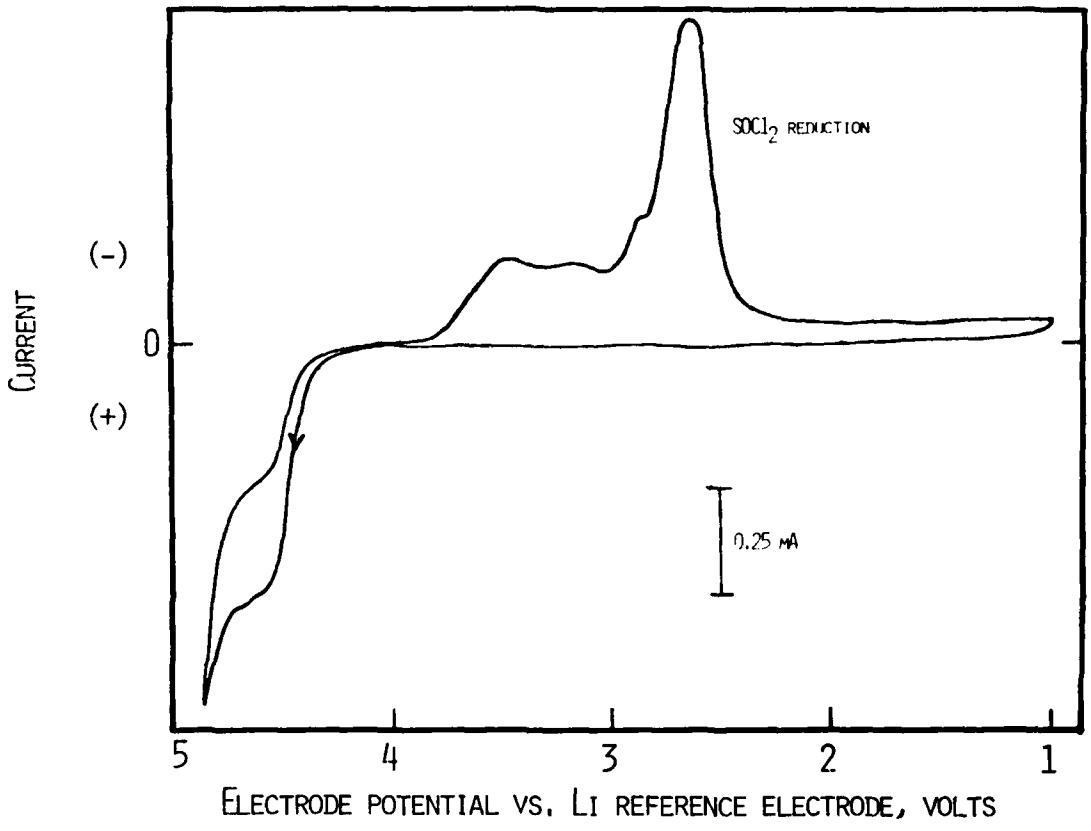

Fig. 18. Cyclic voltammograms of $SOCl_2$/1.8M $LiAlCl_4$ on glassy carbon electrode. Scan rate = 100 mV/sec. The electrode was scanned anodic first from 3.7V.

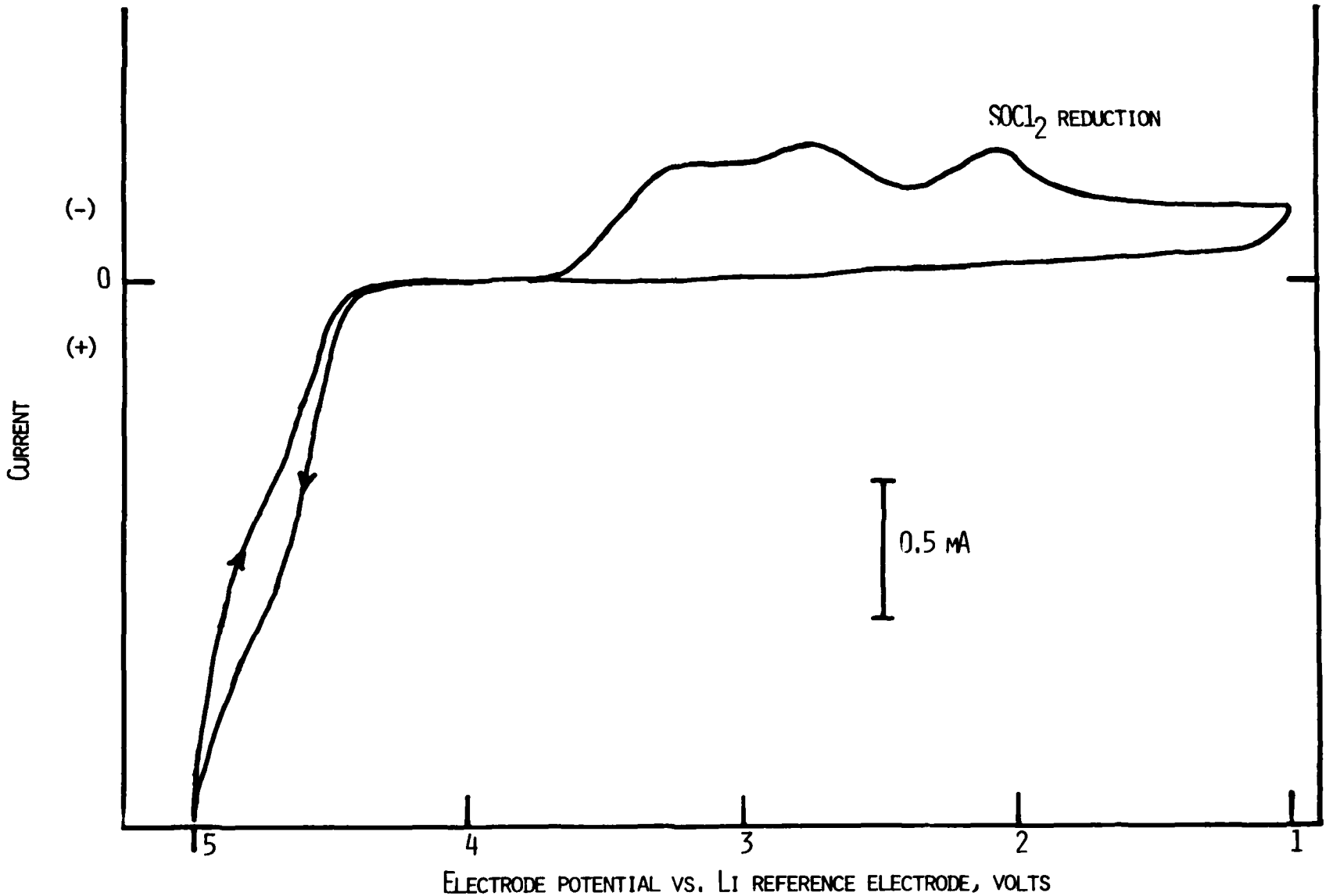

Fig. 19. Cyclic voltammogram of $SOCl_2$/1.8M $LiAlCl_4$ on Ni disc electrode. Scan rate = 50 mV/sec. Electrode was scanned anodic first from 3.7V.

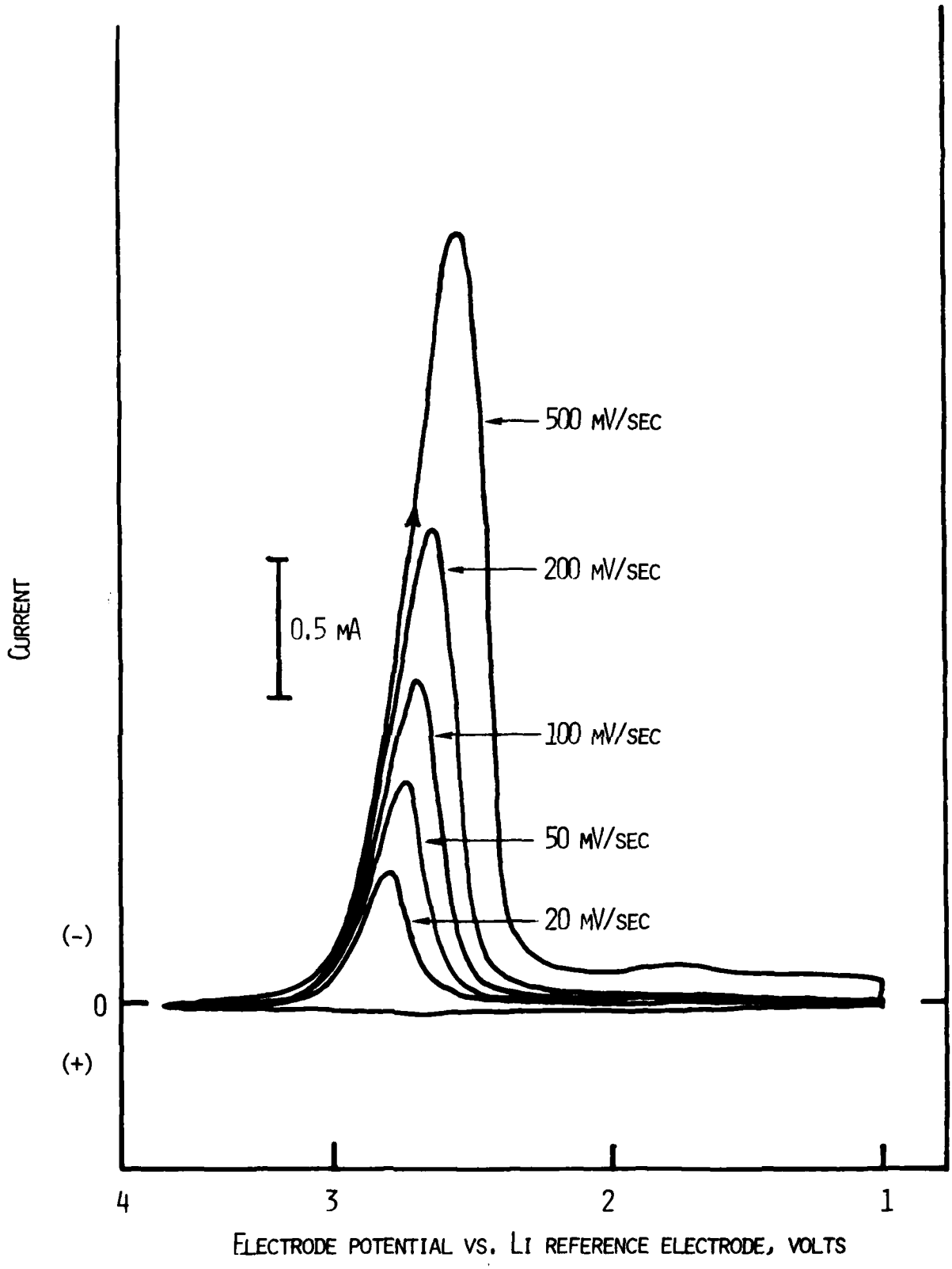

Fig. 20. Cyclic voltammogram of $SOCl_2$/1.8M $LiAlCl_4$ on glassy carbon electrode between 3.8V and 1V as a function of scan rate.

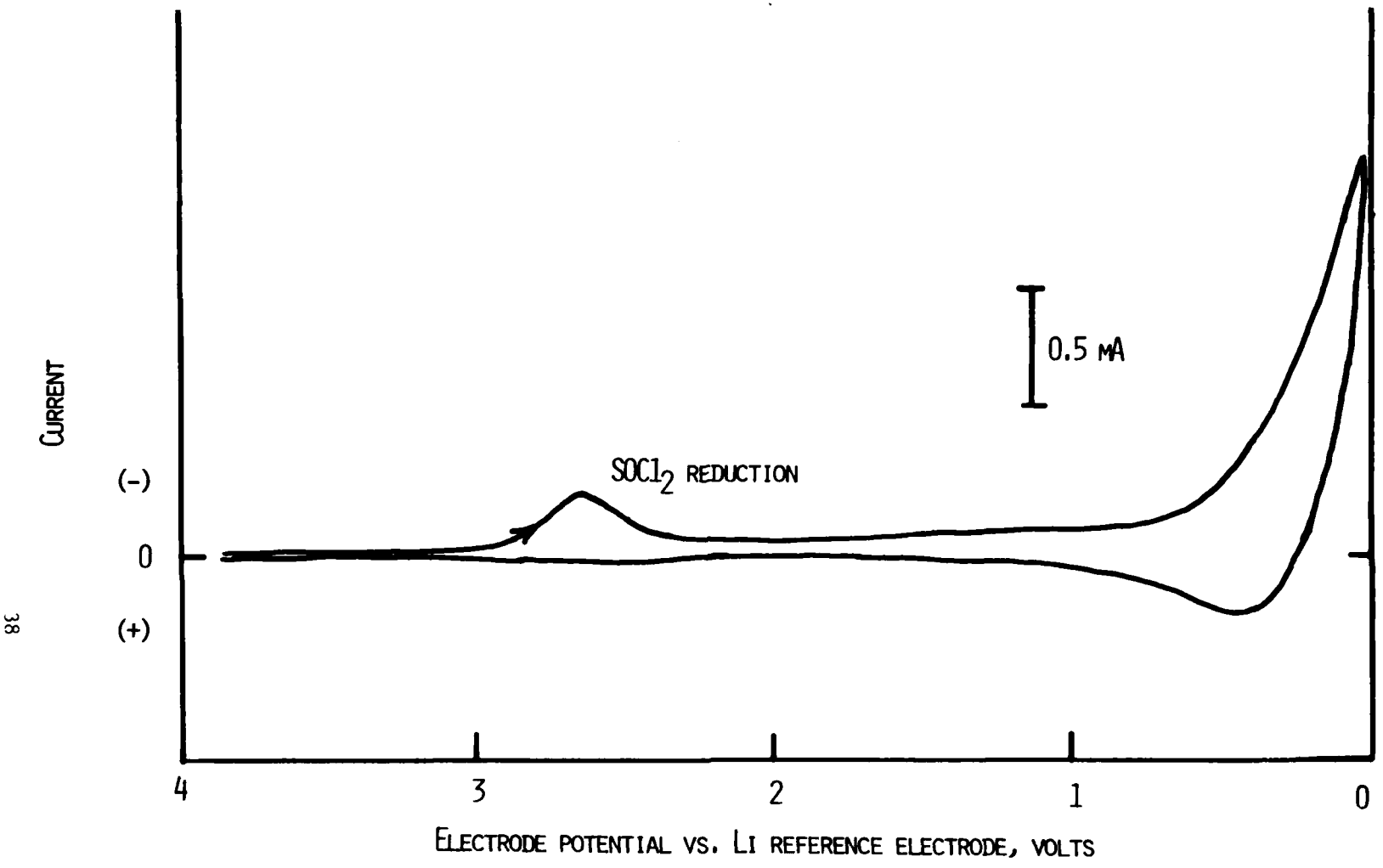

Fig. 21. Cyclic voltammogram of $SOCl_2$/1.8M $LiAlCl_4$ on glassy carbon electrode between 0.0 and 4V. Scan rate = 50 mV/sec.

reduction peak at 1.8V. Because of electrode passivation from the high current reduction process at 2.6V, addition of SO_2 did not result in a significant increase in the height of the peak at 1.8V. The severe passivation of the electrode, probably due to LiCl, was indicated by the observation that after an anodic sweep to 3.6V, second cathode sweep did not show any reduction peak at all. It was necessary to regenerate the electrode by holding it at an anodic potential of ∿4.6V before reproducible results could be obtained. The regeneration of the electrode was achieved in a second electrochemical cell so that products generated while holding the electrode at the anodic potential would not contaminate the test solution.

Various workers have suggested several reactions in the reduction of $SOCl_2/LiAlCl_4$ solutions. The reduction reaction supported by our earlier analytical work and now commonly accepted is

$$2SOCl_2 + 4Li \rightarrow 4LiCl + SO_2 + S \qquad (1)$$

However, other reduction products such as S_2Cl_2, Li_2SO_3 and $Li_2S_2O_4$ have also been suggested and sporadic reports of identification of some of these products have appeared. In order to see whether these products could be identified by cyclic voltammetry, cyclic voltammograms were obtained with addition of S_2Cl_2, $Na_2S_2O_4$ and Na_2SO_3 to $SOCl_2$/1.8M $LiAlCl_4$ solutions. Both Na_2SO_3 and $Na_2S_2O_4$ were insoluble in the electrolyte. The voltammogram obtained with addition of ∿10 v/o S_2Cl_2 showed that S_2Cl_2 reduces at a potential slightly positive of the reduction of $SOCl_2$ so that the positive portion of the $SOCl_2$ reduction peak was slightly broadened with the resulting current peak becoming asymmetrical. The voltammogram in Figure 20 shows that most probably S_2Cl_2 is not produced as a reduction product of $SOCl_2$.

- Electrochemical Oxidation of $SOCl_2/LiAlCl_4$ Solutions

A typical cyclic voltammogram in $SOCl_2$/1.8M $LiAlCl_4$ solution on a carbon electrode is shown in Figure 22. A similar voltammogram was also obtained on a nickel electrode. On scanning the electrode anodically from 4 volts, the onset of an anodic current occurs at ∿4.4V vs. Li^+/Li. The voltammogram shows two broad peaks at 4.55V and 4.65V as well as a sharp and high current peak at 5.0V. In poorly resolved voltammograms, the two peaks at 4.55V and 4.65V merge together and appear as one peak. On cycling the electrode continuously between 4 and 5 volts the heights of the broad peaks decreases although it does not completely disappear even after several cycles. If the electrode was scanned cathodically to 2V or below, the current peaks become large in the subsequent anodic sweep to 5.0V. In these cases, the two peaks at 4.55V and 4.65V generally appear as a single peak.

When the electrode is scanned cathodically below 4V after the anodic scan to 5V, the reduction peaks due to the oxidation products appear in the resulting voltammogram. This is shown in Figure 23.

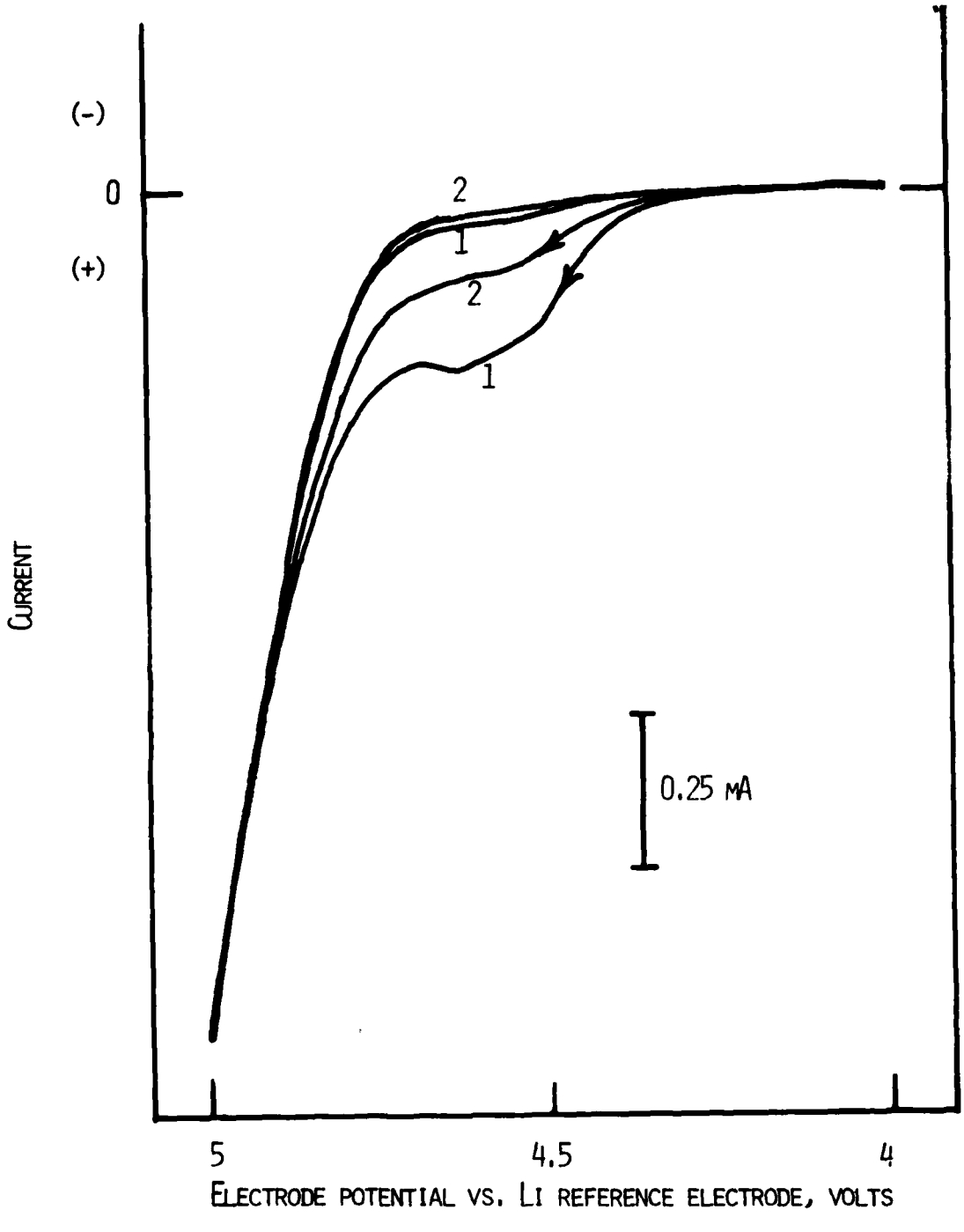

Fig. 22. Cyclic voltammogram of $SOCl_2$/1.8M $LiAlCl_4$ on glassy carbon electrode between 4 and 5 volts. Curves 1 and 2 represent successive scans. Scan rate = 50 mV/sec.

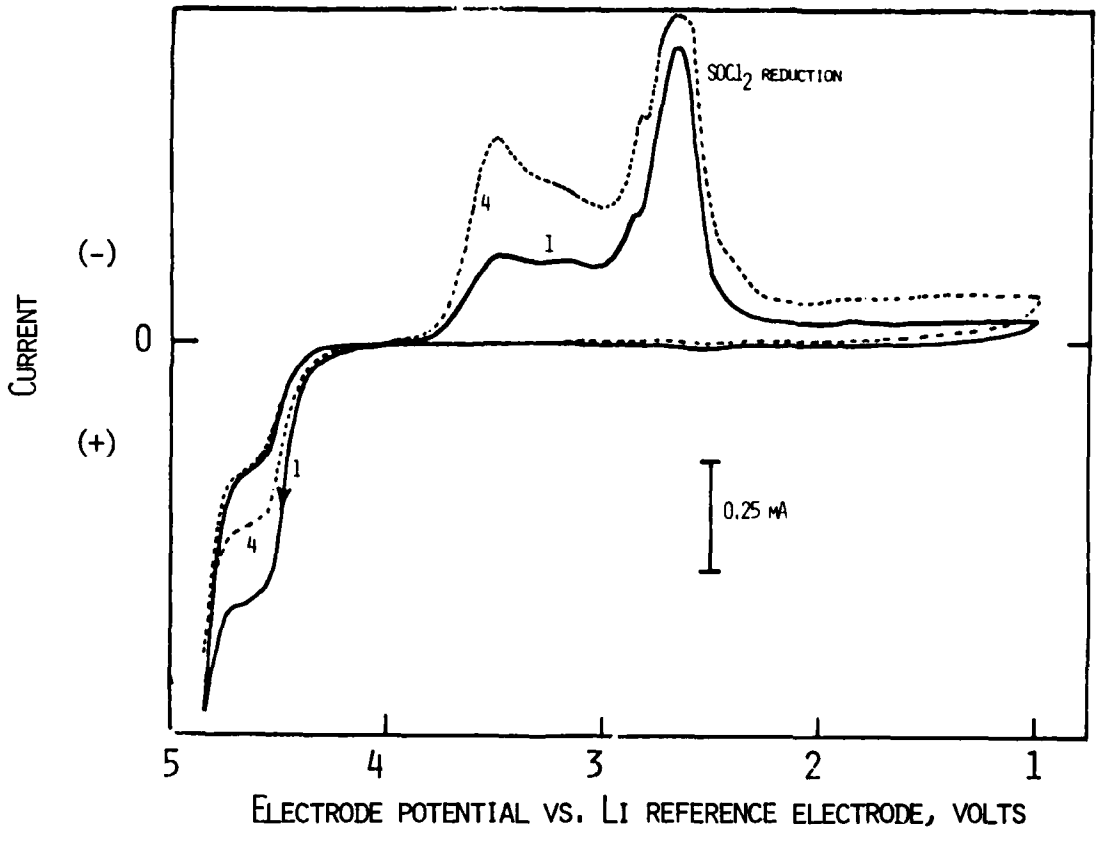

Fig. 23. Cyclic voltammogram of $SOCl_2$/1.8M $LiAlCl_4$ on a glassy carbon electrode. Scan rate = 100 mV/sec. The electrode was scanned anodic first from 3.7V. Cathodic curve 1 was obtained after voltage reversal at ∿4.9V. Curve 4 was obtained after twice cycling the electrode between 4 and 5V.

There are two clearly separated current peaks at ∿3.6V and ∿3.25V which result from the reduction of oxidation products. There is also a third peak at 2.95V, appearing as a shoulder to the $SOCl_2$ reduction peak at 2.6V. The appearance of these peaks and their relative peak heights were found to depend on the potential of scan reversal.

None of these three peaks appear when the scan is reversed at potentials below 4.2 volts. When the scan is reversed at ∿4.6 volts the peak at 3.25V appears as the major one. On increasing the reversal potential to values greater than 4.6V the height of the peak at 3.6V also increases along with the appearance of the shoulder at 2.75V. If the electrode is cycled several times between 4V and 5V before sweeping cathodically, all three peaks show increased peak heights. The voltammograms obtained by addition of Cl_2 to the $SOCl_2$/$LiAlCl_4$ showed an increase in the reduction current peak at 3.25V. As will be seen later the reduction peak at 3.25V was also observed in the cathodic region of SO_2Cl_2/$LiAlCl_4$ solutions after an anodic scan to 5.0V.

In order to identify the other reduction peaks in the voltammograms resulting from oxidation products, the electrode was scanned cathodically from open circuit after adding various reagents to $SOCl_2$/$LiAlCl_4$ solutions. The materials added were SCl_2, S_2Cl_2, SO_2Cl_2, SO_2, $AlCl_3$ and various combinations of these.

The voltammogram obtained by adding 1% SCl_2 to $SOCl_2$/1.8M $LiAlCl_4$ solution is shown in Figure 24. The onset of the cathodic current begins at 3.8V as in the case of the voltammogram in Figure 23. Addition of more SCl_2 resulted in an increase in the current with a peak at ∿3.6V. When larger amounts of SCl_2 were added, the peaks moved slightly to lower potentials.

The reduction peaks at 2.85V could most probably be due to SO_2Cl_2. The voltammogram obtained by adding 30 v/o SO_2Cl_2 to $SOCl_2$/1.8M $LiAlCl_4$ electrolyte is shown in Figure 25. The reduction peak is observed at ∿2.9V as a shoulder to the $SOCl_2$ peak. The voltammogram of SO_2Cl_2/1.8M $LiAlCl_4$ was also recorded to confirm this assignment and is shown in Figure 26. An interesting feature of the voltammogram is the position of the Cl_2 reduction peak. It occurs at about the same position as the one assigned to Cl_2 reduction in $SOCl_2$/$LiAlCl_4$ solutions. Evidently Cl_2 is an oxidation product of SO_2Cl_2 also.

The various other voltammograms with addition of the other reagents or their combinations were not very informative.

It appears that there are two oxidation reactions at potential between 4.4V and 4.65V. The first peak at ∿4.5V most probably corresponds to oxidation of LiCl (Equation 2) and the process may represent the removal of the LiCl film from the electrode surface.

$$LiCl \rightarrow Li^+ + \tfrac{1}{2}Cl_2 + e^- \qquad (2)$$

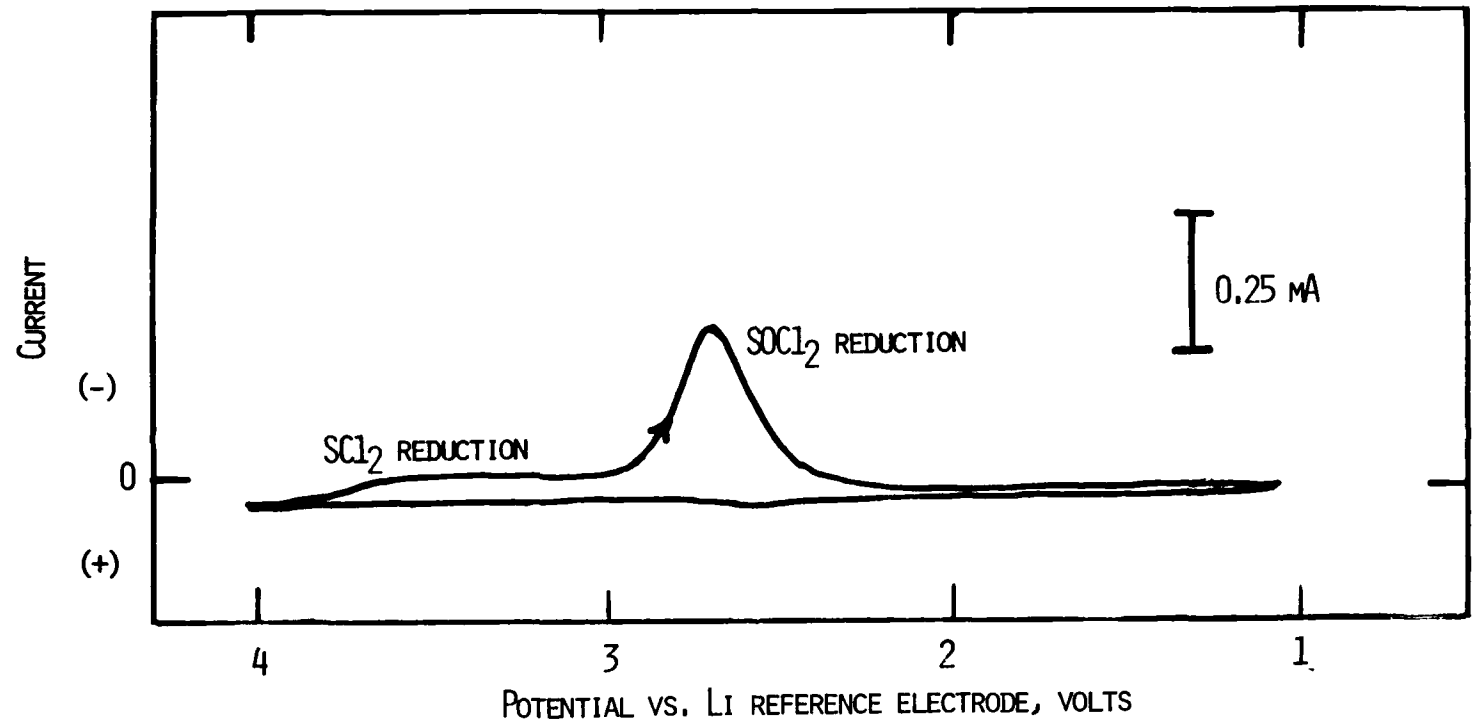

Fig. 24. Cyclic voltammogram of $SOCl_2$/1.8M $LiAlCl_4$ with 1.5 v/o SCl_2 on glassy carbon. Scan rate = 50 mV/sec. Cathodic scan first.

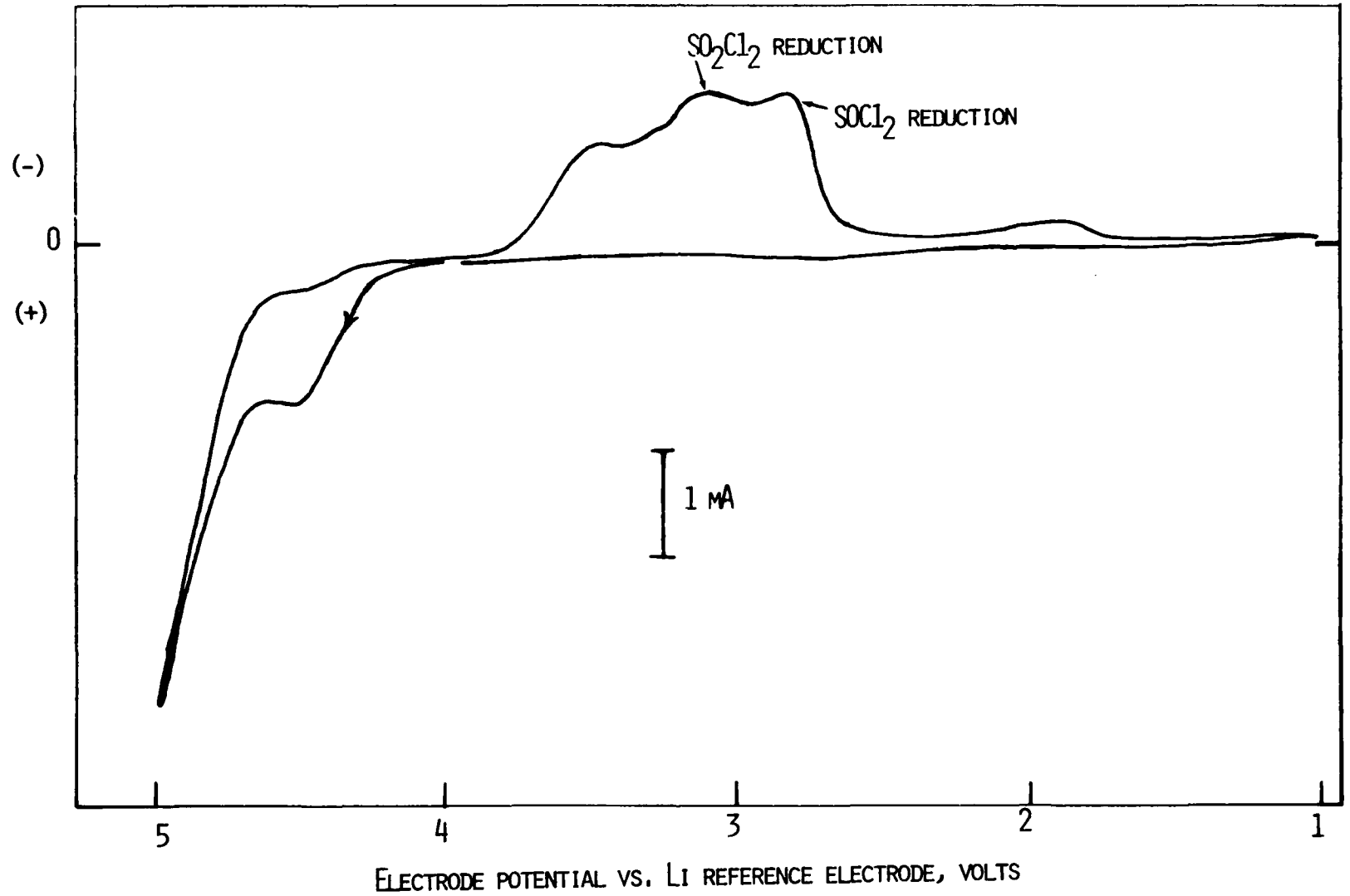

Fig. 25. Cyclic voltammogram of $SOCl_2$/1.8M $LiAlCl_4$ containing 30 v/o SO_2Cl_2 on glassy carbon electrode. Anodic scan first. Scan rate = 50 mV/sec.

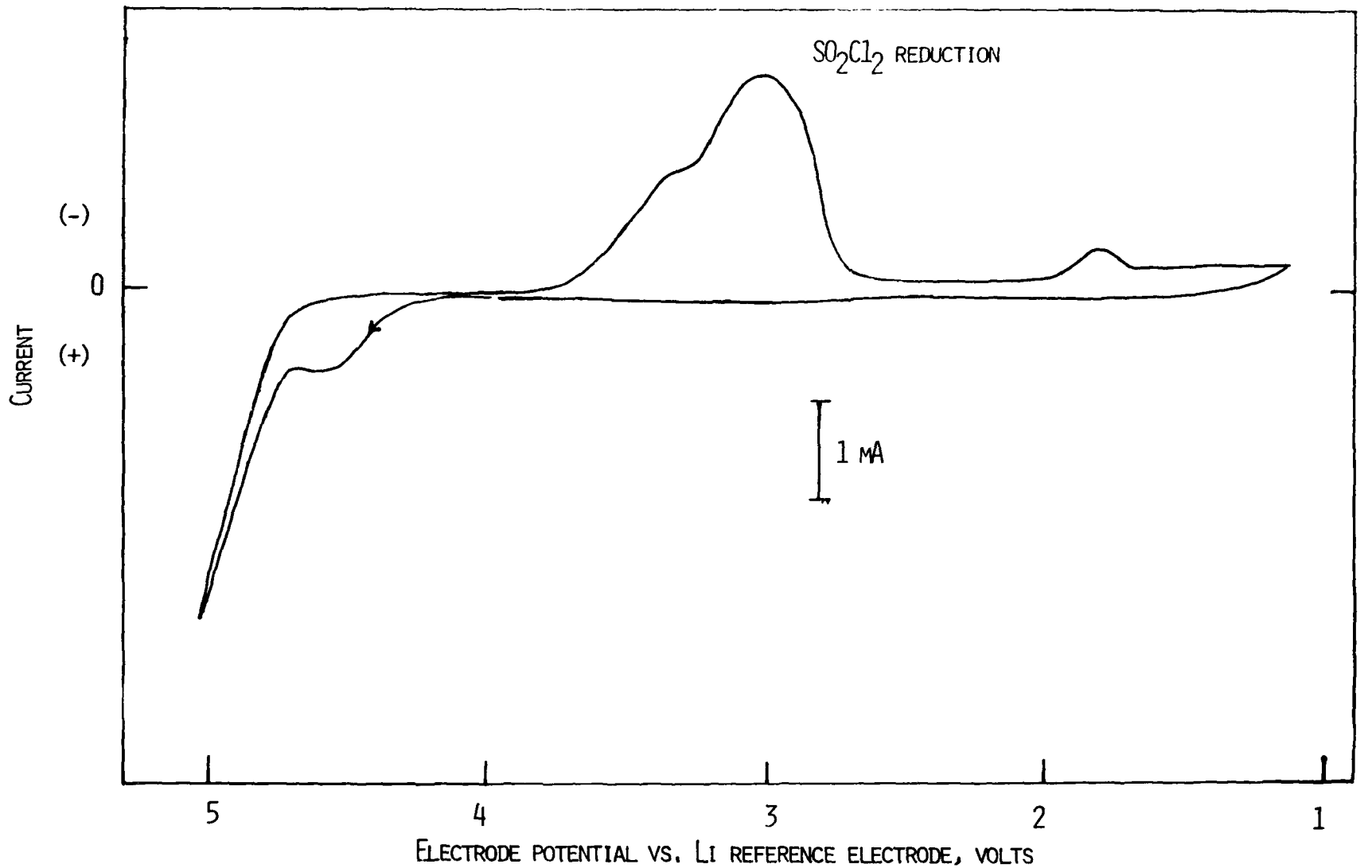

Fig. 26. Cyclic voltammogram of SO_2Cl_2/1.8M $LiAlCl_4$ on glassy carbon electrode between 1 and 5 volts. Scan rate = 50 mV/sec. The electrode was scanned anodic first.

The fact that it was possible to regenerate the electrode surface which had been passivated by holding it at a potential of ∿4.5V substantiate the assignment. The observed increase in the height of the peak after a cathodic sweep to 1V and the continuous decrease in the height of the peak on successive cycling between 4V and 5V are also in agreement for this assignment.

The more positive broad peak at 4.65V may correspond to the oxidation of $AlCl_4^-$, (Equation 2).

$$AlCl_4^- \rightarrow \tfrac{1}{2}Cl_2 + AlCl_3 + e^- \qquad (3)$$

When the voltammograms were run in $SOCl_2/LiAlCl_4$ solutions as a function of the concentration of $LiAlCl_4$ from 0.25 to 2.0M, we found increasing peak heights with increasing concentration of $LiAlCl_4$. It may be recalled that $AlCl_3$ was identified as an oxidation product of $SOCl_2/LiAlCl_4$ solution after constant current electrolysis with the anode potential remaining at ∿4.6V.

The high current peak near 5V is most probably due to oxidation of $SOCl_2$. However, the oxidation may begin at a much lower potential; say, at ∿4.6V in keeping with the fact that products of $SOCl_2$ oxidation were observed in $SOCl_2/LiAlCl_4$ electrolyte after constant current electrolysis with anode potentials at 4.6V.

The predominant reactions at 4.6V could then be reactions (2) and (3) and that shown below in Equation 4.

$$SOCl_2 + AlCl_4^- \rightarrow SOCl^+AlCl_4^- + \tfrac{1}{2}Cl_2 + e^- \qquad (4)$$

Reaction (2) would occur predominantly only if the electrode had been first scanned cathodically from open circuit so as to cause LiCl deposition on the electrode by $SOCl_2$ reduction. Reaction 4 is accepted as the primary oxidation process in $SOCl_2/LiAlCl_4$ solutions (12).

Since the anodic peak at 4.6V and the cathodic peak at 3.25V are interdependent, and since the primary reactions at 4.6V involve the formation of Cl_2, the peak at 3.25V is most probably due to Cl_2 reduction. This assignment is supported by the observation that a solution of Cl_2 in $SOCl_2/LiAlCl_4$ shows a reduction peak at 3.25V and that the Cl_2 reduction peak in $SO_2Cl_2/LiAlCl_4$ is found at ∿3.25V.

The peak at 3.6V can be assigned to SCl_2 reduction . The reduction potential observed here for SCl_2 is in agreement with the value reported by Blomgren et al. (13). They found that SCl_2 reduces at ∿3.7V vs. Li^+/Li in $SOCl_2$. Two other experimental results also suggested that the peak at ∿3.6V is most probably due to SCl_2. In $SOCl_2/LiAlCl_4$ solutions containing S or S_2Cl_2, the reduction peaks at 3.6V showed higher currents than in solutions without the additives, suggesting that these materials may chemically react with an anodic product to give the substance with the 3.6V reduction potential, Since Cl_2 is an oxidation product, the most probable reactions are:

$$S_2Cl_2 + Cl_2 \rightarrow 2SCl_2 \quad (5)$$

$$S + Cl_2 \rightarrow SCl_2 \quad (6)$$

These reactions are well known. For example SCl_2 is prepared by passing dry Cl_2 gas through powdered S. The reaction is exothermic and the intermediate is S_2Cl_2. In this reaction, with a large excess of Cl_2, the unstable SCl_4 can also be prepared by proper low temperature cooling.

The reduction peak at 2.85V may correspond to SO_2Cl_2 in accordance with the results presented in Figures 25 and 26.

3. Mechanisms of Oxidation Reactions in $SOCl_2/LiAlCl_4$ Solutions

The oxidation products which have been identified from constant current electrolysis and cyclic voltammetric studies are, Cl_2, $AlCl_3$, $SOCl^+AlCl_4^-$, SO_2Cl_2 and SCl_2. The various reactions which explain the formation of these materials and consistent with experimental data are:

$$AlCl_4^- \rightarrow AlCl_3 + \tfrac{1}{2}Cl_2 + e^- \quad (7)$$

$$SOCl_2 + AlCl_4^- \rightarrow SOCl^+AlCl_4^- + \tfrac{1}{2}Cl_2 + e^- \quad (8)$$

$$SOCl_2 + SOCl^+AlCl_4^- \rightarrow SCl^+ + SO_2Cl_2 + AlCl_3 + \tfrac{1}{2}Cl_2 + e^- \quad (9)$$

$$SCl^+ + AlCl_4^- \rightarrow SCl^+AlCl_4^- \quad (10)$$

$$SOCl_2 + AlCl_3 \rightarrow SOCl^+AlCl_4^- \quad (11)$$

The cathode process to balance the charges would involve the reduction of $SOCl_2$ as shown in Equation 12.

$$2SOCl_2 + 4Li^+ + 4e^- \rightarrow 4LiCl + S + SO_2 \quad (12)$$

The first oxidation reaction of $SOCl_2$ shown in Equation 8 has been proposed previously (12). We note that $SOCl^+AlCl_4^-$ is structurally similar to $LiAlCl_4$ and could be oxidized at potentials close to that of the oxidation of $LiAlCl_4$. This reaction shown in Equation 9 explains the formation of the various products identified. The complex $SCl^+AlCl_4^-$ is essentially $AlCl_3$ complex of SCl_2 and has been previously characterized (14).

The reaction schemes shown above have been proposed to explain the observed products.

4. Product Analysis from Cells

Analysis of products from discharged, overdischarged and charged $Li/SOCl_2$ cells was carried out using as analytical techniques both IR spectrometry and *in situ* cycle voltammetry. The small prismatic cells in a slightly flooded

state were used for these studies. The larger amounts of electrolyte were needed to have materials left for analysis after the galvanostatic tests. Control experiments with extracts of the electrode package from cells containing lesser amounts of electrolyte did not show results different from flooded cells.

4.1 Experimental Procedures

In the IR spectrometric methods anode and cathode limited cells were subjected to various states of discharge, overdischarge and charge and the electrolyte was analyzed. The electrode package was then extracted with $SOCl_2$ on SCl_2 and spectra were again recorded. In order to identify the absorption peaks, spectra of mixtures of various reagents of known compositions were also obtained.

The IR data were complemented by cyclic voltammetry studies. Attempts to obtain cyclic voltammetry data with a microcarbon electrode incorporated inside the cell between two layers of the electrode package were not successful due to passivation from excessive film formation on the electrode surface. However, informative results were obtained from cyclic voltammetry on a glassy carbon microelectrode (0.07 cm^2) introduced into the cell through a side arm of the specially designed glass cell. The cell and the electrode arrangement is shown schematically in Figure 27. During discharge the microcarbon electrode was placed away from contact with the electrolyte. To record the voltammogram after tests, the electrode was pushed down and secured contact with the electrolyte by placing the cell in a tilted position. Passivation of the electrode was avoided by this procedure and reproducible results were obtained. The cell reference electrode and Li electrode were used as the reference and counter electrodes for CV.

Since the IR spectral data and cyclic voltammetry results are complementary, it is appropriate to discuss the data with respect to cell configurations and the modes of cell operation.

4.2 Forced Overdischarged Anode Limited Cells

- Experimental Results

The anode limited cells and their construction parameters are given in Table 5. A summary of the discharge results, the extent of discharge or overdischarge for each cell before IR spectral or cyclic voltammetry tests are presented in Table 6. The most informative region of the IR spectrum is below 1500 cm^{-1}, the region of S-O absorptions. In cyclic voltammetry, the cathodic region below 4V is the most useful.

Cell P-22 was discharged at 27 mA and yielded 490 mAh capacity, Figure 28. The cell was anode limited as indicated by the potentials of the anode vs. Li reference electrode at the end of discharge. The cell was terminated

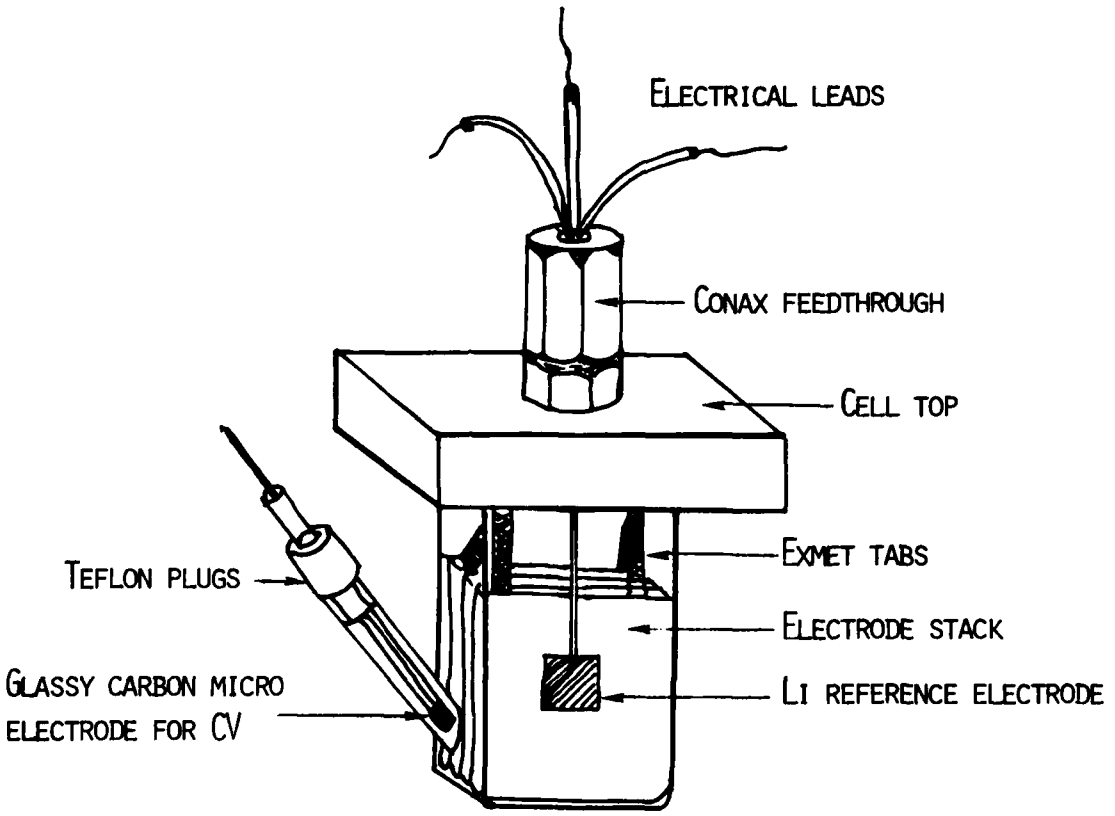

Fig. 27. Schematic view of the cell for <u>in situ</u> cyclic voltammetry.

TABLE 5

CELL PARAMETERS FOR ANODE LIMITED CELLS

Cell No.	Cell Configuration	Carbon Electrode: Average Thickness (mm)	Carbon Electrode: Total Area Facing Li (cm^2)	Carbon Electrode: Approximate Amount of Carbon (mg)	Lithium Electrode: Area (cm^2)	Lithium Electrode: Amount (Ah)	Electrolyte $LiAlCl_4/SOCl_2$: Con. $LiAlCl_4$ (M)	Electrolyte $LiAlCl_4/SOCl_2$: Vol. (ml)	Discharge Current (mA)
P-5	C/Li/C/Li/C(AL*)	0.61	24	320	24	0.70	1.8	3	24
P-18	AL	0.65	24	400	24	0.63	1.8	4.5	24
P-19	AL, without Li on the anode Exmet	0.75	24	530	-	-	1.8	4.0	24
P-21	AL	0.75	24	470	24	0.63	1.8	4.0	24
P-22	AL	0.75	24	450	24	0.63	1.8	4.0	27
P-23	AL, without Li on the anode Exmet	0.70	24	450	-	-	1.8	4.0	50
P-26	AL	0.68	24	480	24	0.63	1.8	3.5	24
P-31	AL, no lithium	0.68	24	400	-	-	1.8	4.0	24
P-32	AL	0.69	24	400	24	0.63	1.8	4.0	24
P-41	AL	0.63	24	420	24	0.63	1.0[a]	4.0	24
P-46	AL	0.62	24	385	24	0.63	1.0[a]	4.0	24
P-48	AL	0.62	24	336	24	0.6	1.8[b]	4.0	24

*AL → anode limited.

[a] $Li_2O/AlCl_3$ based electrolyte, 1M Li^+.

[b] SO_2Cl_2/1.8M $LiAlCl_4$.

TABLE 6

ANALYTICAL TEST SUMMARY OF ANODE LIMITED CELLS

Cell No.	Cell Capacity (mAh)	Test Performed After Discharge, mAh IR	Discharge, mAh CV	Overdischarge, mAh IR	Overdischarge, mAh CV
P-5	470	-	-	1680	-
P-18	396	-	-	240	-
P-19	Cell without Li	-	-	670	-
P-21	260*	260*	-	-	-
P-22	490	490	-	-	-
P-23	Cell without Li	-	-	1150	-
P-26	620	-	-	1100	-
P-31	Cell without Li	-	-	3300	3300
P-32	490	-	490	2160	2600
P-41	560	-	-	304	304
P-46	Cell without Li	-	-	1580	1580
P-48	Cell without Li	-	-	3250	3250

*Partial discharge.

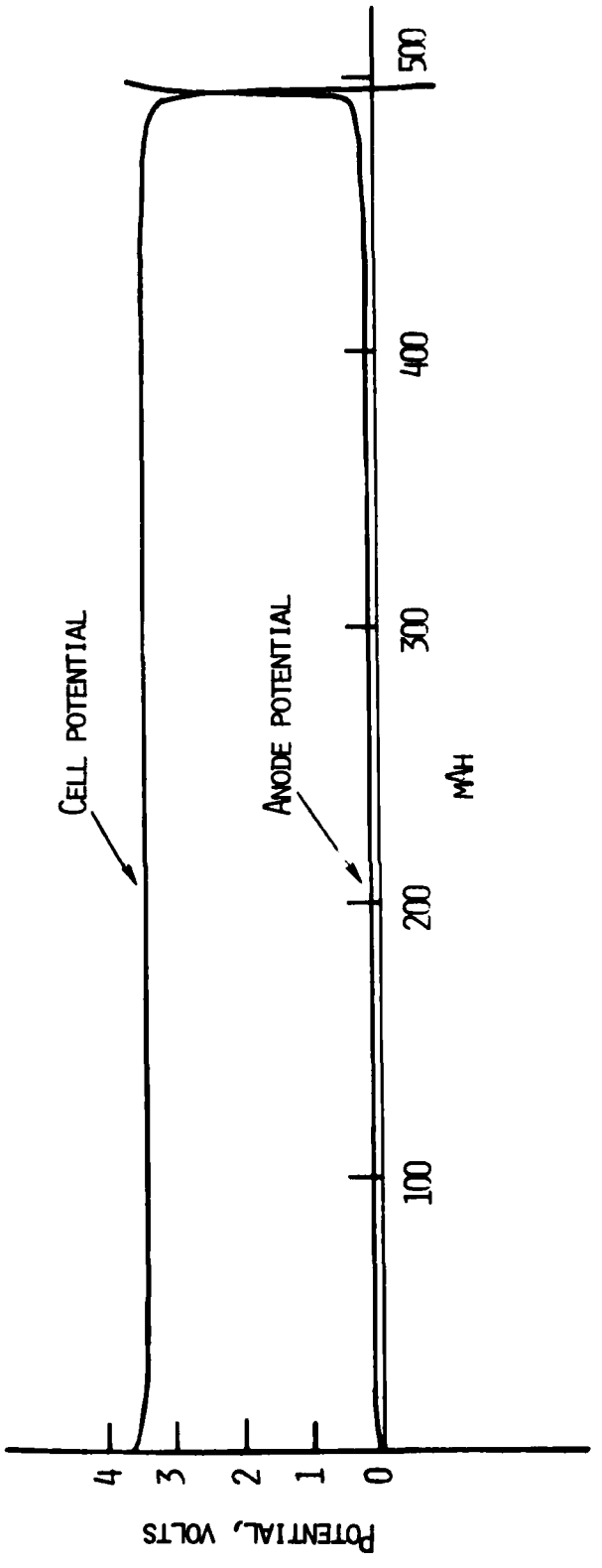

Fig. 28. Discharge curve for Li/$SOCl_2$ cell P-22. Current = 24 mA.

just at the end of discharge when the anode potential was ∿3.5V. The IR spectrum of the electrolyte is shown in Figure 29. The only IR identifiable product is SO_2.

We have also obtained a similar spectrum from Cell P-21 which had been discharged to 260 mAh, ∿2/3 the normal capacity of the cell. At the time of iR spectral recording the cell potential in P-21 was at 3.4V and the anode potential was at +50 mV.

In order to see if any other products with absorptions hidden inside the large $SOCl_2$ peak near 1200 cm^{-1}, we recorded the IR spectra in the double beam spectrometer with $SOCl_2$/1.8M $LiAlCl_2$ solution taken in an identical cell placed in the reference beam. This spectrum for electrolyte from P-22 is shown in Figure 30. The absorptions due to SO_2 are clearly seen at 1340 cm^{-1} and 1155 cm^{-1}. The normal $SOCl_2$ peaks are folded upwards in the spectrum. This technique was found to be a useful one of general utility in the IR spectral studies of this system.

Another anode limited Cell P-18 was discharged at 24 mA and then forced overdischarged also at 24 mA. The overdischarge proceeded with considerable voltage fluctuations as often found (7,8) in anode limited cells during forced overdischarge. The IR spectrum was recorded after 240 mAh of overdischarge and is shown in Figure 31. The spectrum shows SO_2 as the major product. However, another new peak of medium intensity is present at 1070 cm^{-1}. The spectrum obtained with $SOCl_2$/$LiAlCl_4$ solution in the reference beam showed that no material is present which absorbs at 1200 cm^{-1}. The IR spectrum from anode limited Cell P-26 overdischarged for 1.1 Ah was identical to the one in Figure 31 except that the intensity of the peak at 1070 cm^{-1} was relatively higher. We have reproduced this result in yet another cell overdischarged for 2 Ah.

In all the anode limited cells some Li, mostly in loose patches, was still present at the end of discharge. This Li could possibly react with the oxidation product(s) so that some of the products were not available for detection. To eliminate this possibility, two cells were tested without any lithium on the anode. This cell represents an extreme case of anode limited cell. The discharge curve for Cell P-19 is shown in Figure 32. Cell P-23 was tested without the Li reference electrode since the Li could react with oxidation products. Both cells gave identical IR spectra. The spectrum from P-19 is shown in Figure 33. The spectrum shows two other peaks at 1410 cm^{-1} and 1110 cm^{-1} in addition to the peaks present in Figure 31. The peak at 1410 cm-1 is due to SO_2Cl_2 and the peak at 1110 cm^{-1} is due to the complex $SOCl^+AlCl_4^-$.

Cyclic voltammetry data were obtained after various stages of discharge and overdischarge. A typical voltammogram obtained by scanning the C electrode between 1 and 4V in the electrolyte from anode limited Cell P-32 which had been forced overdischarged for 2.16 Ah is shown in Figure 34. The voltammogram shows a reduction peak at 3.25V due to a product of overdischarge. A very low current peak may be present at ∿3.6V. We note that the voltammo-

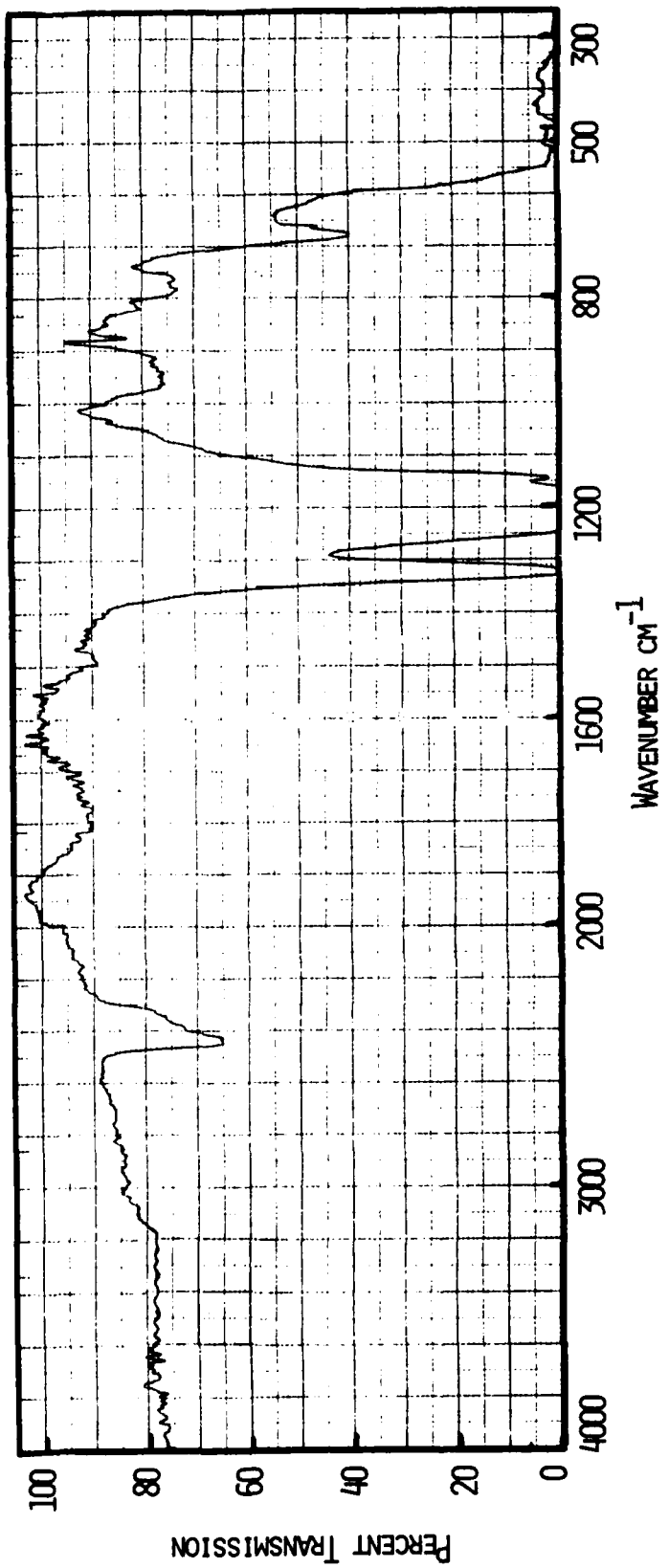

Fig. 29. Infrared spectrum of the electrolyte from Li/$SOCl_2$ cell P-22 after the discharge shown in Fig. 28.

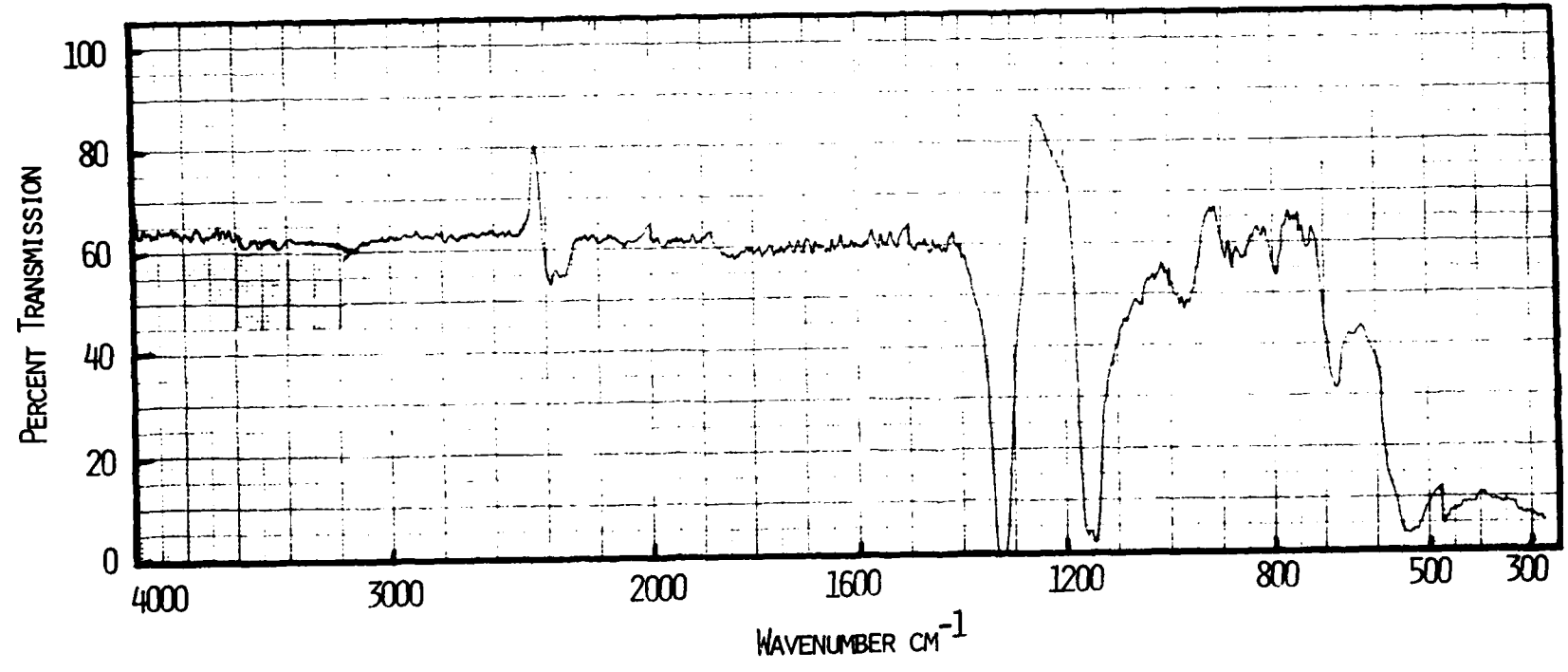

Fig. 30. Infrared spectrum of electrolyte from Li/$SOCl_2$ cell P-22 after 0.49 mAh discharge shown in Fig. 28. The reference cell contained $SOCl_2$.

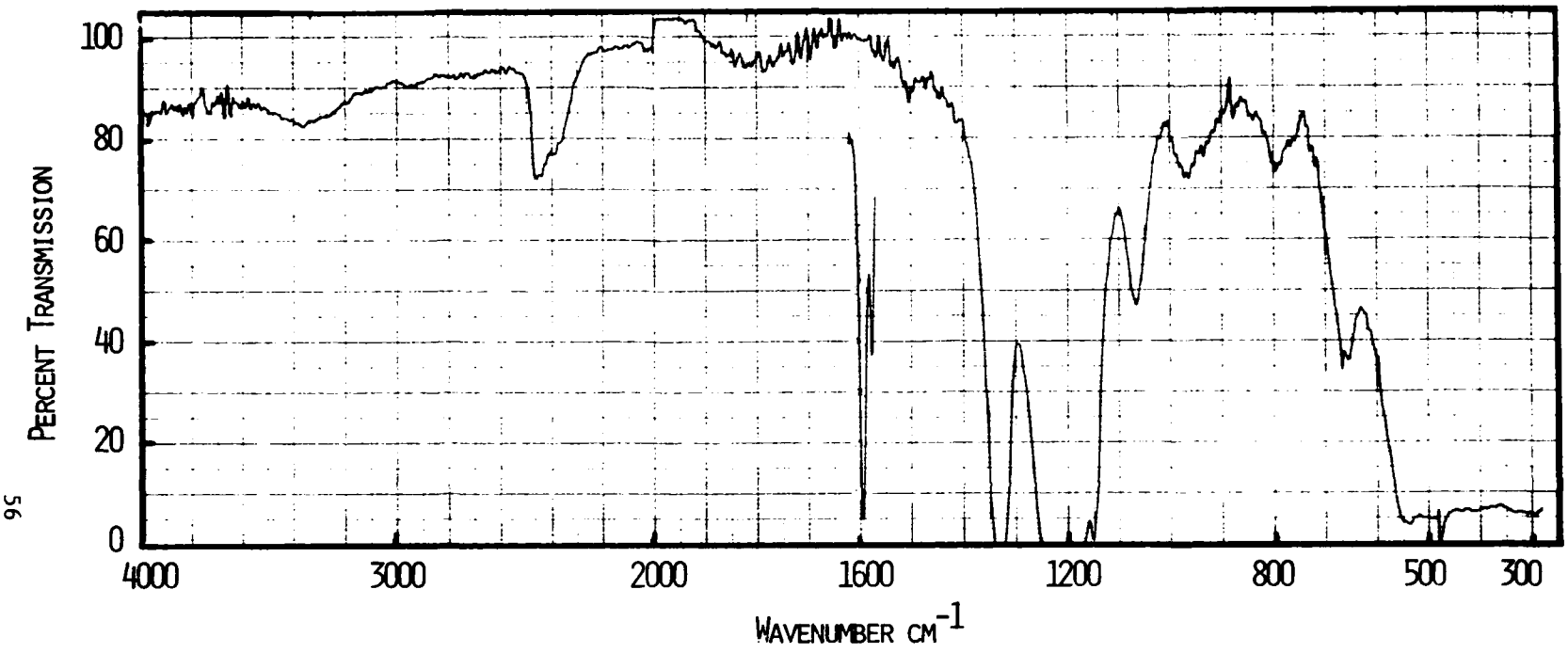

Fig. 31. Infrared spectrum of electrolyte from Li/$SOCl_2$ cell P-18 after the overdischarge shown in Fig. 30.

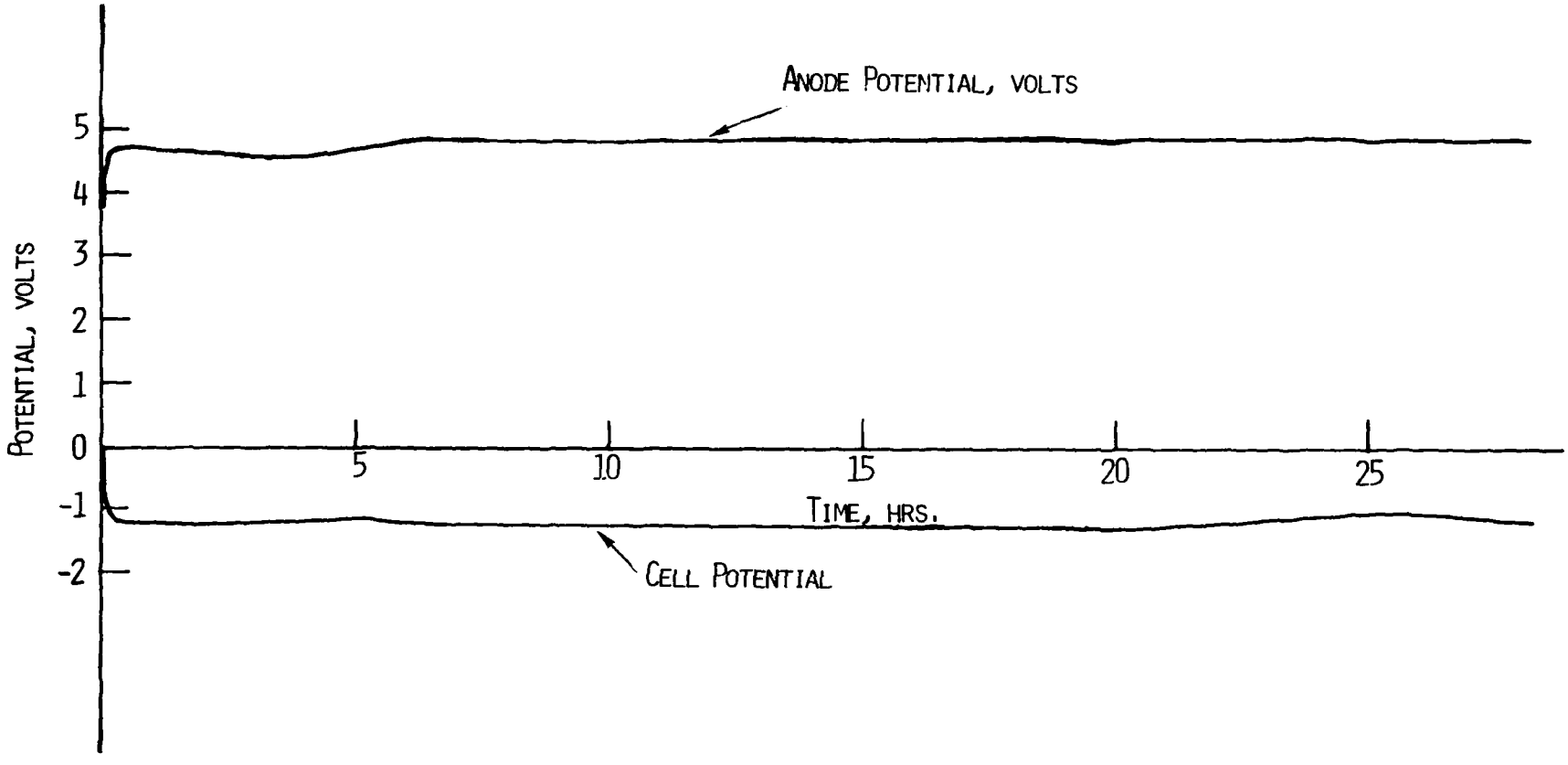

Fig. 32. Discharge curve for cell P-19 without Li on the anode. Current = 24 mA.

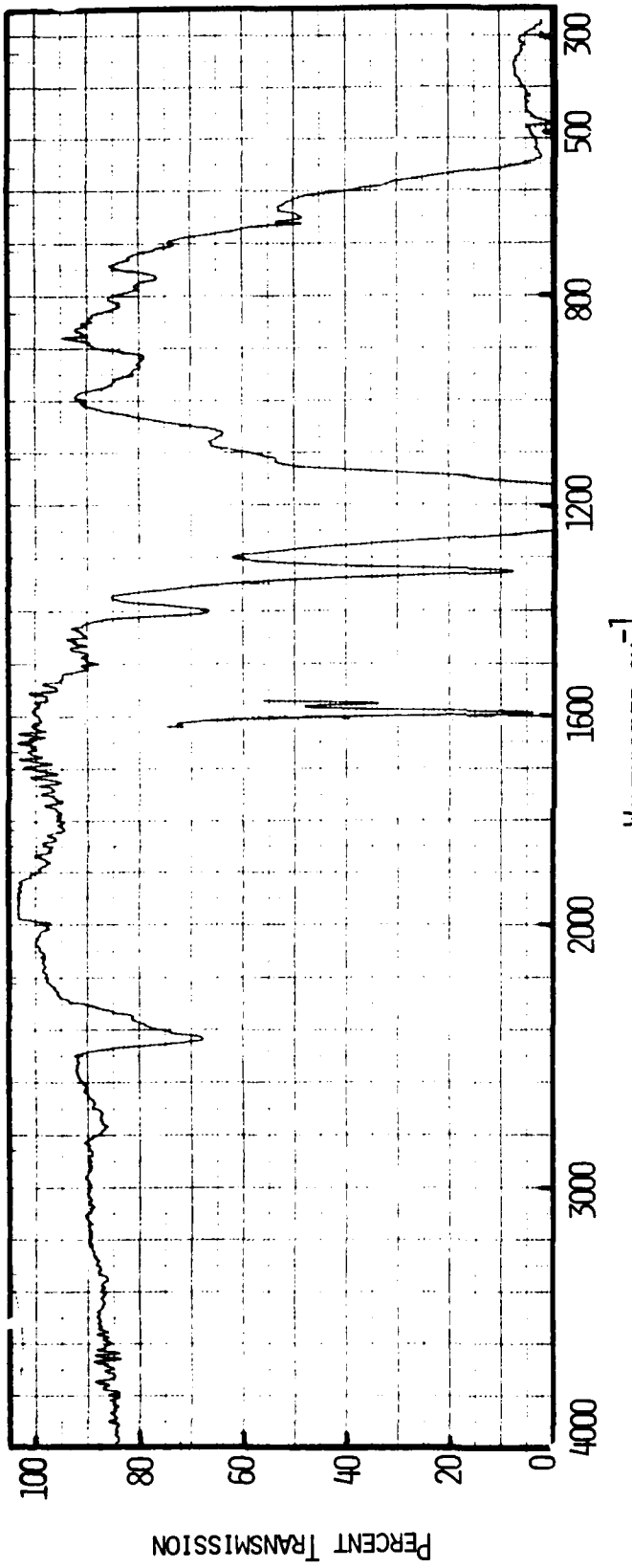

Fig. 33. Infrared spectrum of the electrolyte from cell P-19 shown in Fig. 32.

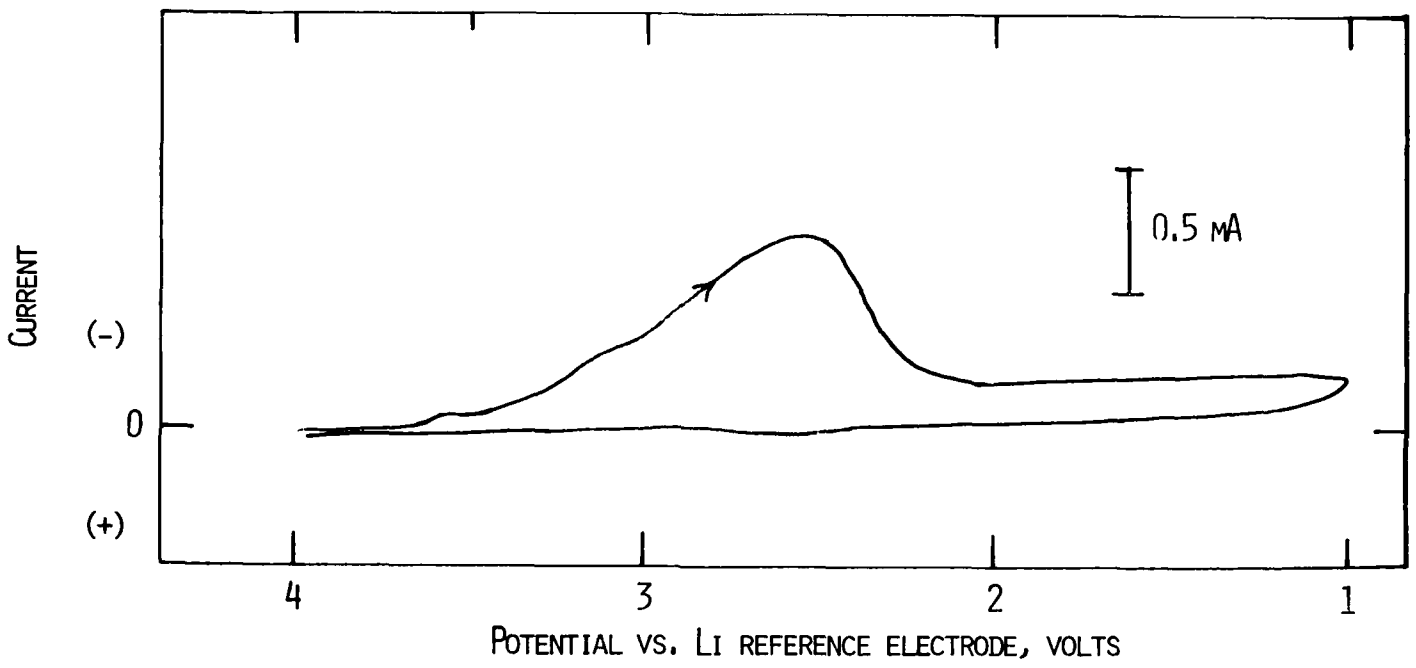

Fig. 34. Cyclic voltammogram of electrolyte from cell P-32 after 550 mAh overdischarge on glassy carbon electrode. Scan rate = 50 mV/sec. Cathodic scan first.

gram obtained after 490 mAh of discharge when the anode potential had just polarized to ~4.0V did not show any peaks at 3.6V and 3.25V. Evidently Cl_2 and SCl_2 are present in the overdischarged cell. The IR spectrum from Cell P-32, obtained immediately after the cyclic voltammetry run, was identical to that shown in Figure 31, showing principally the peak at 1070 cm^{-1} from the product. In addition, SO_2 and a minute amount of SO_2Cl_2 were also present.

A cyclic voltammogram was also obtained in the electrolyte from Cell P-31, discharged without Li on the anode. The voltammogram is shown in Figure 35. It shows the peaks due to Cl_2, and SCl_2.

From anode limited Cell P-5, the electrodes after the overdischarge, were carefully disassembled in the drybox and washed with $SOCl_2$. The IR spectrum of the extract showed absorptions due to SO_2 and the peak at 1070 cm^{-1}. In order to examine the potential presence of new materials whose absorptions are masked by the strongly absorbing $SOCl_2$ peak at 1230 cm^{-1}, the electrodes from another anode limited cell after forced overdischarge were extracted with S_2Cl_2 and the IR spectrum of the extract was recorded. The spectrum was identical to that of the electrolyte from P-5.

The possible role of the supporting electrolyte in controlling the nature of products in anode limited cells during forced overdischarge was investigated in cells utilizing $Li_2O/AlCl_3$ based electrolytes. The cells were P-41 and P-46.

Cell P-41 was essentially identical to the anode limited Cell P-18 containing $SOCl_2$/1.8M $LiAlCl_4$. It was discharged and overdischarged at 24 (1 mA/cm^2 of Li electrode area) the same current density used in P-18. The IR spectrum of the electrolyte after 304 mAh of overdischarge showed the presence of the material exhibiting the absorption at 1070 cm-1. Cyclic voltammogram of the electrolyte showed that Cl_2 was also present. Thus it appears that essentially similar materials are formed in both of the electrolytes under similar regimes of forced overdischarge.

Cell P-46 was constructed without Li on the anode. The electrolyte was analyzed after 1.58 Ah of discharge. IR spectrum showed that SO_2 and the material with absorption at 1070 cm^{-1} were present. However, there was no $SOCl^+AlCl_4^-$, which had been found in similar cells tested with $SOCl_2/LiAlCl_4$. Cyclic voltammetry data showed that SCl_2 and Cl_2 were also present.

Since it has been found that SO_2Cl_2 is one of the oxidation products of $SOCl_2/LiAlCl_4$ solutions and is produced in cells under various oxidizing conditions. We have investigated whether the sensitive chemicals causing explosions in anode limited cells are produced from oxidation reactions of SO_2Cl_2. Thus, Cell P-48 was tested with SO_2Cl_2/1.8M $LiAlCl_4$. This cell did not contain any Li on the anode and therefore was similar to Cells P-23 and P-31. Products identified after 3.25 Ah of overdischarge were SO_2 and Cl_2.

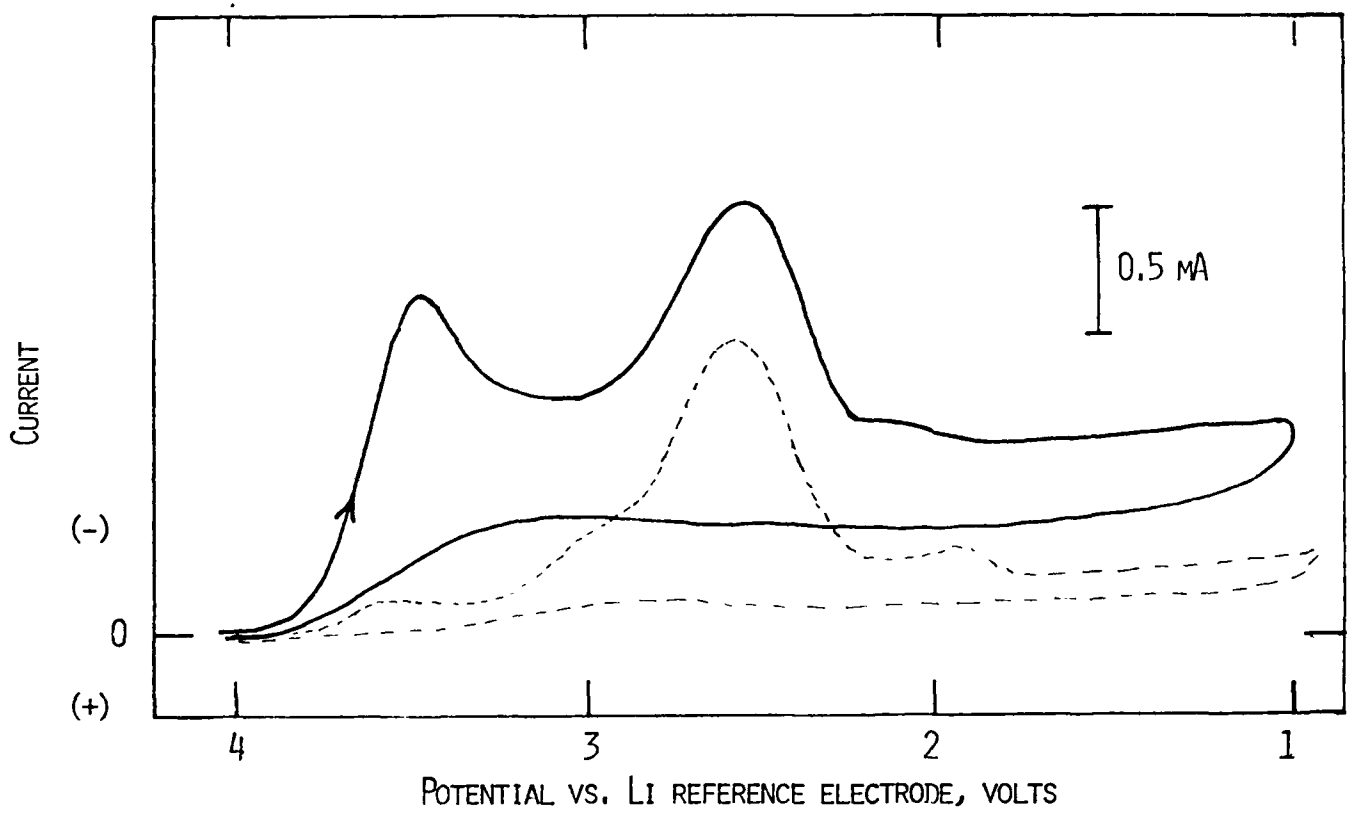

Fig. 35. Cyclic voltammogram of electrolyte from cell P-31 on glassy carbon electrode. The solid curve represents the voltammogram obtained after the discharge shown in Fig. . The voltammogram represented by the broken curve was obtained after 0.10 Ah discharge.

- Discussion of Results

When anode limited cells are forced overdischarged, the anode potential rises to values >4V resulting in oxidation reactions of cell materials with the formation of several products. The identified products are Cl_2 and a material absorbing at 1070 cm^{-1} in the infrared spectrum. In some cells small amounts of SO_2Cl_2 and $SOCl^+AlCl_4^-$ are also found. All these products except the material with the 1070 cm^{-1} absorptions could result from oxidation reactions of the type discussed in the previous section.

It may be noted that the material with the 1070 cm^{-1} absorption was not present in the anolyte from the electrolysis of $SOCl_2/LiAlCl_4$ solution. In the latter experiment the anolyte and the catholyte did not mix. Thus, it appears that the material with the 1070 cm^{-1} absorption may have resulted from either the oxidation of a discharge product or from the reaction of a discharge product with a substance formed in the oxidation.

Several IR experiments with reagent combinations were performed to identify the material exhibiting absorption at 1070 cm^{-1} in the IR spectrum. Only the spectrum of S_2Cl_2 showed a weak band at 1070 cm^{-1}. This is the first overtone band of the S-Cl stretch at 550 cm^{-1}. However, the intensity of the peak at 1070 cm^{-1} in the electrolyte from cells is much higher than even in neat S_2Cl_2 indicating that the material is different. SCl_2 does not have any absorptions at 1070 cm^{-1}. The possibility of SO_3 was investigated by spectral measurements on solutions of SO_3 in $SOCl_2$. However, SO_3 oxidized $SOCl_2$ rapidly to produce SO_2Cl_2 and no absorption at 1070 cm^{-1} was found.

In solutions from cells discharged without Li on the anode, SO_2Cl_2, $SOCl^+AlCl_4^-$ and the material exhibiting absorption at 1070 cm^{-1} were identified from IR spectra. Cyclic voltammetry showed SCl_2 and Cl_2 also. The fact these materials are present in much higher concentrations in these cells than in overdischarged anode limited cells is probably due to the absence of Li. Also in these cells larger amounts of electrolyte are available for oxidation. The reactions in cells without Li on the anode involve regenerative process so that these cells could be "discharged" for long periods of time without changes in electrode polarization. The important cell reactions in the regenerative process may be,

$$AlCl_4^- \rightarrow AlCl_3 + \tfrac{1}{2}Cl_2 + e^- \qquad (13)$$

$$SOCl_2 + AlCl_3 \rightarrow SOCl^+AlCl_4^- \qquad (14)$$

$$SOCl_2 + AlCl_4^- \rightarrow SOCl^+AlCl_4^- + \tfrac{1}{2}Cl_2 + e^- \qquad (15)$$

Anode

$$Li^+ + \tfrac{1}{2}Cl_2 + e^- \rightarrow LiCl \quad (16)$$

$$LiCl + SOCl^+AlCl_4^- \rightarrow LiAlCl_4 + SOCl_2 \quad (17)$$

} Cathode

Note that reaction 17 regenerates the cell materials. However, the presence of SO_2Cl_2 in these cells suggest that some oxidation of $SOCl^+AlCl_4^-$ also occurs. We have found that the reaction of SO_2Cl_2 with Li is extremely fast in the presence of $AlCl_3$. The IR spectrum showed SO_2 as a product of the reaction which may be written as shown in Equation 18.

$$2Li + SO_2Cl_2 + 2AlCl_3 \rightarrow SO_2 + 2LiAlCl_4 \quad (18)$$

$SOCl_2$ also reacts with Li in the presence of $AlCl_3$, but the reaction is much slower.

Although several materials have been identified in anode limited cells after forced overdischarge, none of them appears to be capable of causing the type of explosion observed in these cells. The material exhibiting the absorption at 1070 cm^{-1} in the IR spectrum may be considered a potential candidate. However, the structure of this material is not yet known.

4.3 Cathode Limited Cells

Products from cathode limited cells were analyzed after forced overdischarge and after resistive load overdischarge. The construction parameters for the various cells are shown in Table 7. The extent of discharge and overdischarge for each cell before the analytical test are shown in Table 8.

- Experimental Results

The IR spectrum of the electrolyte from a typical cathode limited cell (P-36) after forced overdischarge is shown in Figure 36. The discharge and overdischarge for the cell are shown in Figure 37. The cell, discharged at 36 mA had a capacity to zero volt of 1.21 Ah and the IR spectrum was obtained after 1.08 Ah of overdischarge. The spectrum shows the SO_2 peaks at 1340 cm^{-1} and 1155 cm^{-1}. A weak shoulder is present at 1065 cm^{-1} and this peak coincides with the first overtone band of the S-Cl stretch in S_2Cl_2 near 550 cm^{-1}. Since the S-Cl stretching absorptions in $SOCl_2$, and the Al-Cl stretching absorptions in $AlCl_4^-$ all occur in the region 500-550 cm^{-1}, it cannot be established unequivocally whether S_2Cl_2 is present in the electrolyte.

The IR spectrum also shows two strong absorptions at 790 cm^{-1} and 665 cm^{-1}. These peaks have been found in the electrolyte from all cathode limited cells after forced overdischarge. In the electrolyte from cathode limited cells, terminated just at the end of discharge or after very little overdischarge, say 50 mAh, these peaks were not present or sometimes present as weak bands.

TABLE 7

CELL PARAMETERS FOR PRISMATIC $Li/SOCl_2$ CELLS

Cell No.	Cell Configuration	Carbon Electrode			Lithium Electrode		Electrolyte $LiAlCl_4/SOCl_2$		Discharge Current
		Average Thickness (mm)	Total Area Facing Li (cm^2)	Approximate Amount of Carbon (mg)	Area (cm^2)	Amount (Ah)	Conc. $LiAlCl_4$ (M)	Vol. (ml)	(mA)
36	Li/C/Li/C/LiC/Li (CL)[a]	0.62	36	360	36	2.01	1.8	4	36
37	CL	0.61	36	340	36	2.01	1.8	4	99[illegible] Load
42	CL	0.62	36	360	36	2.01	1.0[b]	4	36
43	CL	0.62	36	375	36	2.01	1.0[b]	4	36[e]
47	CL	0.62	36	340	36	2.01	1.8	4	36

[a] CL → cathode limited.

[b] $Li_2O/AlCl_3$ electrolyte, 1M Li^+.

TABLE 8

ANALYTICAL TEST SUMMARY OF CATHODE LIMITED Li/$SOCl_2$ CELLS

Cell No.	Cell Capacity (mAh)	Test Performed After Discharge, mAh IR	Discharge, mAh CV	Overdischarge, mAh IR	Overdischarge, mAh CV
36	1210	-	-	1080	1080
37	∿1100	-	-	17 hr thru 99 Ω	17 hr thru 99 Ω
42	1210	-	-	950	950
43	a	-	-	1530[a]	1530[a]
47	a	-	-	3350[a]	3350[a]

[a]The cell was charged.

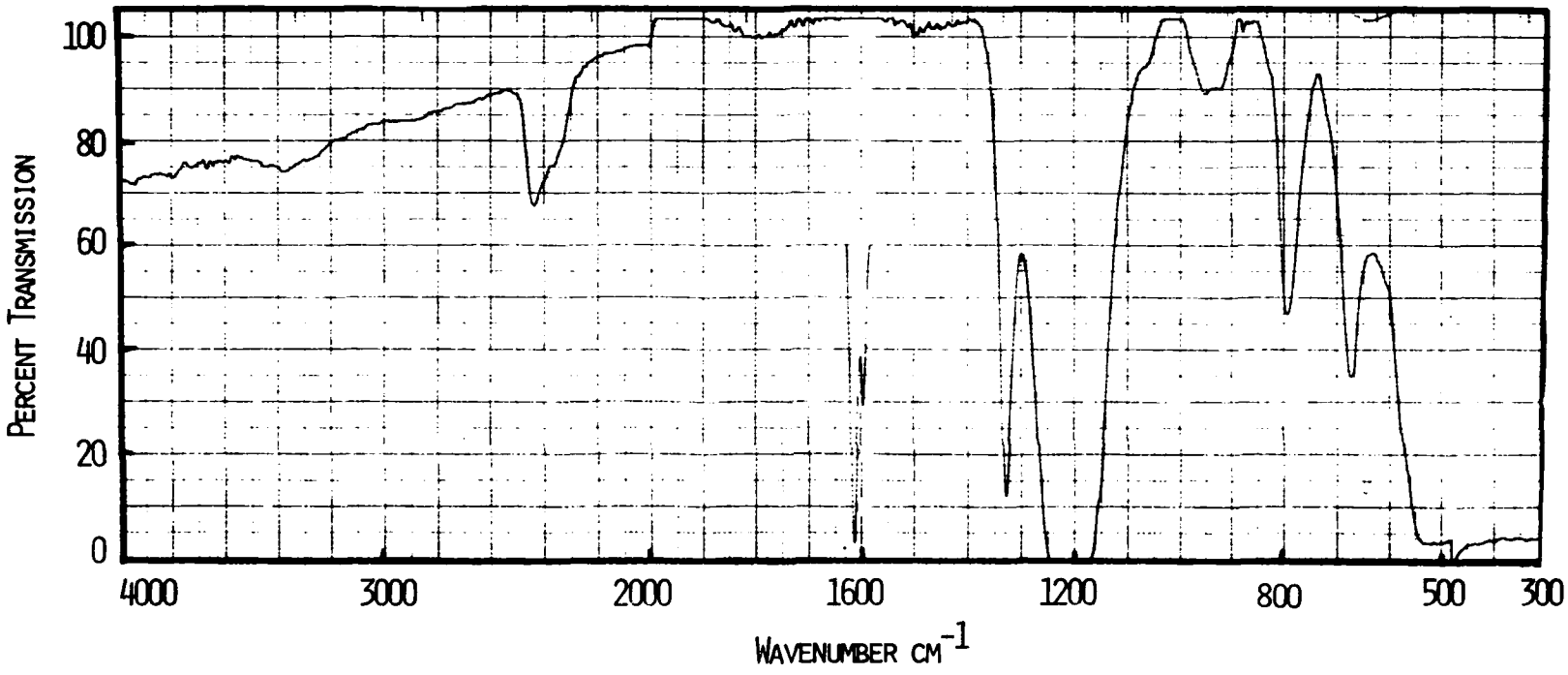

Fig. 36. Infrared spectrum of electrolyte from Li/$SOCl_2$ cell P-36 after forced overdischarge shown in Fig. 37.

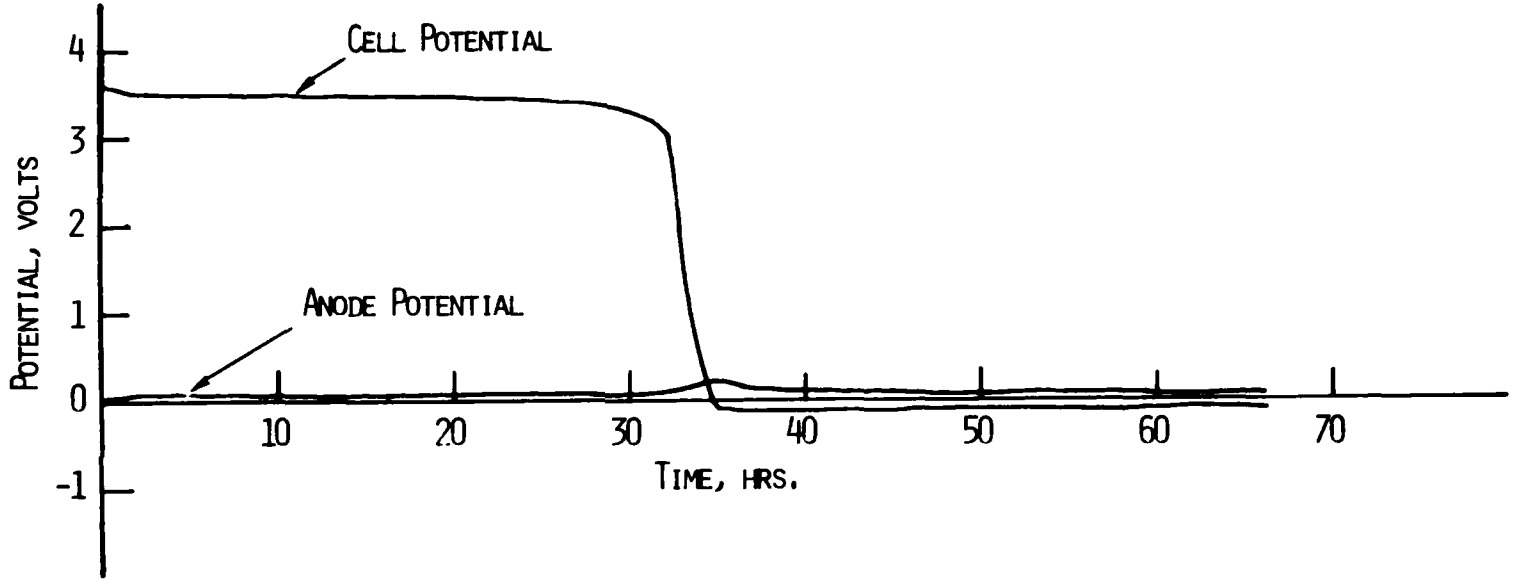

Fig. 37. Discharge and overdischarge curves for Li/$SOCl_2$ cell P-36. Current = 36 mA.

We have also analyzed the electrolyte from forced overdischarged, cathode limited cells which contained $Li_2O/AlCl_3$ based supporting electrolyte. The discharge and overdischarge curves for Cell P-42 with 0.5M Li_2O/1.0M $AlCl_3/SOCl_2$ is shown in Figure 38. The cell capacity of 1.21 Ah to zero volt is virtually identical to that found in similar cells with $SOCl_2/LiAlCl_4$ electrolyte. The IR spectrum of the electrolyte from Cell P-42 was obtained after 0.95 Ah of overdischarge and is shown in Figure 39. The spectrum also shows the peaks at 790 cm^{-1} but at much lower intensities than in the electrolyte from the cell containing $LiAlCl_4$ for the same extent of overdischarge.

The IR spectrum of the electrolyte from a cathode limited cell after resistive load overdischarge was identical to that from forced overdischarged cells.

The discharge and overdischarge behavior of a typical cathode limited cell, P-37, on resistive load is shown in Figure 40. The cell was discharged through 99 Ω load so that the initial current drainage was 35 mA. The cell had a capacity of ∿1.2 Ah, corresponding to 3.23 Ah/g carbon utilization. The cell was allowed to overdischarge (<0.5V) for 17 hours through the 99 Ω load before electrolyte was analyzed by IR spectrometry. The infrared spectrum is shown in Figure 41. Note that the spectrum also shows the absorptions at 790 cm^{-1} and 665 cm^{-1}.

- Discussion of Experimental Results

In order to identify the absorptions at 790 cm^{-1} and 665 cm^{-1}, IR spectra of solutions of various materials in $SOCl_2$ were obtained. From these experiments it was found that these peaks were associated with a product of reaction between Li_2S and $LiAlCl_4$. When Li_2S (anhydrous, Foote Mineral Co.) was added to $SOCl_2$ at room temperature there was no apparent solubility nor was there any apparent reaction between the two materials. On the other hand, when anhydrous Li_2S is added to $SOCl_2/LiAlCl_4$ electrolyte on exothermic reaction ensues with the formation of a white precipitate. The IR spectrum of the solution product from a reaction between Li_2S and $LiAlCl_4$, treated in 1:1 molar ratio in $SOCl_2$ is shown in Figure 42. The spectrum also shows the two peaks at 790 cm^{-1} and 665 cm^{-1} with relative intensities essentially identical to those in Figure 36.

It appears that Li_2S reacts with $LiAlCl_4$ as shown in Equation 19 to form $LiAlSCl_2$ and LiCl of which the former is soluble in $SOCl_2$.

$$Li_2S + LiAlCl_4 \xrightarrow{SOCl_2} LiAlSCl_2 + 2LiCl \qquad (19)$$

In the IR spectrum, the peaks at 790 cm^{-1} and 665 cm^{-1} are most probably due to Al-S stretch and Al-Cl stretch respectively of $LiAlSCl_2$. We have found

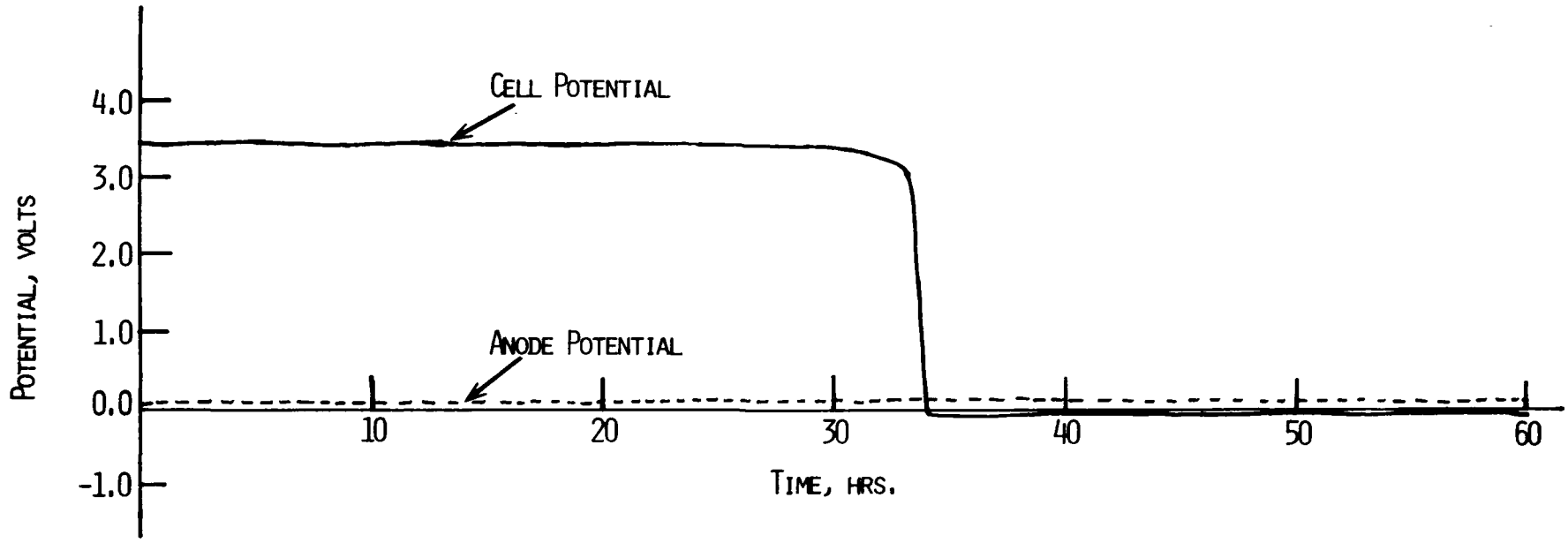

Fig. 38. Galvanostatic discharge curve for cathode limited cell P-42. Current = 36 mA.

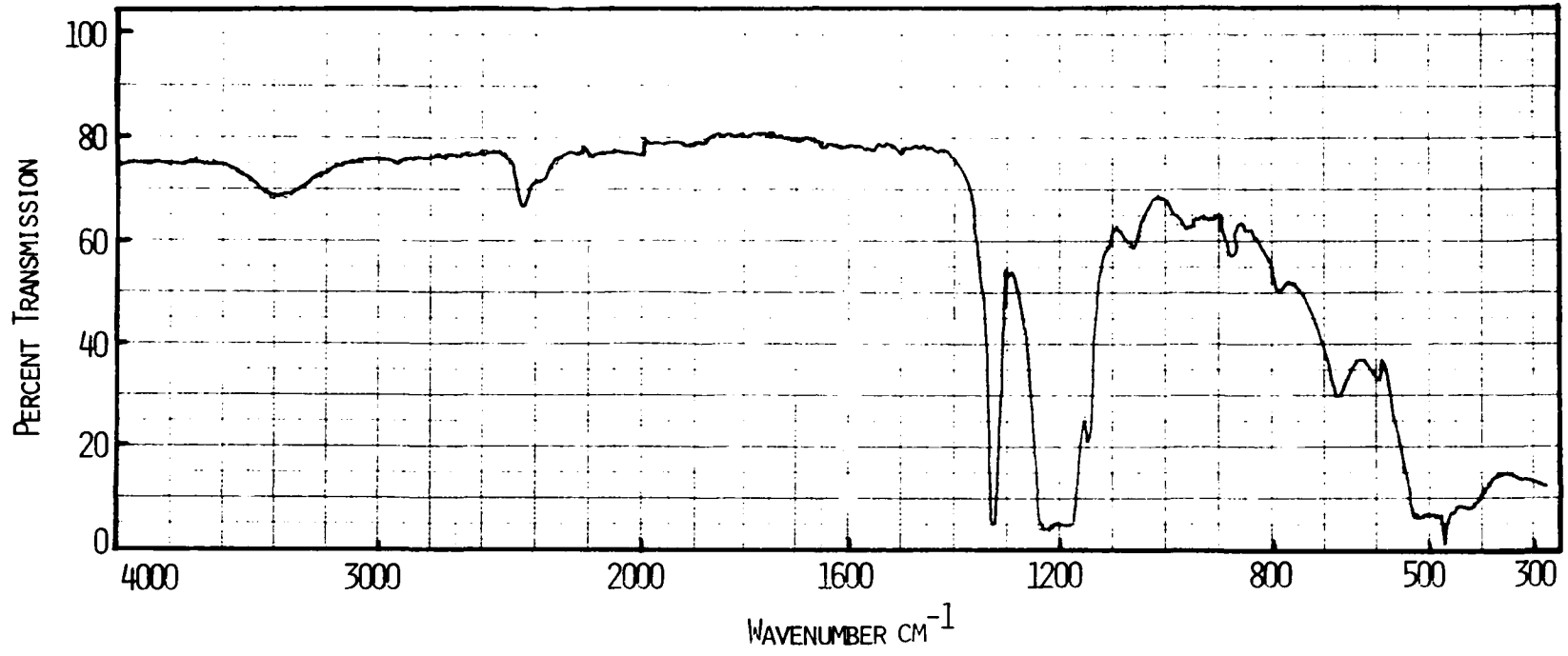

Fig. 39. Infrared spectrum of the electrolyte from cell P-42 after the overdischarge shown in Fig. 38.

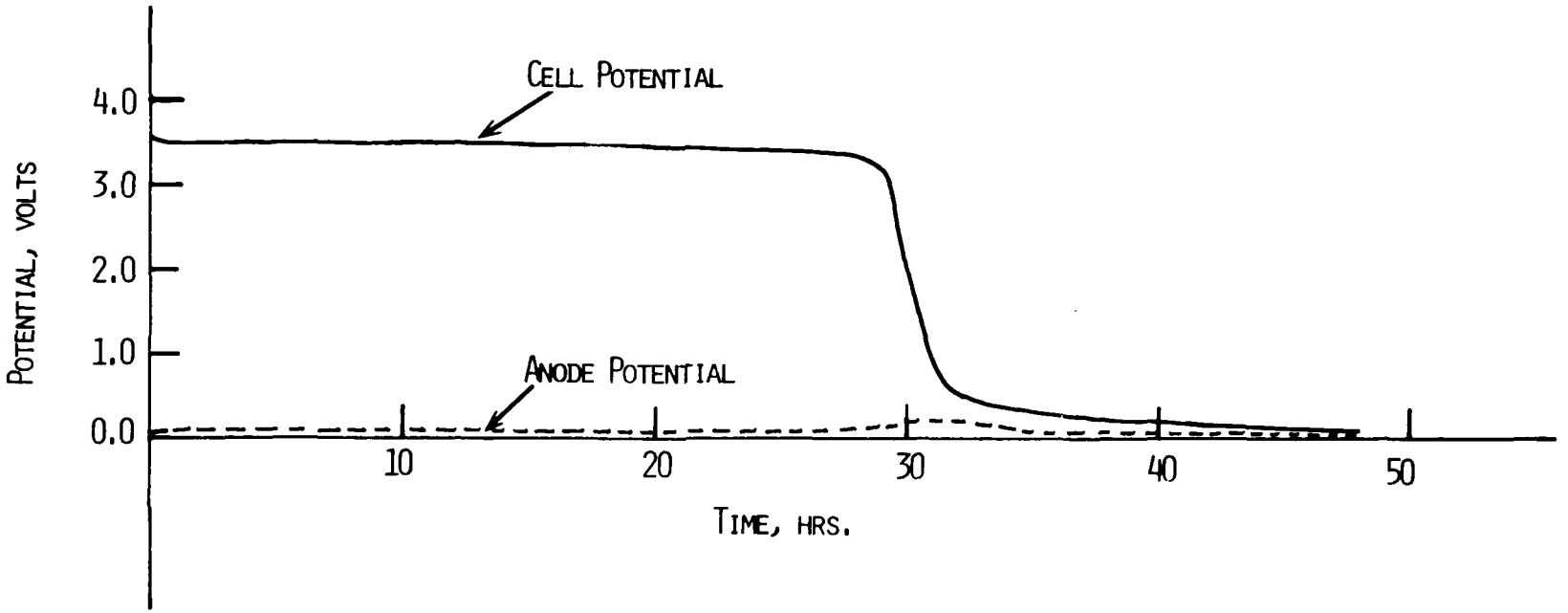

Fig. 40. Discharge of cathode limited cell P-37 through 99Ω load.

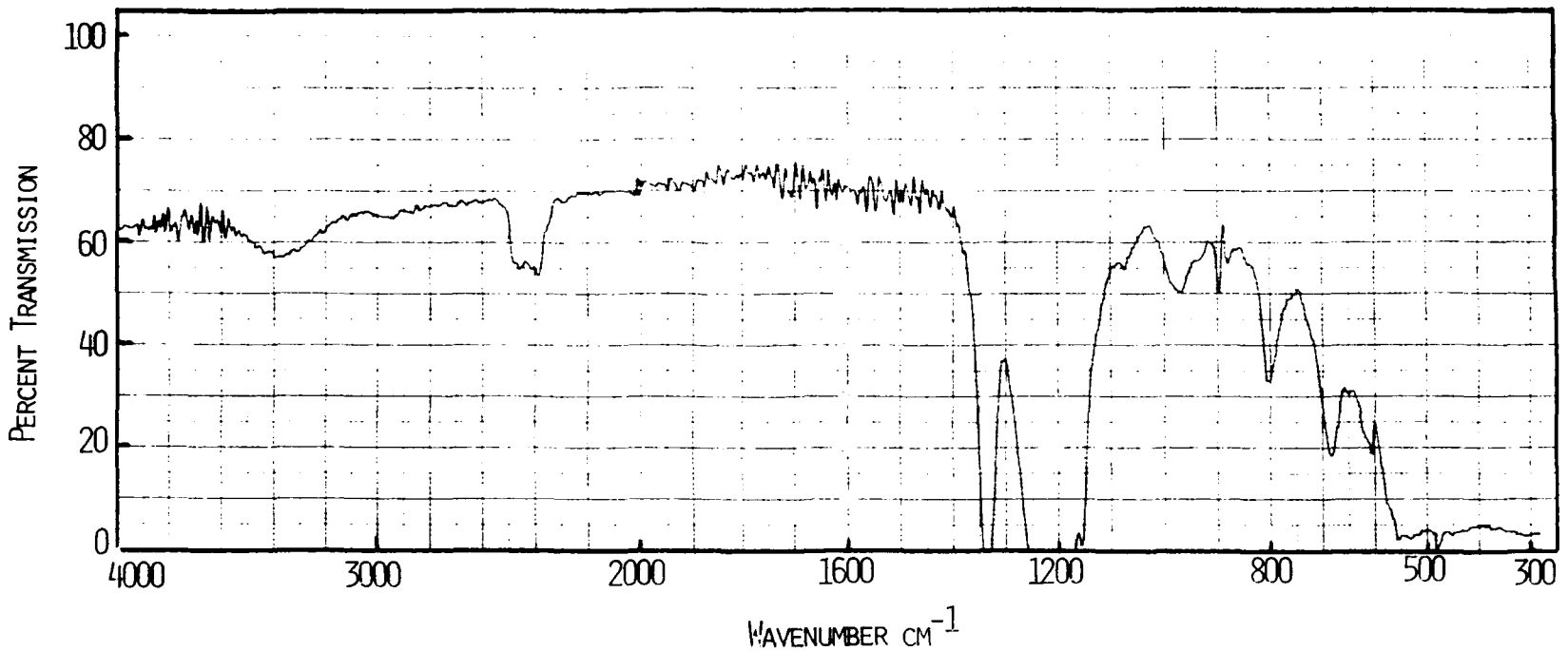

Fig. 41. Infrared spectrum of the electrolyte from cell P-37 after the test shown in Fig. 40.

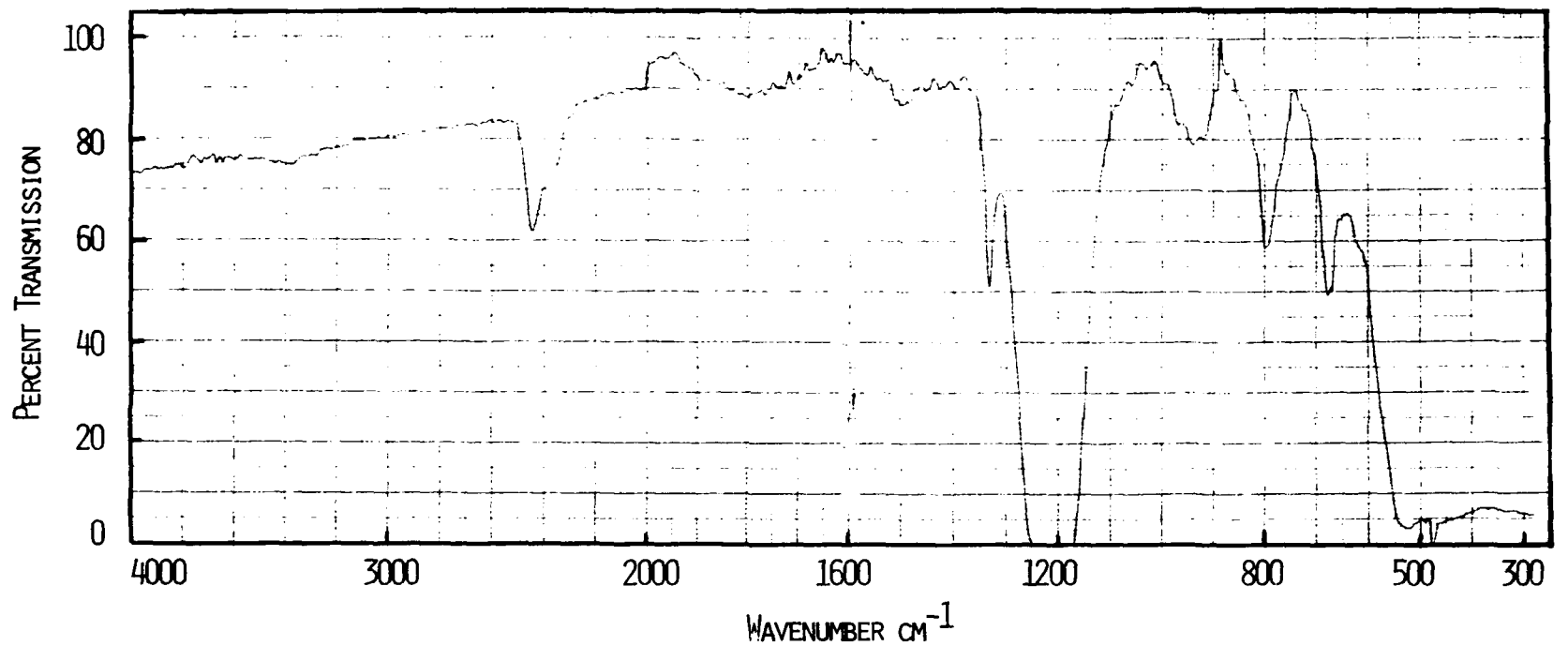

Fig. 42. Infrared spectrum of the solution product from the reaction of equimolar amounts of Li_2S and $LiAlCl_4$ in $SOCl_2$.

that $LiAlSCl_2$ can also be prepared by the reaction of Li_2S and $AlCl_3$ in $SOCl_2$* according to the reactions 20 and 21.

$$Li_2S + AlCl_3 \xrightarrow{SOCl_2} LiAlSCl_2 + LiCl \quad (20)$$

$$Li_2S + 2AlCl_3 \xrightarrow{SOCl_2} LiAlSCl_2 + LiAlCl_4 \quad (21)$$

The IR spectra of the solutions from reactions 20 and 21 are shown in Figures 43 and 44. They have features essentially identical to those in Figure 42. We have also found that solutions of $LiAlSCl_2$ in $SOCl_2$ have conductivities similar to $LiAlCl_4$ and that $LiAlSCl_2$ can be an alternative electrolyte for $Li/SOCl_2$ cells. These aspects of $LiAlSCl_2$ will be discussed later.

When Li_2S and $AlCl_3$ are mixed in a 2:1 molar ratio in $SOCl_2$ or when Li_2S is added to $LiAlSCl_2/SOCl_2$ solutions, the following reactions seem to take place.

$$2Li_2S + AlCl_3 \rightarrow LiAlS_2 + 3LiCl \quad (22)$$

$$Li_2S + LiAlSCl_2 \rightarrow LiAlS_2 + 2LiCl \quad (23)$$

$LiAlS_2$ is apparently insoluble or has very little solubility in $SOCl_2$ and it precipitates out as a dark material along with LiCl. In the IR spectra of these solutions the two absorptions at 790 cm^{-1} and 665 cm^{-1} are present as very weak bands.

The evidences presented here suggest that when cathode limited cells are overdischarged Li_2S is formed and that Li_2S reacts immediately with $LiAlCl_4$ to form $LiAlSCl_2$ and probably $LiAlS_2$. It seems that in discharged cells which invariably contains S as a discharge product, the formation of Li_2S is a spontaneous process, (Equation 24).

$$2Li^+ + S + 2e^- \rightarrow Li_2S \quad (24)$$

*In these solutions we have not ruled out the possibility of parallel reactions such as,

$$Li_2S + SOCl_2 + 2AlCl_3 \rightarrow 2LiAlCl_4 + S_2O$$

$$2S_2O \rightarrow SO_2 + 3S$$

There is no reaction between Li_2S and $SOCl_2$ at room temperature.

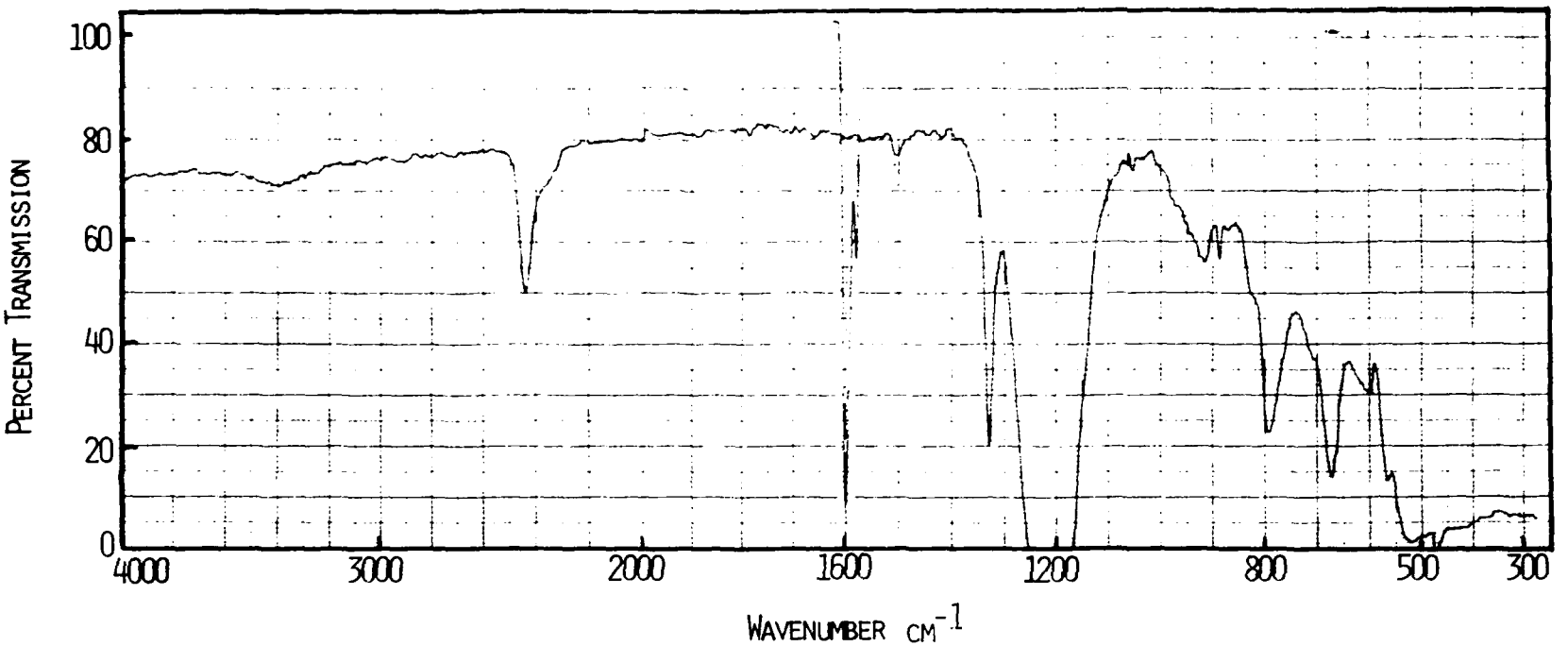

Fig. 43. Infrared spectrum of the solution product from reaction between equimolar amounts of Li_2S and $AlCl_3$ in $SOCl_2$.

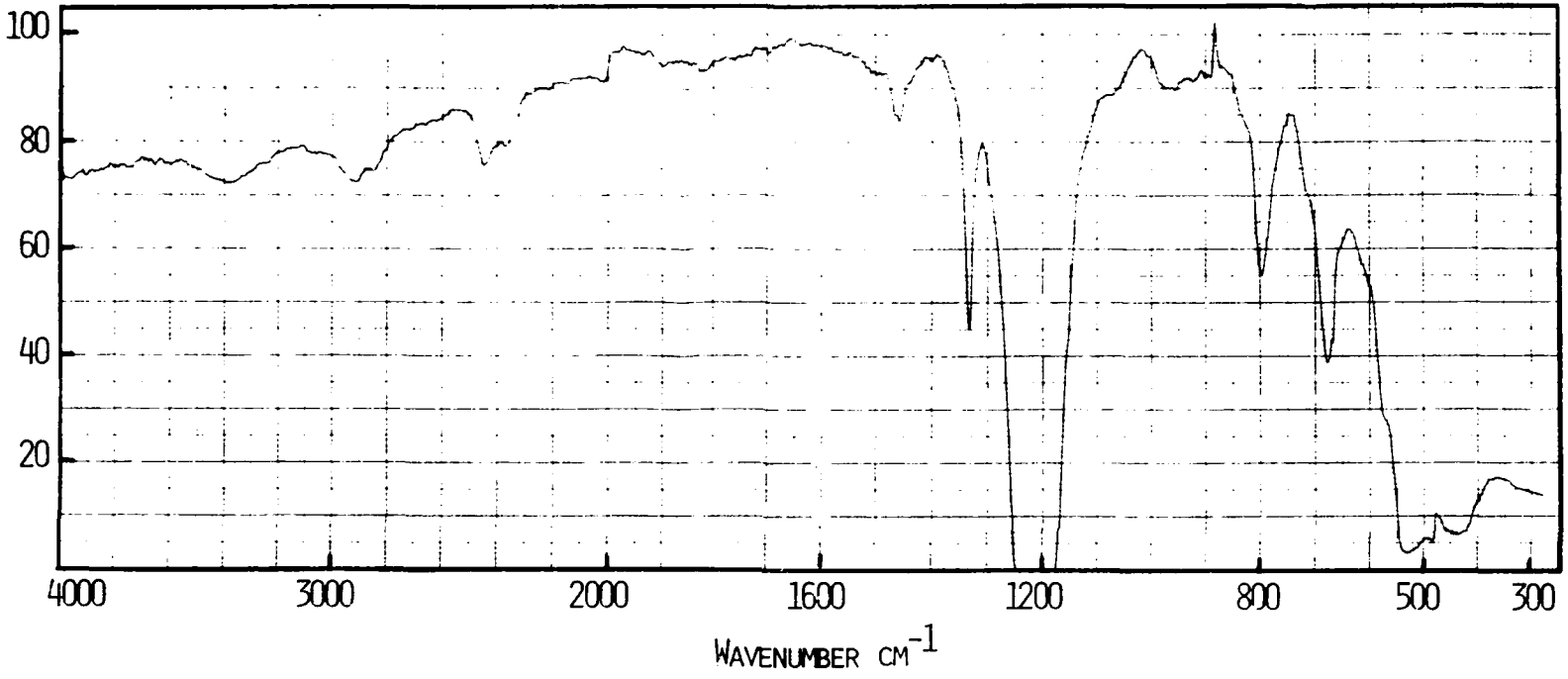

Fig. 44. Infrared spectrum of the solution product from the reaction of one mole of Li_2S with two moles of $AlCl_3$ in $SOCl_2$.

This is in agreement with the fact that the reduction potential of S is ∿2.3V vs. Li. Since both S and SO_2 are discharge products of $Li/SOCl_2$ cells and have closely lying reduction potentials, it is logical to assume that SO_2 also can undergo reduction as shown in Equation 8, probably to form lithium dithionite, $Li_2S_2O_4$, Equation 25.

$$2Li^+ + 2SO_2 + 2e^- \rightarrow Li_2S_2O_4 \qquad (25)$$

To date we do not have any evidence to confirm this. Qualitative tests for $S_2O_4^{-2}$ were negative. It is possible that $Li_2S_2O_4$, if formed, could react with $LiAlCl_4$ forming aluminum dithionite derivatives, which may be unstable and thereby escape qualitative test for $S_2O_4^{-2}$ species.

4.4 Products from "Charged" $Li/SOCl_2$ Cells

In order to characterize the reactions responsible for regenerative processes in the "charging" of $Li/SOCl_2$ cells, electrolyte from charged cells were analyzed by cyclic voltammetry and IR spectrometry. The construction parameters for the cells are shown in Table 9. The test results are summarized in Table 10.

- Experimental Results

The "charging" curve for Cell P-34 at a current of 36 mA is shown in Figure 45. The cyclic voltammogram obtained after 4.6 Ah "charging" is shown in Figure 46. The voltammogram shows that the electrolyte contains SCl_2 and probably some Cl_2. The IR spectrum depicted in Figure 47 shows the presence of SO_2Cl_2, SO_2 and the substance with the 1070 cm^{-1} absorption peak.

Cell P-47 was partially discharged first for 0.61 Ah and then "charged". The charging potentials were at ∿3.8V as opposed to ∿4.2V in fresh cells. Note that we have observed similar behavior in C-cell also. The IR spectrum after 3.35 Ah of charging showed the presence of SO_2 and the material with the 1070 cm^{-1} absorption peak, but no SO_2Cl_2 was present. The cyclic voltammogram showed the presence of Cl_2 but very little or no SCl_2 was present.

In Cell P-43 $Li_2O/AlCl_3$ based electrolyte was used. The IR spectrum and cyclic voltammogram obtained after 1.53 Ah of charging at 36 mA were similar to those obtained from Cell P-34.

- Discussion of Results

"Charging" reactions in fresh or partially discharged $Li/SOCl_2$ cells seem to involve a sequence of regenerative processes so that only small amounts of chemicals accumulate in the cells. Identified products were SO_2Cl_2, SO_2, SCl_2, Cl_2 and a material with IR absorption at 1070 cm^{-1}.

The regenerative processes in fresh cells, consistent with the analytical data and the mechanistic schemes discussed earlier, may be:

TABLE 9

CELL PARAMETERS FOR CHARGED $Li/SOCl_2$ CELLS

Cell No.	Cell Configuration	Carbon Electrode: Average Thickness (mm)	Carbon Electrode: Total Area Facing Li (cm2)	Carbon Electrode: Approximate Amount of Carbon (mg)	Lithium Electrode: Area (cm2)	Lithium Electrode: Amount (Ah)	Electrolyte $LiAlCl_4/SOCl_2$: Conc. $LiAlCl_4$ (M)	Electrolyte $LiAlCl_4/SOCl_2$: Vol. (ml)	Discharge Current (mA)
P-34	CL	0.66	36	420	36	2.01	1.8	4	36
P-47	CL	0.62	36	340	36	2.01	1.8	4	36
P-43	CL	0.62	36	375	36	2.01	1.0[a]	4	36

[a] $Li_2O/AlCl_3$ electrolyte, 1M Li^+.

TABLE 10

ANALYTICAL TEST SUMMARY OF CHARGED $Li/SOCl_2$ CELLS

Cell No.	Cell Capacity (mAh)	Test Performed After Discharge, mAh IR	CV	Overdischarge, mAh IR	CV
P-34	a	-	-	4600	4600
P-47	a	-	-	3350	350
P-43	a	-	-	1530	1530

[a]The cell was charged.

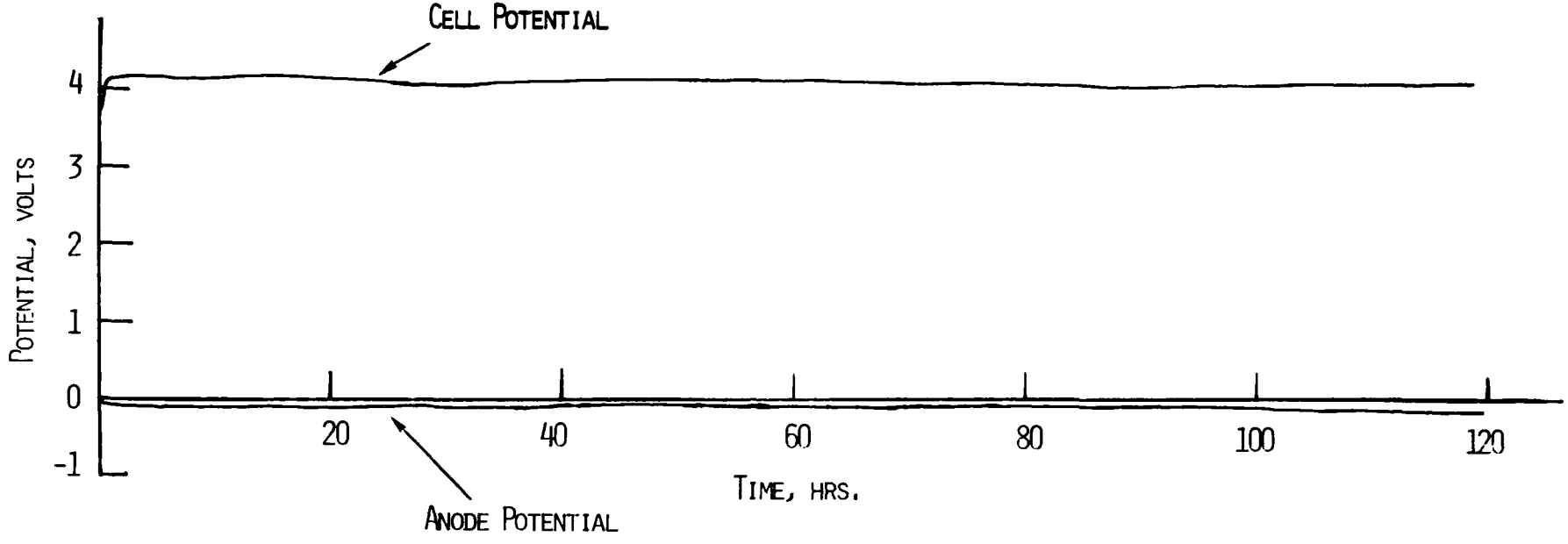

Fig. 45. Galvanostatic "charging" curve for $Li/SOCl_2$ cell P-34. Current = 36 mA.

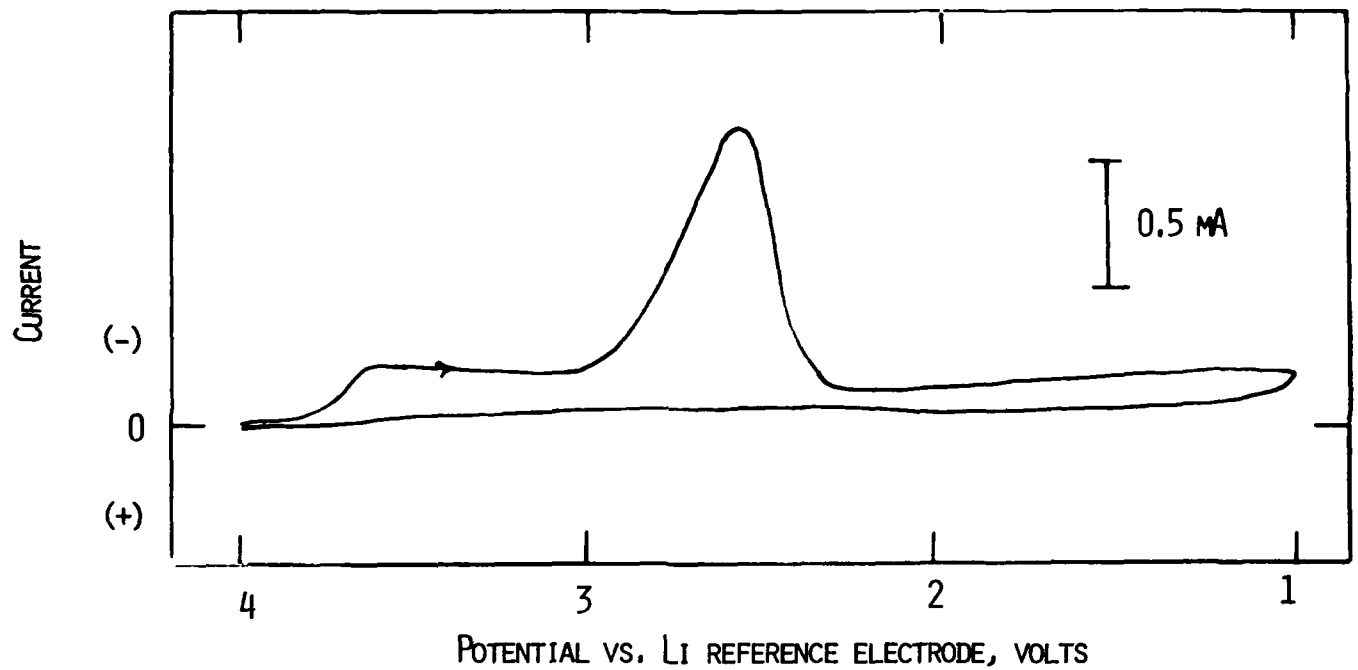

Fig. 46. Cyclic voltammogram of electrolyte from cell P-34 after 750 mAh charge. Scan rate = 50 mV/sec. Cathodic scan first.

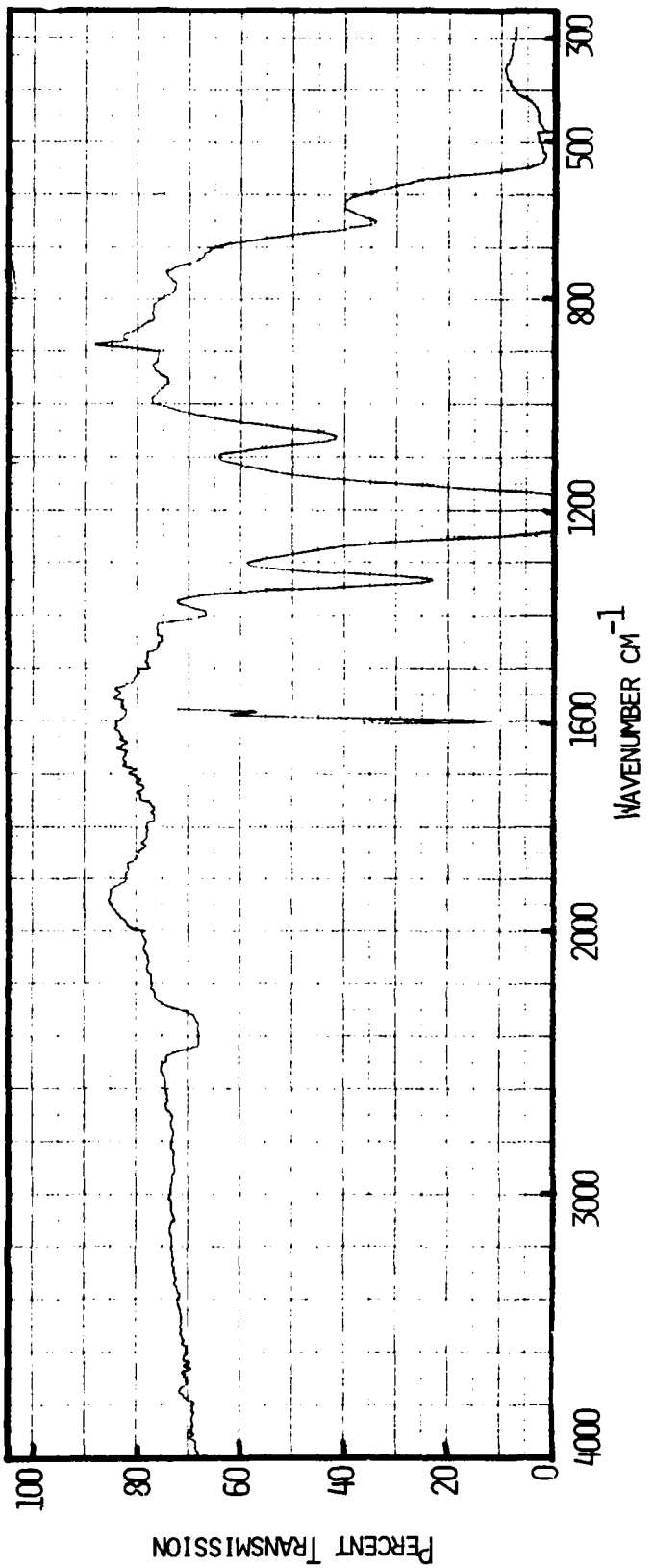

Fig. 47. Infrared spectrum of electrolyte from cell P-34 which was charged, shown in Fig. 45.

$$AlCl_4^- \rightarrow AlCl_3 + \tfrac{1}{2}Cl_2 + e^- \quad (26)$$

$$SOCl_2 \rightarrow SOCl^+AlCl_4^- + \tfrac{1}{2}Cl_2 + e^- \quad (27)$$

Carbon Electrode

$$SOCl_2 + AlCl_3 \rightarrow SOCl^+AlCl_4^-$$

$$\tfrac{1}{2}Cl_2 + Li \rightarrow LiCl \quad (28)$$

$$\tfrac{1}{2}Cl_2 + Li^+ + e^- \rightarrow LiCl \quad (29)$$

Li Electrode

$$LiCl + SOCl^+AlCl_4^- \rightarrow LiAlCl_4 + SOCl_2 \quad (30)$$

Note that the reaction shown in Equation 30 regenerates the cell materials. The presence of SO_2Cl_2 and SCl_2 in these cells may be explained by oxidation reactions of $SOCl^+AlCl_4^-$ as discussed earlier. The regenerative processes in the "charging" of partially discharged cells seem to involve a different set of reactions from those in fresh cells. In these cells SO_2Cl_2 and SCl_2 were absent. Since SO_2Cl_2 and SCl_2 are produced by the oxidation of $SOCl^+AlCl_4^-$, it appears that the latter reaction does not occur during charging of partially discharged cells.

The charging processes in cells containing $Li_2O/AlCl_3$ based electrolytes appear to be the same as in cells with $SOCl_2/LiAlCl_4$.

IV. SUPPORTING ELECTROLYTE BASED ON $Li_2S/AlCl_3$ FOR $Li/SOCl_2$ CELLS

In the previous section we have shown that the reaction of Li_2S with $AlCl_3$ in $SOCl_2$ produces $LiAlSCl_2$ or a mixture of $LiAlSCl_2$ and $LiAlCl_4$ depending upon the stoichiometry of the reactants.* A solution of $LiAlSCl_2$ in $SOCl_2$ can be obtained by treating $AlCl_3$ and Li_2S in a 1:1 molar ratio. When Li_2S and $AlCl_3$ are treated in a 1:2 molar ratio, the products are $LiAlSCl_2$ and $LiAlCl_4$. Both of these solutions were found to be good electrolytes having conductivities similar to that of $SOCl_2/LiAlCl_4$ solutions.

1. Conductivities of $Li_2S/AlCl_3$ Solutions in $SOCl_2$

The conductance data were obtained using a conductivity cell of the Jones and Bollinger type. The variation of specific conductances of 1M $AlCl_3$ solution in $SOCl_2$ as a function of the concentration of added Li_2S is shown in Figure 48. The conductivity of the solution with 0.5M Li_2S is 16×10^{-3} ohm^{-1} cm^{-1} and the solution apparently contains 0.5M each of $LiAlSCl_2$ and $LiAlCl_4$. Upto this concentration of Li_2S there is no precipitate formed in solution with the incremental addition of Li_2S. With further addition of Li_2S a precipitate is formed which is due to LiCl formed according to the reaction

$$LiAlCl_4 + Li_2S \rightarrow LiAlSCl_2 + 2LiCl$$

The conductance data were obtained with precipitate-free electrolytes. The conductance of the solution with 1M Li_2S is $\sim 13 \times 10^{-3}$ ohm^{-1} cm^{-1}. When compared to the specific conductivity of 14×10^{-3} ohm^{-1} cm^{-1} for 1M $LiAlCl_4/SOCl_2$ solutions, the $Li_2S/AlCl_3$ solutions should exhibit discharge performance similar to solutions with $LiAlCl_4$ salt. Preliminary data suggest that this is possible.

2. Performance of Cells with $Li_2S/AlCl_3$ Based Electrolytes

Two cathode limited cells were tested. The construction parameters for these cells are given in Table11. In Cell P-52, the electrolyte was a mixture of $LiAlSCl_2$ and $LiAlCl_4$ obtained by stirring Li_2S (0.5M) and $AlCl_3$ (1M) in $SOCl_2$ so that the Li^+ ion concentration was 1M. The OCV of the cell was 3.7V. It was

*As mentioned previously, it remains to be established whether $SOCl_2$ reacts with Li_2S in the presence of $AlCl_3$.

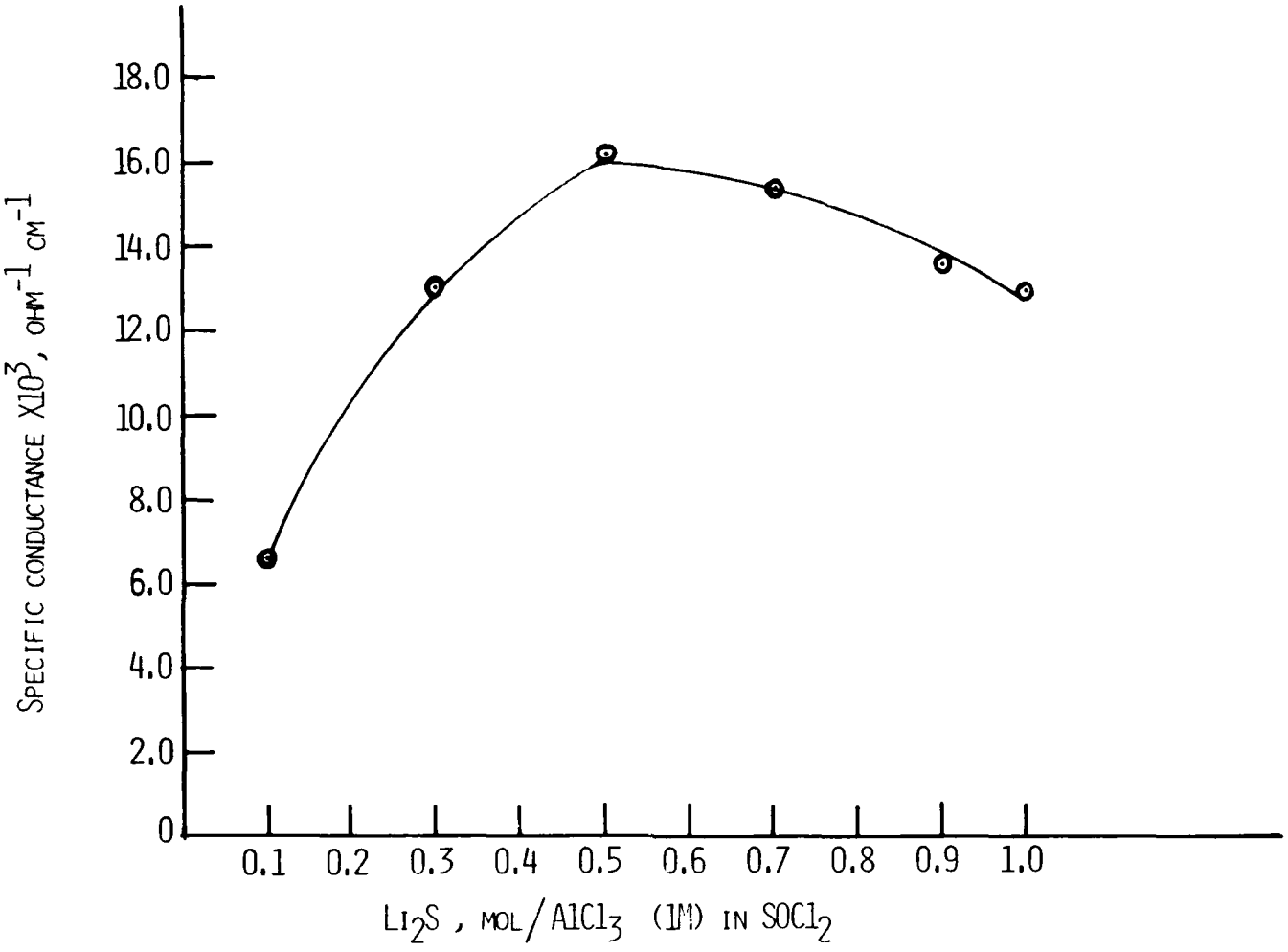

Fig. 48. Conductometric titration of $AlCl_3$ dissolved in $SOCl_2$ (1M) with Li_2S.

TABLE 11

CELL PARAMETERS FOR $Li/SOCl_2$ CELLS WITH $Li_2S/AlCl_3$ BASED ELECTROLYTES

		Carbon Electrode			Lithium Electrode		Electrolyte		
Cell No.	Cell Configuration	Average Thickness (mm)	Total Area Facing Li (cm^2)	Approximate Amount of Carbon (mg)	Area (cm^2)	Amount (Ah)	$[Li^+]$ (M)	Vol. (ml)	Discharge Current (mA)
51	Cathode Limited	0.55	36	340	36	2.01	1.0[a]	4	36
52	Cathode Limited	0.52	36	330	36	2.01	1.0[b]	4	36

[a] 1M $LiAlCl_2$.

[b] ~0.5M $LiAlSCl_2$ + ~0.5M $LiAlCl_4$.

AD-A081 998 EIC CORP NEWTON MASS F/G 10/3
INVESTIGATIONS OF THE SAFETY OF LI/SOCL2 BATTERIES.(U)
FEB 80 K M ABRAHAM, R M MANK, G L HOLLECK DAAB07-78-C-0564
UNCLASSIFIED C-536 DELET-TR-78-0564-F NL

END
DATE FILMED
4 80
DTIC

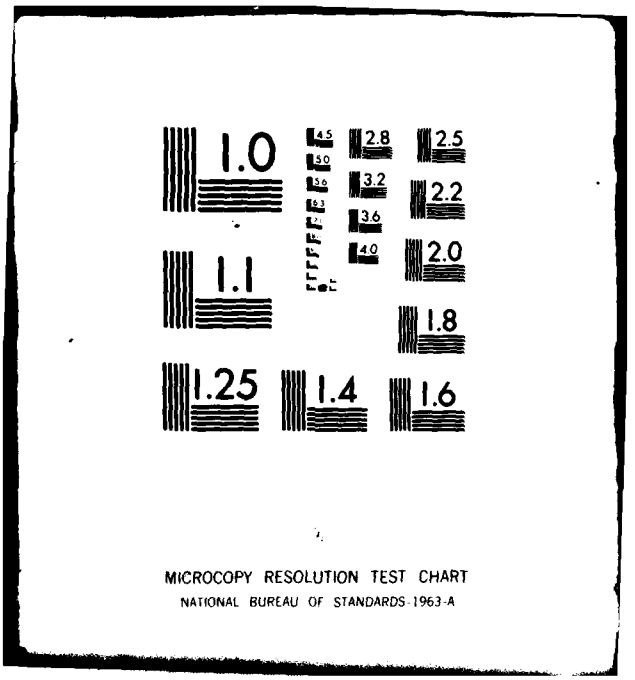
1.0
1.1
1.25
1.4
1.6
1.8
2.0
2.2
2.5
2.8
3.2
3.6
4.0
4.5
5.0
5.6
6.3
MICROCOPY RESOLUTION TEST CHART
NATIONAL BUREAU OF STANDARDS-1963-A

discharged at 36 mA (1 mA/cm^2 of Li electrode area). The discharge curve is shown in Figure 49. The cell yielded 1.0 Ah capacity to zero volt, corresponding to a cathode utilization of 3.07 Ah/g carbon. This utilization is virtually identical to that obtained from cells with $SOCl_2/LiAlCl_4$.

In cell P-51, the electrolyte was solution of $LiAlSCl_2$ (1M) in $SOCl_2$, obtained by treating equimolar amounts of Li_2S and $AlCl_3$ in $SOCl_2$ and filtering off the precipitated LiCl. The OCV of the cell was also 3.7V and it was also discharged at 36 mA, Figure 50. The cell capacity was 0.98 Ah, which corresponded to a cathode utilization of 2.93 Ah/g carbon.

These data suggest that $Li_2S/AlCl_3$ based electrolyte show promise as alternatives for $LiAlCl_4$ in $Li/SOCl_2$ cells.

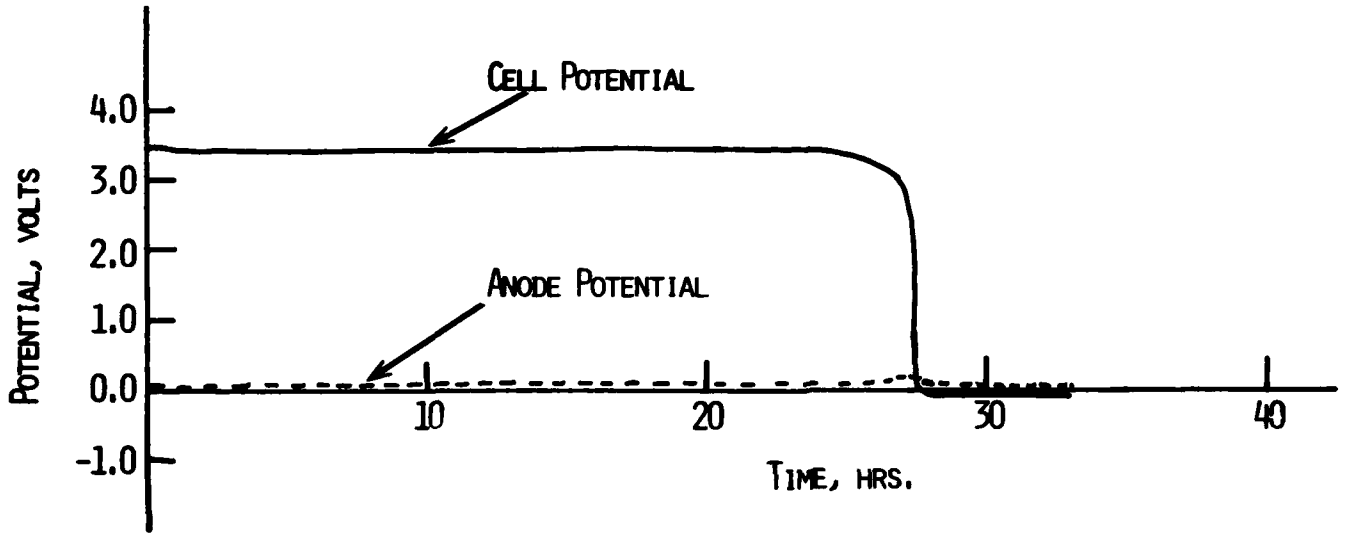

Fig. 49. Galvanostatic discharge curves for cell P-52. Current = 36 mA.

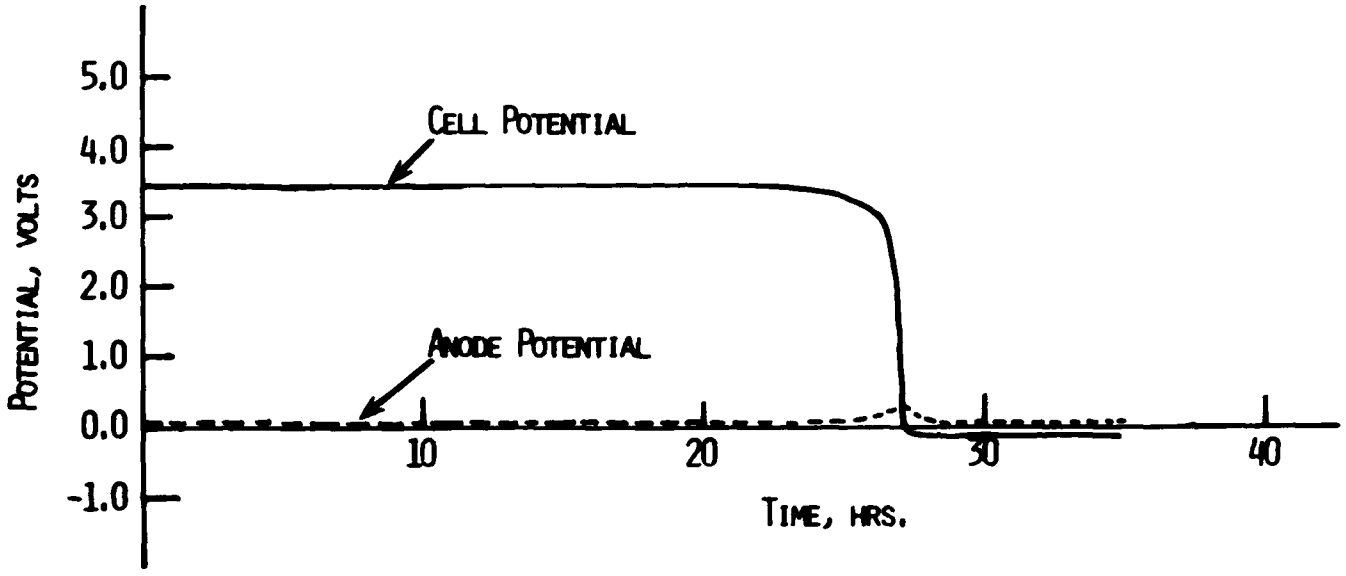

Fig. 50. Galvanostatic discharge curves for cell P-51. Current = 36 mA.

V. SUMMARY AND CONCLUSIONS

The anode limited condition of $Li/SOCl_2$ cells has been identified as a potentially hazardous one. Our data on the forced overdischarge behavior of $Li/SOCl_2$ C-cells suggest that anode limited cells are likely to explode during forced overdischarge.

Cathode limited cells, on the other hand, appeared to be safe. These cells could be forced overdischarged for long periods of time without explosion. The behavior of $Li/SOCl_2$ cells during application of a "charge" current was investigated using C-size cells. It was possible to subject either new or partially discharged cells to a "charging" current without apparent hazard. The charging reactions seem to involve a sequence of regenerative processes so that only small amounts of chemicals accumulate in the cells.

Analysis of reaction products in $Li/SOCl_2$ cells formed during various modes of operation have been carried out using cyclic voltammetry and infrared spectrometry as analytical tools. Sulfur dioxide is formed during early stages of discharge. The nature of products formed during overdischarge depends on whether the cells are anode or cathode limited.

Lithium sulfide (Li_2S) is formed in cathode limited cells during forced and resistive-load overdischarge. The data suggested that once formed the Li_2S reacts immediately with $LiAlCl_4$ to form $LiAlSCl_2$ and probably $LiAlS_2$.

From anode limited cells, Cl_2 and a compound exhibiting IR absorption at 1070 cm^{-1} were detected after forced overdischarge.

Analysis of solutions from cells discharged without Li on the anode showed that SO_2Cl_2, SCl_2, $SOCl^+AlCl_4^-$, Cl_2 and the material exhibitng IR absorption at 1070 cm^{-1} are formed. These materials are formed via oxidation reactions at the anode.

The products detectable after "charging" a $Li/SOCl_2$ cells have been, SO_2Cl_2, SCl_2, SO_2, Cl_2 and the material with the IR absorption at 1070 cm^{-1}. Since identical products are formed in $Li/SOCl_2$ cells during "charging" and in anode limited cells during forced overdischarge, we suggest that sufficient caution should be employed when the cells are charged irrespective of our observation that the mode of operation appeared safe.

VI. REFERENCES

1. W. K. Behl, J. A. Christopulos, M. Ramirez and S. Gilman, J. Electrochem. Soc., 120, 1619 (1973).

2. J. J. Auborn, K. W. French, S. I. Lieberman, V. K. Shah and A. Heller, J. Electrochem. Soc. 120, 1613 (1973).

3. A. N. Dey, P. R. Mallory Company, Second Quarterly Report, ECOM-74-0109-2, November 1974.

4. A. N. Dey and P. Bro, Paper No. 32 presented at the Power Sources Conf., Brighton, 1976.

5. A. N. Dey, P. R. Mallory Company, Interim Report, ECOM-74-0109-13, November 1977 and references therein.

6. N. Marincic and A. Lombardi, GTE Laboratory, Final Report, ECOM-74-0108-F, April 1977.

7. K. M. Abraham, P. G. Gudrais, G. L. Holleck and S. B. Brummer, 28th Power Sources Symposium, Atlantic City, NJ, 1978.

8. K. M. Abraham, G. L. Holleck and S. B. Brummer, Proceedings of the Symposium on Battery Design and Optimization, The Electrochemical Society, Princeton, NJ, 1978.

9. J. P. Gabano and P. Lefant, Proceedings of the Symposium on Battery Design and Optimization, The Electrochemical Society, Princeton, NJ, 1978.

10. V. Gutman in "Halogen Chemistry", V. Gutman, Ed., Academic Press, New York (1967).

11. J. R. Driscoll et al., 27th Power Sources Symposium, Atlantic City, June (1976).

12. W. K. Behl, Proc. 27th Power Sources Symposium, Atlantic City, June (1976).

13. G. E. Blomgren, V. Z. Leger, M. L. Kronenberg, T. Kalnoki-Kis and R. J. Brodd, 11th International Power Sources Symposium, Brighton (1978).

14. S. N. Nabi and M. A. Khaleque, J. Chem. Soc., 3626 (1965).

DISTRIBUTION LIST

Defense Technical Information Ctr. (12)
Attn: DTIC-TCA
Cameron Station (Bldg. 5)
Alexandria, VA 22314

GIDEP Engineering & Support Dept. (1)
TE Section
P.O. Box 398
Norco, CA 91760

Director (1)
Naval Research Laboratory
Attn: Code 2627
Washington, DC 20375

Rome Air Development Center (1)
Attn: Documents Library (TILD)
Griffiss AFB, NY 13441

Deputy for Science & Technology (1)
Office, Asst. Sec. Army (R&D)
Washington, DC 20310

HQDA (DAMA-ARZ-D/ (1)
Dr. F. D. Verderame)
Washington, DC 20310

Director (1)
US Army Materiel Systems Analysis Actv.
Attn: DRXSY-MP
Aberdeen Proving Ground, MD 21005

Command, DARCOM (1)
Attn: DRCDE
50001 Eisenhower Avenue
Alexandria, VA 22333

Cdr, US Army Signals Warfare Lab (1)
Attn: DELSW-OS
Vint Hill Farms Station
Warrenton, VA 22186

Cdr, PM Concept Analysis Ctr. (1)
Attn: DRCPM-CAC
Arlington Hall Station
Arlington, VA 22212

Cdr, Night Vision & Electro-Optics (1)
ERADCOM
Attn: DELNV-D
Fort Belvoir, VA 22060

Cdr, Atomspheric Sciences Lab (1)
ERADCOM
Attn: DELAS-SY-S
White Sands Missile Range, NM 88002

Cdr, Harry Diamond Laboratories (1)
Attn: DELHD-C), TD (In Turn)
2800 Powder Mill Road
Adelphi, MD 20783

Cdr, ERADCOM (1)
Attn: DRDEL-CG, CS (In Turn)
2800 Powder Mill Road
Adelphi, MD 20783

Cdr, ERADCOM (1)
Attn: DRDEL-CT
2800 Powder Mill Road
Adelphi, MD 20783

Commander
US Army Electronics R&D Command
Fort Monmouth, NJ 07703

Attn: DELET-P (1)
DELEW-D (1)
DELET-DD (1)
DELSD-L (Tech Library) (1)
DELSD-L-S (STINFO) (2)
DELET-PR (6)

DISTRIBUTION LIST
(continued)

Commander (1)
US Army Communications R&D Command
Attn: USMC-LNO
Fort Monmouth, NJ 07703

Advisory Group on Electron Devices (2)
201 Varick Street, 9th Floor
New York, NY 10014

Electrochimica (1)
2485 Charleston Road
Mountain View, CA 94040
Attn: Dr. Eisenberg

Sanders Associates, Inc. (1)
24 Simon Street
Mail Stop NSI-2208
Nashua, NY 03060
Attn: J. Marshall

Power Conversion, Inc. (1)
70 MacQueston Pkwy
Mount Vernon, NY 10550
Attn: Stuart Chodosh

Dr. Leonard Nanis (1)
G207
S.R.I.
Menlo Park, CA 94025

Dr. J. J. Auborn, Rm. 1A-317 (1)
Bell Laboratories
600 Mountain Ave
Murray Hill, NJ 07974

Stonehart Associates, Inc. (1)
34 Five Fields Road
Madison, CT 06443
Attn: Mr. Thomas Reddy

Jet Propulsion Laboratory (1)
4800 Oak Grove Drive
Pasadena, CA 91103
Attn: Mr. Harvey Frank
Mail Stop 198-220

Dr. D. Ernst (1)
Naval Surface Weapons Center
White Oak Laboratory, Code
R-33 (M/S A026)
Silver Spring, MD 20910

Mr. J. R. Moden (1)
Energy Conversion Branch Code 3642
Naval Underwater Systems Center
Newport Laboratory
Newport, RI 02840

NASA-Lewis Research Center (1)
Mail Stop 6-1
21000 Brookpark Road
Cleveland, OH 44135
Attn: Dr. Stuart Fordyce

Mr. Joe McCartney (1)
Naval Undersea Center
Code 608
San Diego, CA 92132

Atlus Corporation (1)
440 Page Mill Road
Palo Alto, CA 94306
Attn: Douglas Glader

J. Bene (1)
MS 488
NASA Langley Research Center
Hampton, VA 23665

Mr. Eddie T. Seo (1)
Research & Development Division
The Gates Rubber Company
999 S. Broadway
Denver, CO 80217

Mr. Sidney Gross (1)
Mail Stop 8C-62
Boeing Aerospace Company
P.O. Box 3999
Seattle, WA 98124

DISTRIBUTION LIST
(continued)

Honeywell Technology Center (1)
Attn: Dr. H. V. Venkatasetty
10701 Lyndale Avenue South
Bloomington, MN 55420

Mr. Aiji Uchiyama (1)
Jet Propulsion Laboratory
MS 198-220
4800 Oak Grove Drive
Pasadena, CA 91103

Transportation Systems Center (1)
Kendall Square
Cambridge, MA 02142
Attn: Dr. Normal Rosenberg

GTE Laboratories, Inc. (1)
40 Sylvan Road
Waltham, MA 02154

Foote Mineral Company (1)
Route 100
Exton, PA 19341
Attn: Dr. H. Grady

Honeywell, Inc. (1)
104 Rock Road
Horsham, PA 19044

Eagle-Picher Industries, Inc. (1)
Electronics Division
Attn: Mr. Robert L. Higgins
P.O. Box 47
Joplin, MO 64801

Yardney Electric Company (1)
82 Mechanic Street
Pawcatuck, CT 06379
Attn: Technical Library

P. R. Mallory & Co., Inc. (1)
Northwest Industrial Park
Burlington, MA 01803
Attn: Dr. Per Bro

Exxon Research and Engineering Company (1)
Corporate Research Laboratory
Linden, NJ 07036
Attn: Dr. R. Hamlen

Argonne National Laboratories (1)
9700 South Cass Avenue
Argonne, IL 60439
Attn: Dr. E. C. Gay

GTE Sylvania, Inc. (1)
77 A Street
Needham Heights, MA 02194
Attn: Mr. Richard Pabst

General Motors Corp. (1)
Research Laboratories
General Motors Technical Center
12 Mile and Mounds Roads
Warren, MI 48090
Attn: Dr. J. L. Hartman

Union Carbide Corporation (1)
Parma Research Center
P. O. Box 6116
Cleveland, OH 44101

P. R. Mallory & Company, Inc. (1)
S. Broadway
Tarrytown, NY 10591
Attn: J. Dalfonso

North American Rockwell Corp. (1)
Atomics International Div.
Box 309
Canoga Park, CA 91304
Attn: Dr. L. Heredy

General Electric Research & Development Center (1)
P. O. Box 8
Schenectady, NY 12301
Attn: Dr. Stefan Mitoff

DISTRIBUTION LIST
(continued)

The Electric Storage Battery Co. (1)
Carl F. Norburg Research Center
19 W. College Avenue
Yardley, PA 19067
ATTN: Dr. A. Salkind

Gulton Industries, Inc. (1)
Metuchen, NJ 08840
Attn: Mr. S. Charlip